

Engineering and Characterization of
Cytochrome P450 Enzymes for Nitrogen-Atom
Transfer Reactions

Thesis by
Christopher C. Farwell

In Partial Fulfillment of the Requirements for the degree
of
Doctor of Philosophy



CALIFORNIA INSTITUTE OF TECHNOLOGY
Pasadena, California
2015
(Defended January 27th, 2015)

© 2015

Christopher C. Farwell

All Rights Reserved

ACKNOWLEDGEMENTS

I would like to thank first and foremost my adviser and mentor, Frances H. Arnold, who has successfully married useful and interesting chemistry throughout her career. She has provided an unparalleled environment and opportunity to study fields that I have found interesting since I began studying chemistry: enzymology, evolution, and catalysis.

This work would not have been possible without the contributions of numerous fellow graduate students and post-docs I have had the privilege of working with over the last five years. I am indebted to John McIntosh, Sabine Brinkmann-Chen, Kelly Zhang, Todd Hyster, Jane Wang, Pedro Coelho, and Hans Renata, whose expertise and assistance has made possible much of the work presented here. The knowledge of former lab members Martin Engqvist, Kersten Rabe, Devin Trudeau, and Mike Chen has proved invaluable throughout my Ph.D. studies and I acknowledge their help.

My fellow graduate students in the Chemistry and Chemical Engineering division, Guy Eduouard and John Rittle, are consistent sources of information and expertise in the chemistry of transition metals. Their expertise has also served in the development of the ideas and work presented here.

Finally, I thank my parents, Martha and Bill Farwell, and my brother, Geoff Farwell, for their endless love and support throughout my extended educational period.

ABSTRACT

The creation of novel enzyme activity is a great challenge to protein engineers, but nature has done so repeatedly throughout the process of natural selection. I begin by outlining the multitude of distinct reactions catalyzed by a single enzyme class, cytochrome P450 monooxygenases. I discuss the ability of cytochrome P450 to generate reactive intermediates capable of diverse reactivity, suggesting this enzyme can also be used to generate novel reactive intermediates in the form of metal-carbenoid and nitrenoid species. I then show that cytochrome P450 from *Bacillus megaterium* (P450_{BM3}) and its isolated cofactor can catalyze metal-nitrenoid transfer in the form of intramolecular C–H bond amination. Mutations to the protein sequence can enhance the reactivity and selectivity of this transformation significantly beyond that of the free cofactor. Next, I demonstrate an intermolecular nitrene transfer reaction catalyzed by P450_{BM3} in the form of sulfide imidation. Understanding that sulfur heteroatoms are strong nucleophiles, I show that increasing the sulfide nucleophilicity through substituents on the aryl sulfide ring can dramatically increase reaction productivity. To explore engineering nitrenoid transfer in P450_{BM3}, active site mutagenesis is employed to tune the regioselectivity intramolecular C–H amination catalysts. The solution of the crystal structure of a highly selective variant demonstrates that hydrophobic residues in the active site strongly modulate reactivity and regioselectivity. Finally, I use a similar strategy to develop P450-based catalysts for intermolecular olefin aziridination, demonstrating that active site mutagenesis can greatly enhance this nitrene transfer reaction. The resulting variant can catalyze intermolecular aziridination with more than 1000 total turnovers and enantioselectivity of up to 99% *ee*.

TABLE OF CONTENTS

Abbreviations	vi
Chapter I: Expanding P450 Catalytic Reaction Space Through Evolution and Engineering	1
Abstract.....	2
Introduction.....	3
Cytochrome P450: a platform for C–H activation.....	5
P450 catalytic intermediates facilitate diverse natural chemistry.....	7
Manipulating conserved features enables non-natural chemistry	12
Conclusions.....	17
References.....	19
Chapter II: Enantioselective Intramolecular C–H Amination Catalyzed by Engineered Cytochrome P450 Enzymes	21
Abstract.....	22
Main Text.....	23
Supplementary Materials.....	31
References.....	44
Chapter III: Enantioselective Imidation of Sulfides via Enzyme-Catalyzed Intermolecular Nitrogen-Atom Transfer	45
Abstract.....	46
Introduction.....	47
Results and Discussion.....	49
Conclusions.....	61
Supplementary Materials.....	63
References.....	82
Chapter IV: Enzyme-Controlled Nitrogen-Atom Transfer Enables Regiodivergent C – H amination	84
Abstract.....	85
Main Text.....	86
Supplementary Materials.....	96
References.....	106
Chapter V: Enantioselective Enzyme-Catalyzed Aziridination Enabled by Active-Site Engineering of a Cytochrome p450	109
Abstract.....	110
Introduction.....	111
Results and Discussion.....	114
Conclusions.....	123
Supplementary Materials.....	125
References.....	143

ABBREVIATIONS

CYP	Cytochrome P450 monooxygenase identifier
P450	Cysteine-ligated cytochrome P450 monooxygenase
P411	Serine-ligated cytochrome P450 enzyme
BM3	Cytochrome P450 from <i>Bacillus megaterium</i> (CYP102A1)
CO	Carbon monoxide
DMSO	Dimethyl sulfoxide
KPi	Potassium monophosphate
NADPH	Reduced nicotinic adenine dinucleotide phosphate
TTN	Total turnover number
HPLC	High performance liquid chromatography
LC-MS	Liquid chromatography with mass spectrometry
M9-N	M9 minimal media with no nitrogen source added

*Chapter 1*EXPANDING CYTOCHROME P450 REACTION SPACE THROUGH EVOLUTION
AND ENGINEERING

This chapter is published as J. A. McIntosh, C. C. Farwell, F. H. Arnold “Expanding Cytochrome P450 Reaction Space Through Evolution and Engineering” in *Current Opinion in Chemical Biology* 2014, 19, 126-134. U. Bornscheuer, J. C. Moore, eds. J.A.M., F.H.A., and myself wrote the paper, where I contributed to the first, second, and fourth sections and also created all figures.

Abstract

Advances in protein and metabolic engineering have led to the broad use of enzymes to synthesize important molecules. However, many desirable transformations are not catalyzed by any known enzyme, driving interest in understanding how new enzymes can be created. The cytochrome P450 enzyme family, whose members participate in xenobiotic metabolism and natural products biosynthesis, catalyzes an impressive range of difficult chemical reactions that continues to grow as new enzymes are characterized. Recent work has revealed that P450-derived enzymes can also catalyze useful reactions previously accessible only through synthetic chemistry. The evolution and engineering of these enzymes provides an excellent case study for how to genetically encode new chemistry and expand biology's reaction space.

Introduction

Impressive demonstrations of the use of engineered microbes to produce fuels and chemicals in recent years have led some to predict a future in which microbes can produce nearly all of the organic molecules upon which society depends from renewable resources.¹ This future may be desirable from the standpoint of energy efficiency and environmental sustainability, but it is also a ways off. Successful metabolic engineering efforts have, for the most part, depended on reassembling natural enzymes into biosynthetic pathways. Many desired products unfortunately fall outside the reach of the rather limited set of known enzyme-catalyzed transformations. Eventually, progress in biological production will depend on our ability to genetically encode new catalysts for known and novel chemical reactions.

Generating new enzymes *de novo* is difficult, although progress is being made with some relatively simple transformations—for example, computationally designed enzymes that catalyze the Kemp elimination and Diels-Alder reactions have been reported.² Nature, it seems, agrees with this assessment, preferring to repurpose existing enzyme scaffolds rather than create whole new enzymes.³ Some scaffolds appear to be used more frequently than others: for example, the enolase and crotonase superfamilies (and many others) support several different reactions,⁴ whereas the dihydrofolate reductase family is only known to carry out a single reaction.⁵ Thus a biomimetic alternative to *de novo* protein design might exploit enzymes that nature has already used for chemical innovations. But can nature's past successes with catalytic diversification guide future efforts to generate new enzyme catalysts? Recent work suggests that the versatility of cytochrome P450 enzymes—which catalyze a multitude of reactions in nature—can indeed be replicated and

even expanded upon by enzyme engineers to genetically encode new biosynthetic capabilities.

Cytochrome P450 enzymes are most commonly associated with the hydroxylation and dealkylation of xenobiotic molecules in mammals, and in this case the substrate scope is vast. But their natural roles far exceed this one niche. Biosynthetic pathways to many natural products, such as terpenes (including steroids), alkaloids, and polyketides, involve P450-mediated oxidations, which add functional groups to simpler hydrophobic skeletons. P450s also occur in primary catabolic pathways for degradation of alkanes and other recalcitrant molecules. Beyond their large substrate scope, many different reaction types have been characterized for naturally occurring and engineered P450s,⁶ including hydroxylation, epoxidation, sulfoxidation, aryl-aryl coupling, nitration, oxidative and reductive dehalogenations, and recently several synthetically important non-natural reactions (*vide infra*). Given future challenges in synthetic biology, the ability of P450 enzymes to assume new catalytic functions in natural and artificial contexts merits close inspection for insights into how we might discover or create new biocatalysts.

In this review, we present examples of the broad catalytic range of P450 enzymes from papers published during the last two years, with an emphasis on newly characterized reactions, both naturally occurring and artificially conceived. To help distinguish between the many natural P450 reactions and newly discovered non-natural reactions, we first review key aspects of P450 catalysis and describe how these characteristics allow access to a diverse set of reactions. Next, we describe recently published non-natural P450 reactions and contrast features of natural and non-natural chemical reactivity. Finally, we discuss the broader relevance of P450 reaction diversity to the goal of engineering new enzymes.

Cytochrome P450: a platform for C–H activation

Here we introduce the P450 catalytic cycle and the key reactive intermediates that are responsible for much of the natural reactivity of P450 enzymes. Additionally, we make note of some of the key conserved residues involved in oxygen activation; mutations to some of these key residues lead to increased activity in non-natural reactions, as we describe below. For a more detailed treatment of the P450 mechanism, we refer the reader to more specialized reviews.^{6a,7}

In the resting state of the enzyme, the catalytic iron is in the ferric (+3) oxidation state (intermediate A in Figure 1). P450s produce intermediates that are sufficiently reactive to attack even inert hydrocarbons. Consequently, P450 enzymes have evolved mechanisms that prevent initiation of the catalytic cycle in the absence of substrate. Substrate binding initiates the catalytic cycle by increasing the redox potential of the heme prosthetic group, which makes it possible for an associated reductase to reduce the heme to the ferrous (+2) state. The catalytic cycle continues with binding of molecular oxygen to the iron center to give a ferric superoxide complex (intermediate B in Figure 1). A second electron transfer generates an iron-peroxo intermediate (C1 in Figure 1), which is then protonated to give an iron-hydroperoxy intermediate (C2 in Figure 1). Subsequent protonation effects heterolytic cleavage of the O–O bond to form the high-valent iron-oxo intermediate known as compound I (intermediate D in Figure 1). In hydroxylation reactions, compound I abstracts a hydrogen atom from a substrate C–H bond (formally a proton-coupled 1-electron oxidation of the substrate), yielding compound II and a substrate radical. These two radical species then rapidly recombine to produce the hydroxylated product and the ferric resting state of the enzyme.

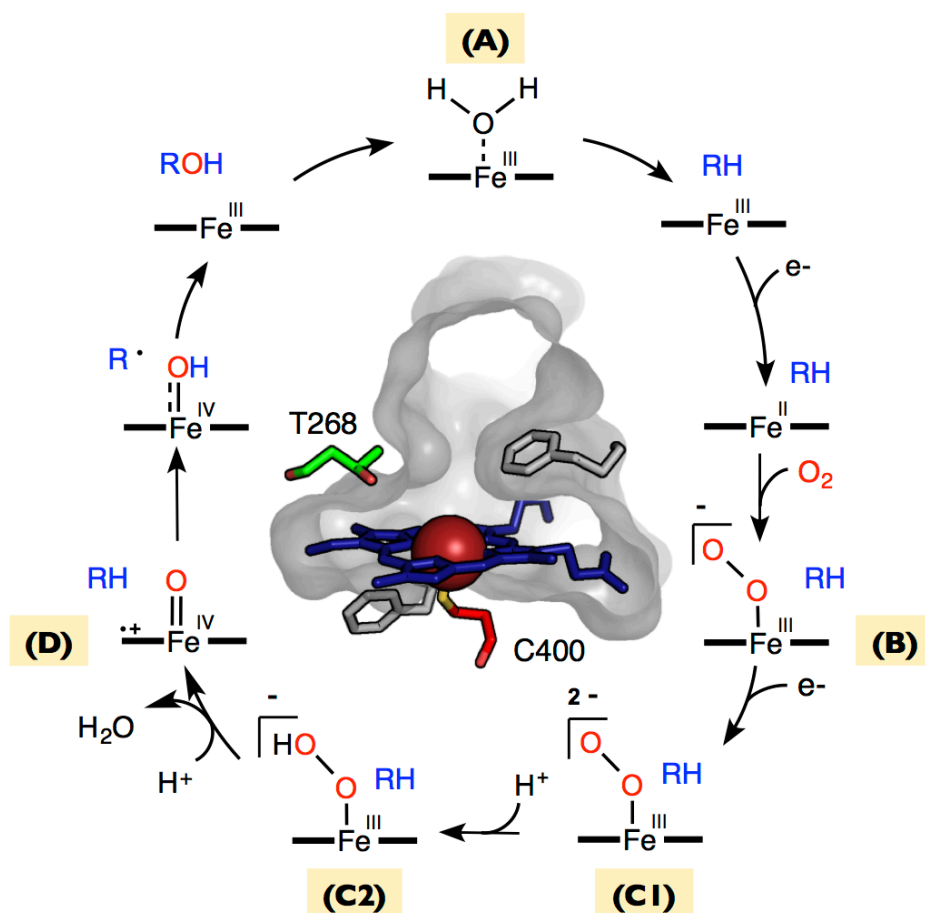


Figure 1. The P450 catalytic cycle. The active site structure of P450_{BM3} is shown at center with conserved threonine (T268) and axial cysteine (C400) highlighted. Key intermediates include the ferric resting state (A), the ferric superoxide intermediate (B), the iron-peroxo or hydroperoxy intermediates (C1, C2), and compound I (D).

Although many interactions between the protein, its reductase partner, and the heme prosthetic group contribute to the smooth operation of the catalytic cycle, a few key residues merit special mention. One is a conserved active-site threonine (T268 in Figure 1), which, through water, helps to protonate the iron-peroxo and iron-hydroperoxy intermediates, thus promoting O–O bond scission to generate compound I. Another key residue universally conserved among P450 enzymes is the axial cysteine that ligates the heme iron. Thiolate ligation is thought to serve several functions. For one, the electron-

rich thiolate ligand makes the ferric heme a worse electron acceptor. This decrease in redox potential helps to prevent triggering of the catalytic cycle in the absence of substrate. Another key role of the axial cysteine is to promote heterolytic O–O bond scission of the iron-hydroperoxy intermediate. Finally, as Green has argued, thiolate ligation may bias compound I toward hydrogen abstraction chemistry.^{7c} In particular, the electron donating ability of the thiolate ligand makes compound I worse at performing 1-electron oxidations, but makes the 1-electron reduced form (known as compound II) much more basic, thus favoring proton-coupled 1-electron oxidations (i.e., hydrogen abstractions).

Intermediates in the P450 catalytic cycle drive diverse natural chemical reactivity

The expansive catalytic scope of P450 enzymes is obvious from even a partial listing of known P450-catalyzed reactions: aryl-aryl coupling, ring contractions and expansions, S- N- and O-dealkylations, decarboxylation, oxidative cyclization, alcohol and aldehyde oxidation, desaturation, sulfoxidation, nitrogen oxidation, epoxidation, C–C bond scission, decarbonylation, and nitration. Many of these transformations (heteroatom demethylations, decarboxylation, alcohol and aldehyde oxidation, desaturation, and others) are mechanistically very similar to hydroxylation (Figure 1) and result from the ability of compound I to perform hydrogen atom abstractions; others involve compound I-mediated oxidations distinct from hydrogen atom abstraction. P450 enzymes, however, do not rely exclusively on compound I, as other intermediates in the catalytic cycle are responsible for some P450 transformations (Figure 2). For example, the iron-peroxo (or hydroperoxide) intermediate can mediate epoxidation and sulfoxidation under some circumstances;⁸ in others this species carries out C–C bond cleavage, as described below. Likewise, the

initial oxygen adduct with ferrous heme (the ferric-superoxide intermediate, Figure 2, blue) is proposed to play a key role in P450-catalyzed nitration.⁹ P450 catalytic diversification in nature is thus enabled by the generation of multiple potentially reactive species during the P450 catalytic cycle, as well as the potency of P450-derived oxidants, which can react with substrates in different ways. Though many potential oxidants occur during the cycle, natural P450s are often quite specific in the reactions that they catalyze. Specificity is directed by protein sequences molded by the force and filter of natural selection to favor certain intermediates while tuning their reactivity and selectivity.

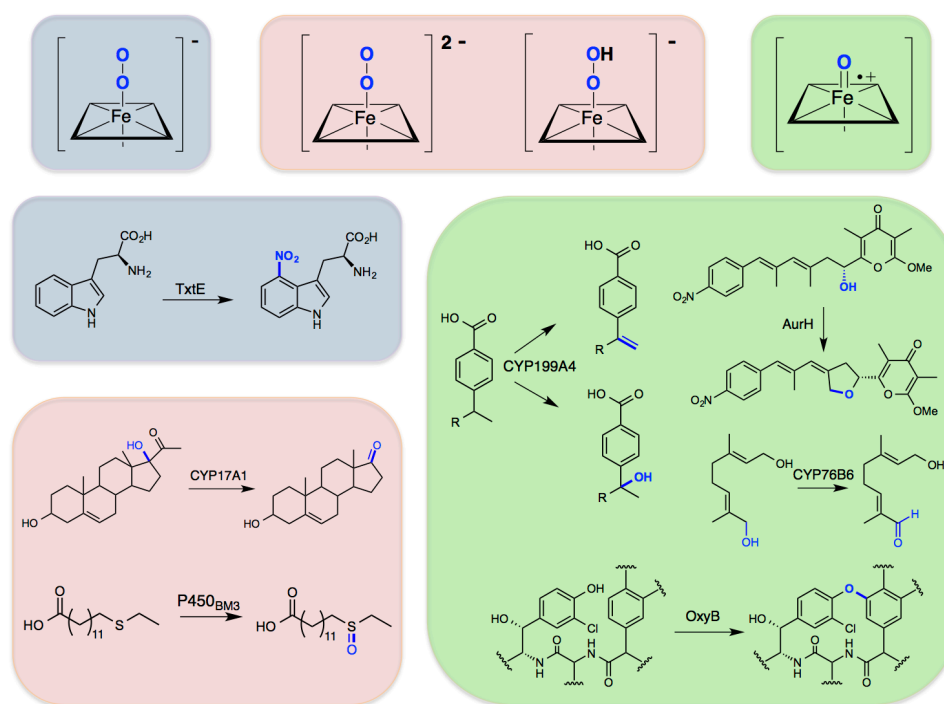


Figure 2. Key catalytic intermediates in the P450 cycle and examples of chemical reactions that rely on them. In blue are highlighted the ferric superoxide intermediate and the nitration reaction that is associated with this intermediate.⁹ In pink are highlighted the iron-peroxo and iron-hydroperoxy intermediates and C–C bond scission¹⁹ and sulfoxidation¹⁴ reactions. Highlighted in green are compound I and desaturation,¹³ ring closure,¹⁰ sequential oxidation,^{12b} and aryl coupling reactions.¹⁶

Beginning with compound I-derived oxidations, one particularly interesting P450-mediated reaction occurs during biosynthesis of the natural product aureothin (Figure 2, green). The P450 enzyme AurH first catalyzes hydroxylation of the aureothin precursor, followed by intramolecular C–O bond formation, to give a tetrahydrofuran ring, with both reactions presumably occurring with the intermediacy of compound I.¹⁰ Hertweck and coworkers have exploited this unusual enzyme to accomplish a biomimetic total synthesis of aureothin, as well as the synthesis of several aureothin derivatives;¹¹ one example^{11c} describes an active site mutation that converts AurH into a six-electron oxidase, leading to the conversion of a substrate methyl group all the way to a carboxylic acid.

Several natural examples of sequential hydroxylations to yield ketones or carboxylates from unactivated C–H bonds have been described recently.¹² For example, in xiamycin biosynthesis, the P450 enzyme XiaM was shown to catalyze sequential hydroxylation of a methyl group to a carboxylate.^{12a} Another example of multiple P450-catalyzed oxidations was published by Höfer et al. in their investigation of the first steps of the biosynthesis of bioactive alkaloids vinblastine and secologanin (Figure 2, green).^{12b}

Though more typical of di-iron monooxygenases and α -ketoglutarate-dependent dioxygenases, desaturation has been observed with a few P450 enzymes.^{6b} An interesting example of P450-catalyzed desaturation was recently reported by Bell et al.¹³ CYP199A4 was previously found to catalyze demethylation of several aromatic compounds, including 4-methoxybenzoic acid and veratric acid, as well as hydroxylation (major product) and desaturation (minor product) of 4-ethylbenzoic acid. In their recent report, these authors found two active site mutations (F185V and F185I) that markedly increase desaturation of

4-ethylbenzoic acid to yield 4-vinylbenzoic acid, with the isoleucine variant giving exclusively the desaturation product (Figure 2, green).

Several examples of P450-catalyzed decarboxylation are associated with biosynthesis and drug metabolism. One biotechnologically interesting P450-catalyzed decarboxylation leads to the synthesis of terminal alkenes from fatty acids.¹⁴ The authors propose a mechanism in which compound I abstracts the β -hydrogen, followed by 1-electron oxidation of the resulting radical to yield a β -carbocation, which spontaneously decarboxylates to give the product.

The above compound I-mediated transformations most likely proceed via hydrogen atom abstraction. Another mechanism by which compound I can mediate oxidation is through sequential 1-electron oxidations. Vancomycin and related antibiotics contain aryl C–C and C–O crosslinks catalyzed by P450-mediated 1-electron oxidations (Figure 2, green). Recent work on the biosynthesis of these antibiotics includes the solution of two crystal structures of P450s involved in aryl coupling reactions,¹⁵ as well as a study that examines the timing of P450-catalyzed crosslinking during vancomycin biosynthesis.¹⁶

Biochemical evidence suggests that the iron-peroxo intermediate can behave as an alternative oxidant in epoxidation and sulfoxidation reactions,⁸ though until recently¹⁷ theoretical studies cast doubt on its role in sulfoxidation.¹⁸ It is generally accepted that the iron-peroxo species is the active oxidant in C–C cleavage reactions.¹⁹ For example, recent work by Kincaid and coworkers supports the role of a substrate-influenced selectivity switch that promotes the stability of the iron-peroxo species, favoring C–C lyase chemistry for certain steroid derivatives (Figure 2, pink).¹⁹

One of the most interesting P450 reactions characterized recently is that of tryptophan nitration in thaxtomin biosynthesis (Figure 2, blue).⁹ Here, neither compound I nor the iron-peroxo intermediate is thought to play the key role. Instead, the initial adduct between ferrous heme and dioxygen, the ferric superoxide intermediate (Figure 1, B), is proposed to react with *in situ* generated nitric oxide to form ferric peroxynitrite. The peroxynitrite species can then decompose via one of two pathways (neither of which has been directly supported so far). In pathway (1), peroxynitrite decomposes homolytically to yield NO_2^\bullet and an iron-ferryl intermediate (compound II). Compound II then performs a 1-electron oxidation of tryptophan, giving a radical which recombines with NO_2^\bullet to give the product. In pathway (2), heterolytic decomposition of the ferric peroxynitrite intermediate gives the ferric-hydroxide resting state and NO_2^+ , which reacts with tryptophan by electrophilic aromatic substitution.

A recently characterized reaction of uncertain mechanism is P450-catalyzed synthesis of alkanes from fatty aldehydes to form insect protective coatings.²⁰ In contrast to other known P450-catalyzed decarboxylation or decarbonylation reactions,¹⁴ the product here is a fully saturated alkane. Although strong evidence that a P450 was responsible for this reaction was first presented in the 1990s,²¹ only recently has the specific P450 enzyme been identified.²⁰

Manipulating conserved features enables non-natural chemistry

The diverse set of naturally occurring P450 reactions has proven a rich source of inspiration for the field of biomimetic oxidation in synthetic chemistry. In an interesting reversal of roles, several classic papers as well as more recent works have shown that P450s can catalyze reactions first discovered by synthetic chemists. Unlike natural P450 reactions, which rely on various reactive oxygen intermediates, these new P450 reactions stem from alternative reactive species created through the use of activated reagents such as diazo compounds and azides. Some of the inspiration for non-natural P450 reactions came from the rich literature on P450 model complexes. Originally synthesized as functional or spectroscopic mimics of P450 enzymes, model P450 complexes (i.e., iron-porphyrins) were later found to catalyze several reactions distinct from oxygen transfers. Breslow and Gelman first demonstrated that iron-tetraphenyl porphyrin model complexes could catalyze intra- and intermolecular nitrene transfers to form benzosultams and substituted cyclohexanes when provided with iminoiodinane nitrene precursors.²² Following up on this, Dawson and coworkers found that rabbit liver P450 enzymes could catalyze low levels (< 5 total turnovers, TTN) of the same reactions that had been described for the synthetic P450 model.²³

More recently, our group demonstrated several new P450 reactions that had previously been shown only for metalloporphyrins. It has been known since the 1990s that iron porphyrins catalyze the reaction of olefins with diazo carbene precursors to yield cyclopropanes²⁴. Metalloporphyrin-catalyzed cyclopropanation is thought to proceed via a metal-carbenoid intermediate, analogous to P450 epoxidations that proceed through compound I. However, it was only recently shown by Coelho et al.²⁵ that this reaction

could be catalyzed at low levels by hemin in water as well as by several heme proteins, including P450_{BM3}, although at levels even lower than free hemin. The selectivities of most of the heme proteins mirrored the *trans*-selectivity of hemin for the cyclopropanation of styrene with ethyl diazoacetate. P450_{BM3} showed very low activity, but in contrast to the other heme proteins produced the cyclopropane product with low but measurable enantioselectivity. Mutations in P450_{BM3}, including at highly conserved residues such as the active site threonine T268, which when mutated to alanine dramatically improved the productivity as well as the diastereo- and enantioselectivity of this reaction (Figure 3A). Although in natural P450s, this conserved active site threonine acts as a proton shuttle, for non-natural chemistry, mutation of T268 to less bulky alanine presumably relieves steric impediments to reactivity, as evidenced by strong alterations in the stereoselectivity of cyclopropanation; future studies may shed light on the effect of this mutation by assaying alternative substitutions at this position. Enzyme engineering could even overcome the natural selectivity of the prosthetic group to achieve >90% *cis* selectivity. And, while free hemin gives a racemic mixture of products, the P450_{BM3} cyclopropanation catalysts exhibited enantioselectivities of up to 97%. In a second publication, Coelho and coworkers demonstrated that mutation of the axial coordinating cysteine, universally conserved among P450s, to serine was highly activating, particularly *in vivo* (*vide infra*).²⁶ The strong effect of axial ligand substitution was attributed in part to the significant increase in reduction potential (>100 mV increase) for the serine-ligated enzyme, facilitating reduction to the active ferrous state. Axial thiolate ligation, absolutely essential for monooxygenation, is unnecessary for this non-natural reaction. Whereas thiolate ligation is important for O–O

bond scission, no such strong electron donation is required to decompose the less-stable diazo substrates employed by Coelho et al.

Another metalloporphyrin reaction shown to be catalyzed by P450s is C–H amination from azides as nitrene sources (Figure 3B).²⁷ The iminoiodinane precursors that Dawson and coworkers had used to obtain low levels of C–H amination with P450s²³ are problematic due to their insolubility in protein-compatible solvents. Thus we tested the more atom-efficient and convenient azide-based nitrene precursors. In spite of the fact that azide-based C–H amination reactions have been found to be markedly less efficient with iron-porphyrins (as compared to cobalt or ruthenium complexes) and require high temperatures and anhydrous conditions,²⁸ we found that wild-type P450_{BM3} could catalyze low levels of intramolecular C–H amination to yield benzosultams.²⁷ As found for cyclopropanation, enzyme engineering could improve the enantioselectivity and activity of the new C–H amination enzymes. Indeed several of the mutations that increased cyclopropanation activity (at the active site threonine and axial cysteine) were found to strongly modulate C–H amination activity, leading to catalysts that were capable of catalyzing several hundred turnovers *in vitro* and roughly double that amount *in vivo*. Here again, mutation to the conserved axial cysteine was highly activating: its positive effect on C–H amination *in vitro* was even greater than that observed for cyclopropanation.

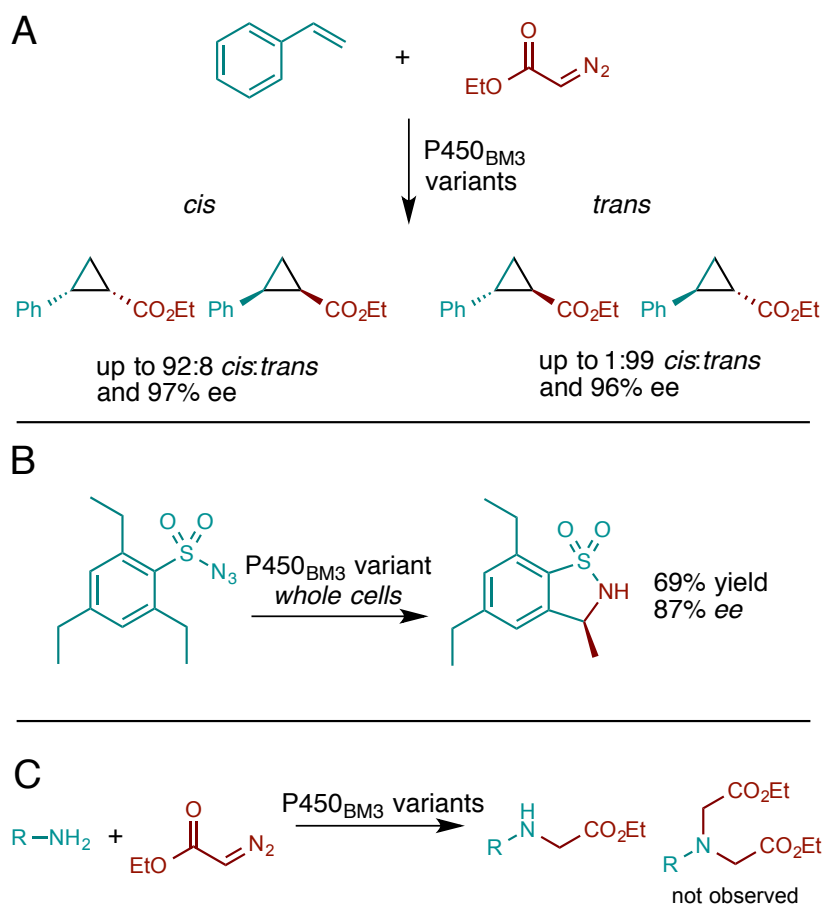


Figure 3. Several recent examples of non-natural P450 reactions: (A) cyclopropanation of styrene catalyzed by P450_{BM3} variants,²⁵ (B) intramolecular C–H amination catalyzed by P450_{BM3} variants expressed in whole cells²⁷ and (C) intermolecular carbene insertion into N–H bonds yielding secondary amines.²⁹

In another approach to P450-catalyzed C–N bond formation, Wang et al. have shown that engineered P450 enzymes can also catalyze carbene N–H insertions.²⁹ The reaction of ethyl diazoacetate with a diverse set of amine acceptors was found to proceed with high turnover numbers. Although many other C–N bond forming methodologies lead to product mixtures via multiple nucleophilic additions, the enzyme-catalyzed N–H insertions gave only the desired secondary amines (Figure 3C). Of note is that free hemin

produces a mixture of secondary and tertiary amines, which emphasizes the important role of the enzyme in regulating substrate access to the reactive center.

An interesting aspect of these new reactions is that both cyclopropanation and C–H amination proceed well in whole cells. P450_{BM3}-derived cyclopropanation catalysts, in particular, were more than six-fold faster when used in whole cells (on a per enzyme basis) and catalyzed more than 60,000 total turnovers under saturating substrate concentrations.²⁶ Thus the enzyme is as good as any transition metal catalyst reported to date. Although NADPH-driven heme reduction *in vitro* requires P450_{BM3}'s reductase domain, in whole cells the reductase was not strictly necessary: even the isolated heme domain could catalyze over 1,000 total turnovers of styrene cyclopropanation. In the reducing environment of anaerobic whole cells, other electron donors apparently can facilitate reduction to the active ferrous state. For C–H amination the effect of carrying out reactions in whole cells was less profound (roughly two-fold higher activity), perhaps due to the higher levels of azide reduction (which competes with C–H amination) in whole cells than *in vitro*.

A simplifying feature of enzyme-catalyzed carbene and nitrene transfers is the enzyme's decreased dependence on the reductase domain for activity. For C–H amination and carbene transfers, although initial reduction to ferrous heme is necessary, after bond formation the heme is returned to the active ferrous state, thus eliminating the need for stoichiometric NADPH. Decreased dependence on the reductase may also prove to be problematic, as it may lead to the generation of reactive carbon or nitrogen species in the absence of substrate, which for stronger electrophiles may lead to heme or protein destruction.

An interesting lesson from these efforts to generate enzymes for whole new reactions is that conserved residues whose function was highly specific to the chemistry catalyzed by the natural enzyme became particularly important for tuning the new activities. The active site threonine, which normally helps to catalyze O–O bond scission via protonation, and the axial coordinating cysteine, whose importance in oxygenation reactions is profound,^{7c} can both be substituted to greatly increase activity for C–H amination and cyclopropanation (and abolish monooxygenase activity). Many other protein residues contribute to oxygen activation in P450s, and it is likely that at least some can be mutated to further enhance non-natural reactivity. As observed with natural P450 enzymes, enhancing the reactivity of enzyme-carbenoid and nitrenoid intermediates may facilitate an expanded catalytic scope for these new chemistries.

Conclusions

What information can be gleaned from the diverse natural and non-natural chemistry catalyzed by P450 enzymes that might inform other efforts to genetically encode new reactions? As noted above, much of the natural diversity of P450 chemistry is driven by the reactive nature of oxygen activation intermediates. In this vein, it is worth noting that many other natural enzymes are capable of generating highly reactive species, such as other oxygenase enzymes (di-iron monooxygenases, Rieske monooxygenases, etc.), radical SAM enzymes, and adenosylcobalamin-dependent enzymes, among others.³⁰ Although they may prove more difficult to engineer than P450s, these enzymes should not be overlooked in the search for new biocatalytic transformations.

For recent non-natural P450 chemistry, the reactive intermediates are derived from the reaction of enzyme with synthetic reagents. That these reactions do not require the sophisticated P450 catalytic cycle with its well-timed reductions and bond cleavages can be attributed to the activated nature of the reagents, which undergo relatively facile decomposition to yield reactive carbon and nitrogen species. Exploring the reactions of synthetic reagents with natural enzymes has proven fruitful for finding new genetically encoded catalysts in other contexts³¹ and is likely to bring more synthetic chemistry into biology. While the reactivity of a free prosthetic group is not necessarily predictive of activity within an enzyme, for each reaction type we explored thus far,^{25,26-27,29} free heme was found to give at least some basal activity with most (though not all) substrates under the assay conditions. Thus investigations of metal/cofactor-reagent pairs may yield useful starting points for identifying possible new enzyme reactivities. Of course, what is different from past efforts²³ is the availability of enzyme engineering tools such as directed evolution, which can reliably improve even very low activities, especially when the activities are exhibited by an (evolvable) enzyme rather than some other protein framework.

Although non-natural chemistries that rely on synthetic reagents may be challenging to employ within cellular biosynthetic pathways, a great deal of useful biocatalysis is conducted *in vitro*³² where access to the synthetic reagent is not a problem. Current efforts to develop biosynthesis in cell-free extracts³³ could allow for relatively straightforward integration of non-natural prosthetic groups and reagents in biosynthetic pathways. Thus, working within the constraints of biology may ultimately prove unnecessary—even for enzyme engineers.

References

- (1) Keasling, J. D.; Mendoza, A.; Baran, P. S. *Nature* **2012**, 492, 188.
- (2) (a) Rothlisberger, D. *et al. Nature* **2008**, 453, 190; (b) Siegel, J. B. *et al. Science* **2010**, 329, 309.
- (3) Gerlt, J. A.; Babbitt, P. C. *Curr Opin Chem Biol* **2009**, 13, 10.
- (4) Glasner, M. E.; Gerlt, J. A.; Babbitt, P. C. *Curr Opin Chem Biol* **2006**, 10, 492.
- (5) Dellus-Gur, E. *et al. J Mol Biol* **2013**, 425, 2609.
- (6) (a) Guengerich, F. P.; Munro, A. W. *J. Biol. Chem.* **2013**, 288, 17065; (b) Guengerich, F. P. *Chem Res Toxicol* **2001**, 14, 611; (c) Podust, L. M.; Sherman, D. H. *Nat. Prod. Rep.* **2012**, 29, 1251.
- (7) (a) Whitehouse, C. J.; Bell, S. G.; Wong, L. L. *Chem. Soc. Rev.* **2012**, 41, 1218; (b) Krest, C. M. *et al. J Biol Chem* **2013**, 288, 17074; (c) Green, M. T. *Curr. Opin. Chem. Biol.* **2009**, 13, 84; (d) Fasan, R. *ACS Catal.* **2012**, 2, 647.
- (8) (a) De Voss, J. J.; Cryle, M. J. *Angew. Chem. Int. Ed. Engl.* **2006**, 45, 8221; (b) Jin, S. *et al. J. Am. Chem. Soc.* **2003**, 125, 3406.
- (9) Barry, S. M. *et al. Nat. Chem. Biol.* **2012**, 8, 814.
- (10) He, J.; Muller, M.; Hertweck, C. *J Am Chem Soc* **2004**, 126, 16742.
- (11) (a) Henrot, M. *et al. Angew Chem Int Ed Engl* **2012**, 51, 9587; (b) Richter, M. *et al. ChemBioChem* **2012**, 13, 2196; (c) Zocher, G. *et al. J Am Chem Soc* **2011**, 133, 2292.
- (12) (a) Zhang, Q. *et al. Org Lett* **2012**, 14, 6142; (b) Hofer, R. *et al. Metab Eng* **2013**.
- (13) Bell, S. G. *et al. Chemistry* **2012**, 18, 16677.
- (14) Rude, M. A. *et al. Appl Environ Microbiol* **2011**, 77, 1718.
- (15) (a) Li, Z. *et al. Proteins* **2011**, 79, 1728; (b) Cryle, M. J.; Staaden, J.; Schlichting, I. *Archives of Biochemistry and Biophysics* **2011**, 507, 163.
- (16) Schmartz, P. C. *et al. Angew Chem Int Ed Engl* **2012**, 51, 11468.
- (17) Wang, B. *et al. J. Chem. Theory Comput.* **2013**, 9, 2519.
- (18) Li, C. *et al. Angew Chem Int Ed Engl* **2007**, 46, 8168.
- (19) Gregory, M. *et al. Angew. Chem. Int. Ed. Engl.* **2013**, 52, 5342.
- (20) Qiu, Y. *et al. Proc. Natl. Acad. Sci. USA* **2012**, 109, 14858.
- (21) Reed, J. R. *et al. Proc Natl Acad Sci U S A* **1994**, 91, 10000.
- (22) Breslow, R.; Gellman, S. H. *J. Chem. Soc. Chem. Commun.* **1982**, 1400.
- (23) Svastis, E. W. *et al. J. Am. Chem. Soc.* **1985**, 107, 6427.
- (24) Wolf, J. R. *et al. J. Am. Chem. Soc.* **1995**, 117, 9194.
- (25) Coelho, P. S. *et al. Science* **2013**, 339, 307.
- (26) Coelho, P. S. *et al. Nat. Chem. Biol.* **2013**, 9, 485.
- (27) McIntosh, J. A. *et al. Angew. Chem. Int. Ed. Engl.* **2013**, 52, 9309.
- (28) Ruppel, J. V.; Kamble, R. M.; Zhang, X. P. *Org. Lett.* **2007**, 9, 4889.
- (29) Wang, Z. J. *et al. Submitted* **2013**.
- (30) Lewis, J. C.; Coelho, P. S.; Arnold, F. H. *Chem Soc Rev* **2011**, 40, 2003.
- (31) (a) Muller, A. *et al. Angew Chem Int Ed Engl* **2007**, 46, 3316; (b) Hasnaoui-Dijoux, G. *et al. ChemBioChem* **2008**, 9, 1048; (c) Savile, C. K.; Magloire, V. P.; Kazlauskas, R. J. *J. Am. Chem. Soc.* **2005**, 127, 2104.
- (32) Huisman, G. W.; Collier, S. J. *Curr Opin Chem Biol* **2013**, 17, 284.

- (33) Harris, D. C.; Jewett, M. C. *Curr Opin Biotechnol* **2012**, 23, 672.

*Chapter 2*ENANTIOSELECTIVE INTRAMOLECULAR C–H AMINATION CATALYZED BY
ENGINEERED CYTOCHROME P450_{BM3} ENZYMES

This chapter is published as J. A. McIntosh, P. S. Coelho, C. C. Farwell, Z. J. Wang, J. C. Lewis, T. R. Brown F. H. Arnold “Enantioselective Intramolecular C–H Amination Catalyzed by Engineered Cytochrome P450 Enzymes *in vitro* and *in vivo*.” in *Angewandte Chemie Int. Ed.* 2013, 52, 9309-9312. I contributed to all characterization of enzymes, including protein expression and purification, *in vitro* and *in vivo* reactions, and quantification of all enzyme reaction products. J.A.M., P.S.C., Z.J.W., and T.R.B. performed chemical syntheses and characterization of standards.

Abstract

The ease with which cytochrome P450 enzymes can install oxygen atoms within otherwise unreactive chemical structures has fascinated scientists from all branches of chemistry. Although many studies have examined the use of protein engineering to modify the substrate specificity of these enzymes, few studies have examined the possibility of catalyzing entirely unnatural reactions with P450s. Here, inspired by innovative work in synthetic porphyrin chemistry, we show that engineered variants of P450 BM3 catalyze C–H amination upon reaction with arylsulfonyl azides. Wild-type BM3 enzyme exhibits some activity, but it is greatly enhanced by the mutation of two residues that are highly conserved within P450s, demonstrating a strong ‘tuning’ effect of enzyme residues on the efficiency of the reaction. These new nitrene-insertion enzymes are also highly active *in vivo* in *E. coli* cells, where they catalyze several hundreds of turnovers.

Main Text

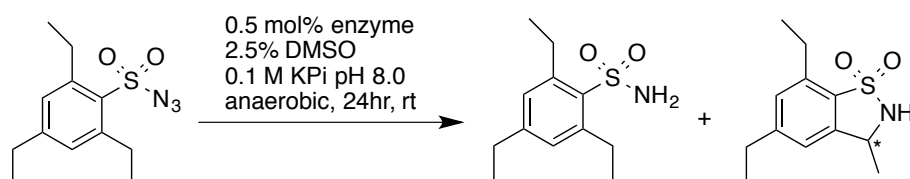
Iron containing monooxygenases play diverse roles in nature, ranging from the primary metabolic functions of alkane hydroxylases to the xenobiotic detoxification and secondary metabolic roles of cytochrome P450 enzymes.¹ Common to these enzymes is the ability to reductively activate molecular oxygen to generate highly electrophilic oxygen species, whose reactivity is comparable with that of ‘oxenes’ (oxygen atoms containing six-valence electrons).² P450 enzymes in particular possess the remarkable ability to insert oxygen atoms at virtually any position within otherwise unreactive carbon skeletons, leading to the synthesis of alcohols or epoxides in diverse natural products.

Whereas enzymes are capable of inserting oxygen atoms into even unactivated C–H bonds, the sites into which nitrogen can be incorporated are more constrained. Transaminases, ammonia lyases, and amino acid dehydrogenases, for example,³ target oxidized or otherwise chemically activated carbons for reaction. Enzymes that catalyze the concerted oxidative amination of C–H bonds are apparently absent from nature's repertoire of chemical catalysts.

Synthetic chemists, who are not limited to biologically accessible reagents and metals, have developed highly useful methods for the oxidative formation of C–N bonds.⁴ These C–H amination reactions often proceed through a nitrenoid intermediate that has no parallel in natural enzymes. Although these reactions do not require preoxidized or otherwise activated carbon atoms, they do require specialized nitrene-precursors such as azides, haloamines, or iminoiodinanes. Of the many transition-metal catalysts based on Rh, Ru, Mn, Co, and Fe that catalyze intra- and intermolecular C–H amination, we were especially interested in the metal-porphyrin systems,⁵ which react

with iminoiodinanes in the +3 oxidation state to catalyze nitrene transfers that are isoelectronic with the well-established formal oxene transfer reaction of ferric-P450 enzymes with iodosylbenzene.^{5a,6} Trace levels (3 total turnovers; TTNs) of intramolecular C–H amination were reported more than 25 years ago for mammalian cytochrome P450 preparations reacting with iminoiodinanes.⁷ We decided to revisit the possibility of finding or engineering an enzyme catalyst for this useful and challenging transformation.

Iminoiodinanes, however, are problematic for biocatalytic application, given their polymeric nature⁸ and insolubility⁹ in aqueous media. As an alternative to iminoiodinanes, we decided to focus on the synthetic reaction of sulfonylazides with reduced (+2 oxidation state) metal porphyrins.¹⁰ We reasoned that such a "chemomimetic" approach to achieving direct C–H to C–N conversion could provide a biocatalytic route to amines and amides using biochemically compatible and atom-efficient azide-based nitrene precursors, with the usual enzyme advantages of selectivity and mild reaction conditions. Here we report the first highly active enzyme catalysts of C–H amination.



Scheme 1. Initial reaction screening substrate and products

In initial experiments, we tested a panel of 24 purified cytochrome P450_{BM3} variants developed for monooxygenation reactions. Enzymes were reacted with 2,4,6-triethylbenzene-1-sulfonylazide (**1**) under anaerobic, reducing conditions at an enzyme loading of 0.5 mol% in aqueous media (phosphate buffer, 2.5% v/v DMSO). Most reactions gave sulfonamide **2** as the major product, though all of the tested enzymes, including wild-type (4 TTN), yielded small amounts of the C–H amination product, **3**. The most active enzyme for C–H amination in the initial screen contained only a single mutation (T268A) relative to wild-type P450_{BM3}. The T268A mutation was recently shown to promote P450_{BM3}-catalyzed carbene transfers yielding cyclopropanes.¹¹ Thus, in spite of the significant differences between carbene and nitrene chemistry, we proceeded to test several P450_{BM3}-based cyclopropanation catalysts, including several serine-heme ligated ‘P411’¹² enzymes (so called because the Soret peak in the ferrous CO-bound spectrum is shifted to 411 nm rather than 450 nm for cysteine ligated enzymes) in which the axial coordinating cysteine C400, absolutely required for monooxygenation activity, is mutated to serine. The most active enzyme here was the serine-heme ligated P411_{BM3}-CIS (14 mutations from wild-type), which also contained the T268A mutation and supported over 140 total turnovers (73% yield of **3** by HPLC). Variant P450_{BM3}-CIS, which lacks the C400S mutation at the axial heme ligand, was significantly less active (9 TTN), indicating that serine-heme ligation strongly enhances BM3-catalyzed C–H amination. The P450_{BM3}-C400S single mutant (P411_{BM3}) also exhibited markedly improved activity (49 TTN) relative to its cysteine-ligated counterpart, P450_{BM3} (4 TTN). To clarify the roles of the T268A and C400S mutations in BM3-catalyzed amination, we performed further experiments at 0.1 mol% catalyst

loading with the P450_{BM3}-T268A and P411_{BM3} single mutants as well as the T268A/C400S double mutant in reaction with sulfonyl azide **1** (Table 1). We found that the T268A and C400S mutations combined to yield a highly active enzyme (120 TTN for the double mutant versus 310 TTN for P411_{BM3}-CIS, Table 1), indicating that the T268A and C400S mutations were major contributors to the high activity of P411_{BM3}-CIS. In fact, reverting the T268A mutation in P411_{BM3}-CIS markedly reduced activity (82 TTN).

Table 1. Comparison of activities (TTN) and enantioselectivities of purified P450 and P411 variants (0.1 mol % catalyst loading) for the reaction of azide **1** to sulfonamide **2** and sultam **3**.

<i>In vitro</i> catalyst	TTN ^a	% <i>ee</i> ^b
P450 _{BM3}	2.1	n.d.
P450 _{BM3} -T268A	15	36
P411 _{BM3}	32	20
P411 _{BM3} -T268A	120	58
P411 _{BM3} -CIS	310	67
P411 _{BM3} -CIS-A268T	82	47
P411 _{BM3} -CIS-T438S	383	73

^a TTN = total turnover number. ^b (*S*-*R*)/(*S*+*R*). n.d. = not determined. Reaction conditions described in the supplementary materials. TTNs and enantioselectivities determined by HPLC analysis.

Control experiments revealed that the enzyme-catalyzed reaction was inhibited by carbon monoxide, air, and heat denaturation of the enzyme, all of which suggests that catalysis occurs at the enzyme-bound heme (Table S2). Hemin also was capable of catalyzing this reaction when reduced with dithionite (Figure 1). However, whereas enzyme reactions with prochiral substrate **1** resulted in asymmetric induction (up to 67% *ee*, Table 1), reaction with hemin unsurprisingly yielded only racemic **3**, strongly

suggesting that BM3-catalyzed amination occurs within the chiral environment of the enzyme active site. Addition of sub-stoichiometric amounts of NADPH was sufficient for activity (Table S3), supporting the hypothesis that ferrous-heme is the azide-reactive state, akin to P450-catalyzed cyclopropanation.¹¹ Dithionite could be used in place of NADPH to drive catalysis, where its effect was comparable to that of NADPH for both cysteine- and serine-ligated enzymes P450_{BM3}-T268A and P411_{BM3}-T268A (Table S4), indicating that reduction to ferrous heme was not limiting.

To examine the effect of C–H bond strength on amination activity, P411_{BM3}-CIS and P411_{BM3}-T268A were reacted with the trimethyl and triisopropyl analogs of **1** (substrates **4** and **6**, respectively). The desired benzosultam products were obtained, though the productivity was lower with both substrates (Figure 1). Free hemin activity was inversely correlated with the substrate C–H bond strength, showing no measurable activity on substrate **4**, minimal activity on substrate **1** (3 TTN), and the highest activity on substrate **6** (55 TTN). The differing patterns of activity observed with hemin and enzyme-catalyzed reactions suggest that the enzyme itself plays a critical role in catalyzing C–H bond formation beyond providing a chiral active site that guides the stereochemical outcome of the reaction. In particular, enzyme reactions with triethyl and trimethyl sulfonylazide substrates **1** and **4** were markedly more productive than the corresponding hemin reactions. The reduced activity of the enzyme toward triisopropyl substrate **6** suggests that the active site structure currently favors smaller substrates, though it is likely that this can be modulated by further enzyme engineering.

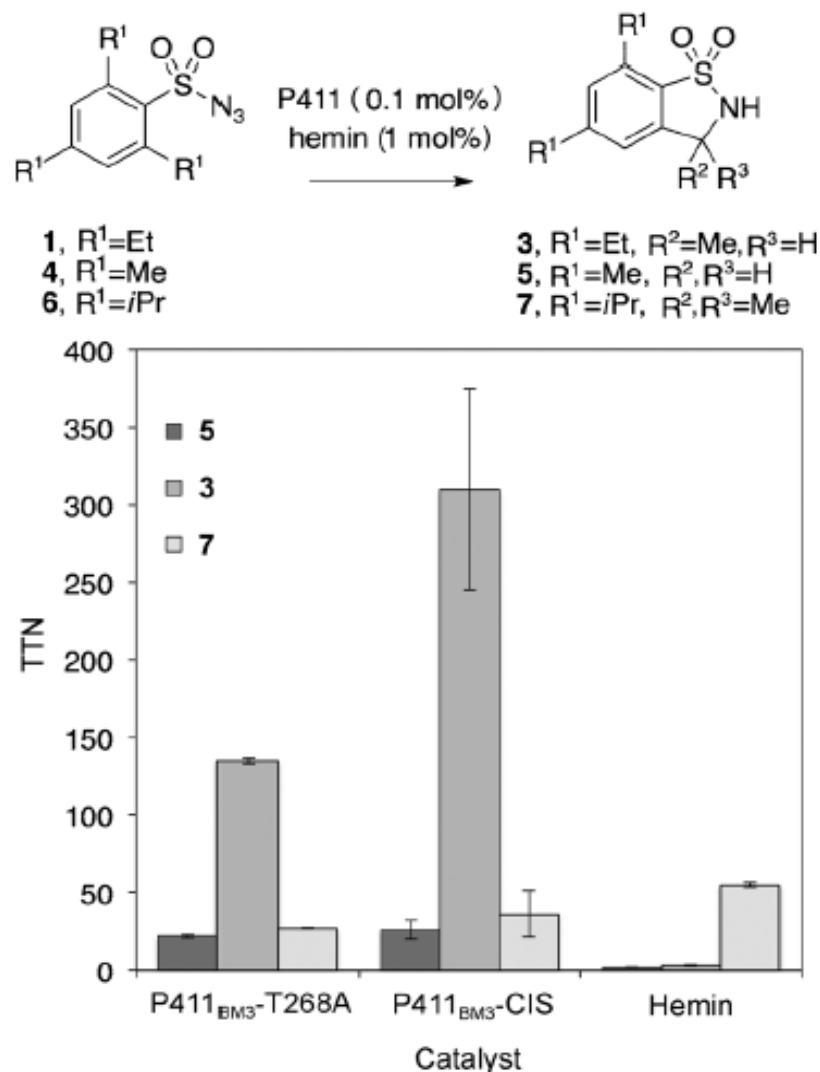


Figure 1. Substrate selectivity of P411 enzymes compared with free hemin. Compounds used to test the dependence of amination activity on C–H bond strength in reaction catalyzed by enzyme (0.1 mol%) or hemin (1 mol%) are shown. Reaction conditions are described in the Supporting Information.

To determine whether this new reactivity could be exploited *in vivo*, we next investigated whether these enzymes expressed in intact *E. coli* cells could catalyze amination reactions when provided with azide substrate. Remarkably, both the P411_{BM3}-T268A and P411_{BM3}-CIS enzymes were highly active on **1**, catalyzing hundreds of

turnovers (245 TTN, 89% *ee* P411_{BM3}-T268A, 680 TTN, 60% *ee* P411_{BM3}-CIS) under anaerobic conditions with added glucose (Tables 2, S4).

Table 2. Comparison of C–H amination activities (TTN) of intact *E. coli* cells expressing P450 and P411 variants

<i>In vivo</i> catalyst	[Enzyme] (μM)	% Yield 3	TTN ^a	% <i>ee</i> ^b
pCWori-empty	0	0	0	n.d.
P450 _{BM3}	6.6	0.5	5.1	n.d.
P450 _{BM3} -T268A	5.8	7.8	26	84
P411 _{BM3}	4.3	6.7	29	16
P411 _{BM3} -T268A	2.2	30	250	89
P411 _{BM3} -CIS	1.4	46	680	60
P411 _{BM3} -CIS-T438S	2.7	58	430	87

^a TTN = total turnover number. ^b (*S*-*R*)/(*S*+*R*). n.d. = not determined. Reaction conditions described in Supporting Information.

Lyophilized cells containing P411_{BM3}-CIS could also support catalysis, with productivity similar to freshly-prepared cell suspensions (750 TTN, 61% *ee*). Enantioselectivity was comparable or enhanced for whole-cell catalysts relative to purified enzymes (Table 2). Including the previously characterized T438S mutation in P411_{BM3}-CIS strongly increased enantioselectivity (430 TTN, 86% *ee*).^{11,13} Optimization of expression conditions increased the productivity of whole-cell C–H amination catalysts, enabling conversions of nearly 70% in small-scale reactions (Table S6). Inspired by the simplicity of employing whole cells as amination catalysts, we performed a preparative scale reaction (50 mg) using anaerobic resting cells expressing the P411_{BM3}-CIS-T438S catalyst, affording sultam **3** (77% yield by HPLC, 69% isolated yield, 87% *ee*).

The beneficial effects of the T268A and C400S mutations for C–H amination is striking in that both residues play critical roles in P450-catalyzed monooxygenation.¹⁴ While important for protonation of iron-peroxo intermediates that occur during dioxygen activation, T268 may sterically hinder binding of bulkier azide substrates in C–H amination. Consistent with a steric role, the T268A mutation enhances the stereoselectivity of C–H amination; it also strongly impacts diastereo and enantioselectivity of styrene cyclopropanation.¹¹ The C400S mutation is not necessary for dithionite-driven *in vitro* cyclopropanation, and its strong effect *in vivo* can be attributed to the higher reduction potential of the serine-ligated heme, which facilitates reduction by NADPH.¹² In contrast, here we find that the C400S mutation is absolutely necessary for high levels of *in vitro* amination activity (Table 1). This effect persists even when dithionite is used as a reductant (Table S4), suggesting that the C400S mutation does not simply facilitate NADPH-driven reduction to the active ferrous state, but rather exerts a strong effect on subsequent steps of the reaction. That mutations to both T268 and C400 appear necessary for enzymatic C–H amination suggests that naturally occurring P450s, in which these two residues are highly conserved, will likely be poor catalysts of C–H amination.

Many enzyme-catalyzed reactions, such as ketoreduction, monooxygenation, and transamination, are increasingly useful in chemical synthesis,¹⁵ and applications of these and other naturally-occurring reaction types will continue to develop. However, it is no longer necessary to limit biocatalysis to reactions that have natural antecedents.^{11,16} Rather, the scope of biocatalysis can be expanded by directing natural enzymes to imitate

the artificial, accessing whole new chemistries by judicious choice of reaction conditions, synthetic reagents, and protein engineering.

Supplementary Materials for

Enantioselective Intramolecular C–H Amination Catalyzed by Engineered Cytochrome P450 Enzymes

Contents	Page
1. Materials and Methods	32
2. Confirmation of Enzymatic Activity	34
3. Reaction Optimization and Conditions	36
4. Synthetic Procedures	41
5. Assignment of Absolute Configuration	43

1. Materials and Methods

General. Unless otherwise noted, all chemicals and reagents for chemical reactions were obtained from commercial suppliers (Sigma-Aldrich, Acros) and used without further purification. Silica gel chromatography purifications were carried out using AMD Silica Gel 60, 230-400 mesh. ^1H and ^{13}C NMR spectra were recorded on either Varian Inova 500 MHz or 600 MHz instruments in CDCl_3 , and are internally referenced to residual solvent peak. Optical rotation values were measured on a Jasco J-2000 polarimeter. Reactions were monitored using thin layer chromatography (Merck 60 silica gel plates) using an UV-lamp for visualization or stains where indicated.

Analytical high-performance liquid chromatography (HPLC) was carried out using an Agilent 1200 series, an UV detector, and a Kromasil 100 C18 column (Peeke Scientific, 4.6 x 50 mm, 5 μm). Semi-preparative HPLC was performed using an Agilent XDB-C18 (9.4 x 250 mm, 5 μm). Analytical chiral HPLC used a Chiralpak AD-H column (Daicel, 4.6 x 150), while preparative chiral HPLC used a Chiralpak AD-H column (Daicel, 21 x 250 mm, 5 μm). Azides **1** and **4**, and benzosultam standards **3**, **5**, and **7** were prepared as reported.¹⁷ Azide **7** is commercially available (Sigma, 723045-1G). These standards were used in co-injection experiments to determine the authenticity of benzosultams. Enzymatically-produced benzosultam **3** was prepared as described below and was characterized by NMR (^1H and ^{13}C).

pCWori was used as a cloning and expression vector for all enzymes described in this study. Site-directed mutagenesis of P411_{BM3}-CIS to yield P411_{BM3}-CIS-A268T was performed via overlap extension PCR, followed by digestion of vector and PCR products with BamHI and SacI. The PCR products were gel purified and ligated into digested

pCWori using T4 ligase (NEB, Quickligase). Primer and vector sequences available upon request.

Determination of P450/P411 concentration. Concentration of P450 or P411 enzymes was determined from ferrous carbon monoxide binding difference spectra using previously reported extinction coefficients for cysteine-ligated ($\epsilon = 91,000 \text{ M}^{-1} \text{ cm}^{-1}$) and serine-ligated enzymes ($\epsilon = 103,000 \text{ M}^{-1} \text{ cm}^{-1}$).¹⁸

Table S1. Mutations (relative to wild-type P450_{BM3}) in enzymes used in this study.

Enzyme	Mutations relative to wild-type P450 _{BM3}
P450 _{BM3}	none
P450 _{BM3} -T268A	T268A
P411 _{BM3}	C400S
P411 _{BM3} -T268A	T268A, C400S
P450 _{BM3} -CIS	V78A, F87V, P142S, T175I, A184V, S226R, H236Q, E252G, T268A, A290V, L353V, I366V, E442K
P411 _{BM3} -CIS	BM3-CIS C400S
P411 _{BM3} -CIS-A268T	BM3-CIS A268T, C400S

Protein expression and purification. Enzymes used in purified protein experiments were expressed from *E. coli* cultures transformed with plasmid encoding P450 or P411 variants. BL21(DE3) was used for expression of P411_{BM3}-CIS, while DH5 α was used as an expression host for all other enzymes. Expression and purification was performed as described elsewhere,¹⁹ with the exception that the agitation rate was lowered to 150 RPM for P411 after induction. Following expression, cells were pelleted and frozen at -20 °C. For purification, frozen cells were resuspended in lysis buffer (25 mM tris pH 7.5, 4 mL/g

of cell wet weight) and disrupted by sonication (2 x 1 min, output control 5, 50% duty cycle; Sonicator 3000, Misonix, Inc.). To pellet insoluble material, lysates were centrifuged at 24,000xg for 0.5 h at 4 °C. Cleared lysates were then purified on a Q Sepharose column (5 mL HiTrap™ Q HP, GE Healthcare, Piscataway, NJ) using an AKTApurifier FPLC system (GE healthcare). P450 or P411 enzymes were then eluted on a linear gradient from 100% buffer A (25 mM tris pH 8.0), 0% buffer B (25 mM tris pH 8.0, 1 M NaCl) to 50% buffer A/50% buffer B over 10 column volumes (P450/P411 enzymes elute at around 0.35 M NaCl). Fractions containing P450 or P411 enzymes were pooled, concentrated, and subjected to three exchanges of phosphate buffer (0.1 M KPi pH 8.0) to remove excess salt. Enzyme concentrations were determined by CO binding difference spectra as described above. Concentrated proteins were aliquoted, flash-frozen on powdered dry ice, and stored at -20 °C until later use.

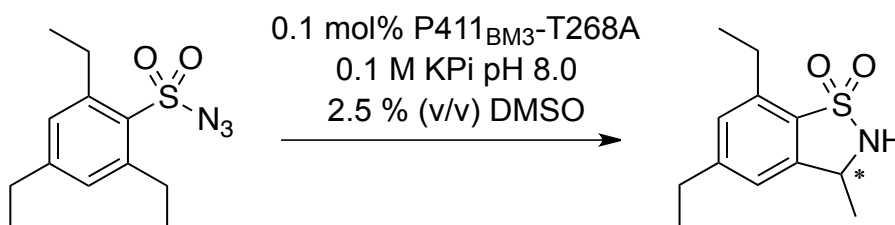
2. Confirmation of Enzymatic Activity

Controls to confirm the enzymatic amination activity of variant P411_{BM3}-T268A.

Small-scale reactions (400 µL total volume) were set up and worked up as described above. Control reactions were performed with both the holoenzyme (BM3 with covalently linked reductase domain) and the isolated heme domain. Reactions denoted by complete system (CS) indicate holo enzyme with reaction conditions as displayed in the scheme below. Reactions of the complete system with heme domain (CS heme) included 2 mM Na₂S₂O₄ rather than NADPH unless otherwise indicated in Table S2. Carbon monoxide (CO) inhibited and heat-denatured enzyme controls were performed as previously described.¹¹ Buffer for the CO controls was supplemented with 2 mM Na₂S₂O₄ in both holoenzyme and

heme domain experiments. For the hemin experiment, 0.8 mL of a hemin solution (1 mM in 50% DMSO-H₂O) was added to a final concentration of 2 mM to afford a direct comparison with the enzyme reactions. TTNs and enantioselectivities were determined as described above.

Table S2. Controls experiments for variant P411_{BM3}-T268A. Conditions are as described in the supporting methods. Reactions denoted by complete system (CS) indicate holo enzyme with reaction conditions as displayed in the above scheme. Reactions of the complete system with heme domain (CS heme) included 2 mM Na₂S₂O₄ rather than NADPH unless otherwise indicated in the table.



Conditions	TTN	% activity ^a	% ee [*]
Complete system (CS)	110	-	38
CS-NADPH+ Na ₂ S ₂ O ₄	130	120	44
CS+CO	5	4.4	-
Boiled P450 _{holo}	33	30	1
CS aerobic	10	9.1	60
CS-P450	0	0	-
CS heme-Na ₂ S ₂ O ₄ +NADPH	4	3.6	-
CS heme	160	145	91
CS heme + CO	0	0	-
Boiled P450 _{heme}	10	9.1	3
CS heme aerobic	0	0	-
CS-P450+Hemin	0	0	-

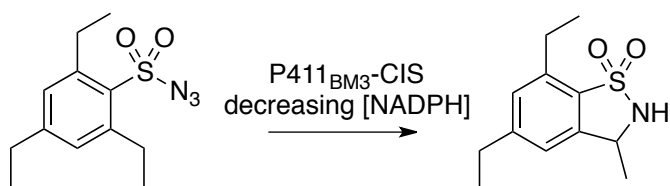
^aPercent residual activity (CS = 100%). ^{*}%ee=(S-R)/(S+R)

3. Reaction Optimization and Conditions

Typical procedure for small-scale amination bioconversions under anaerobic conditions using purified enzymes. Small-scale reactions (400 μ L) were conducted in 2 mL crimp vials (Agilent Technologies, San Diego, CA) containing buffer (0.1 M potassium phosphate pH 8.0), enzyme (0.1-0.5% catalyst loading), and oxygen depletion mixture (10X stock solution containing 14,000 U/mL catalase, 1,000 U/mL glucose oxidase dissolved in 0.1 M KPi pH 8.0). Enzyme (P450 or P411) and oxygen depletion mixture were added to the vial with a small stir bar before crimp-sealing. Portions of phosphate buffer (190 μ L, 0.1 M, pH = 8.0), glucose (40 μ L, 250 mM) and NADPH (40 μ L, 20 mM), or multiples thereof, were combined in a larger crimp sealed vial and degassed by sparging with argon for at least 5 min. In the meantime, the headspace of the sealed 2 mL reaction vial with the P450 solution was made anaerobic by flushing argon over the protein solution (with no bubbling). The buffer/reductant/glucose solution (270 μ L) was syringed into the reaction vial with continuous argon purge of the vial headspace. An arylsulfonyl azide solution in DMSO (10 μ L, 80 mM) was added to the reaction vial via a glass syringe, and the reaction was left stirring for 24 h at room temperature under positive argon pressure. Final concentrations of the reagents were typically: 2 mM arylsulfonyl azide, 2 mM NADPH, 25 mM glucose, 2 or 10 μ M P450. Reactions were quenched by adding 30 μ L 3 M HCl under argon. To the vials were then added acetonitrile (430 μ L) and internal standard (*o*-toluenesulfonamide 10 mM in 50% acetonitrile 50% water, 1 mM final concentration). This mixture was then transferred to a microcentrifuge tube, and centrifuged at 17,000xg for 10 minutes. A portion (20 μ L) of the supernatant was then analyzed by HPLC. For LC-MS analysis, the quenched reaction mixture was extracted

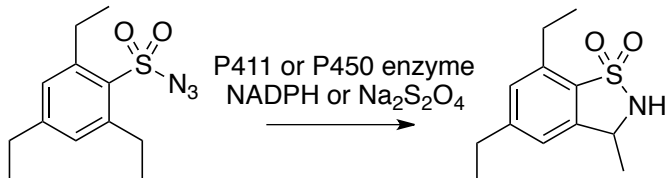
twice with ethyl acetate (2 x 350 μ L), dried under a light argon stream, and resuspended in 50% water-acetonitrile (100 μ L). For chiral HPLC the reactions were extracted as above with ethyl acetate, dried and resuspended in DMSO (100 μ L), and then C18 purified as described above. The C18 purified material was dried, and resuspended in acetonitrile, and then injected onto the chiral HPLC system for analysis. Sultam formation was quantified by comparison of integrated peak areas of internal standard and sultam at 220 nm to a calibration curve made using synthetically produced sultam and internal standard.

Table S3: Dependence of holoenzyme activity on NADPH concentration. Small-scale reactions (400 μ L) were assembled and worked up as described above. NADPH concentration was varied within the concentration range of sultam product formation to assess stoichiometry of iron reduction in the enzyme-catalyzed reactions. The P411_{BM3}-CIS enzyme was used at 0.2 mol % loading (4 μ M) relative to azide substrate **1** (2 mM) with indicated reductant concentration, 0.1 M KPi pH 8.0, and 2.5 % (v/v) DMSO co-solvent.



[NADPH] (mM)	[sultam] (mM)
2.0	0.322
0.1	0.486
0.02	0.164
0.01	0.053
0	0

Table S4: Comparison of NADPH and dithionite in reaction of P450_{BM3}-T268A and P411_{BM3}-T268A with azide 1. Small scale reactions containing either NADPH (2 mM) or dithionite (2 mM) as reductant, enzymes were used at 0.1 mol% loading (2 μ M) relative to azide substrate **1** (2 mM) 0.1 M KPi pH 8.0, 2.5 % DMSO co-solvent. Enzyme activities are given in TTNs.



P411 or P450 enzyme
NADPH or Na₂S₂O₄

Catalyst	Product TTN	
	Dithionite	NADPH
P450 _{BM3} -T268A	25	22
P411 _{BM3} -T268A	110	110

Typical procedure for small-scale amination bioconversions under anaerobic conditions using whole cells. *E. coli* BL21(DE3) cells containing P450 or P411 enzymes were expressed and prepared as described elsewhere.¹² Following expression, cells were resuspended to an OD600 of 30 in M9 salts lacking NH₄Cl (M9-N), and then degassed by sparging with argon in a sealed 6 mL crimp vial for at least 0.5 h. Separately, glucose (250 mM dissolved in 1X M9-N, 40 μ L, or multiples thereof) was degassed by sparging with argon for at least 5 minutes. The oxygen quenching mixture was added to sealed 2 mL crimp vials containing stir bars and the headspace of the vials was purged with argon for 5 minutes, at which time glucose, and then cells were added by syringe. Substrate (80 mM arylsulfonyl azide, 10 μ L in DMSO) was added via syringe, and the reactions were stirred at room temperature for 24 h under positive argon pressure. Reactions were quenched in a manner identical to reactions containing purified enzymes, as described above. For chiral

HPLC, the reactions were extracted and purified in an identical manner as for reactions that employed purified enzymes. Lyophilized intact cells containing sucrose as a cryoprotectant were prepared as described elsewhere.¹² The resulting cell powder, containing expressed P411_{BM3}-CIS (26 mg), was added along with a stir bar to a 2 mL crimp vial and then sealed. The headspace of the vial was degassed, oxygen quenching system (40 μ L) was added via syringe, followed by degassed glucose (250 mM, 40 μ L), M9-N (310 μ L), and finally substrate (80 mM **1**, 10 μ L). Lyophilized cell reactions were stirred for 24 h at room temperature, then quenched and analyzed as described above.

Table S5. Comparison of amination activity of whole-cell catalysts. This table provides additional data regarding *in vivo* catalysts, some of which are also presented in Table 2 in the main text.

<i>In vivo</i> catalyst	Cell density (g _{cdw} /L)	[P450] μ M	% Yield (2)	% Yield (3)	TTN	% ee*
pCWori-empty	11	0	92	0	0	nd
P450 _{BM3}	8.5	6.6	33	0.5	5.1	nd
P450 _{BM3} -T268A	9.5	5.8	51	7.8	26	84
P411 _{BM3}	8.8	4.3	80	6.7	29	16
P411 _{BM3} -T268A	9.4	2.2	45	30	250	89
P411 _{BM3} -CIS	9.1	1.4	50	46	680	60
P411 _{BM3} -CIS-T438S	11	2.7	27	58	430	87

Optimization experiments for whole-cell reactions. Different media conditions were tested according to the standard procedure described above, except that the seed culture was grown in LB rather than M9Y, and the expression culture was grown in the alternative medium. Tested media TB+power-mix, C-*, and FB were selected based on previously published work concerning P450 expression.²⁰ Hyperbroth was purchased from Athena

Environmental Sciences (Baltimore, MD) and used according to the manufacturer's instructions.

Table S6. Effect of growth medium on productivity of forming sultam 3. Expression conditions were varied as described in the supporting information. Yields determined by HPLC quantification.

Medium	Cell density (g _{cdw} /L)	[P450] μM	% Yield (2)	% Yield (3)
M9Y-ALA	10.5	0.45	35	14
TB _p	10.5	0.89	33	29
FB	10.7	4.9	46	48
Hyperbroth	12.7	11	26	66
M9Y + ALA	10.5	4.1	39	43
C*	8.3	2.6	32	41

Preparative-Scale Bioconversions. The preparative reaction was scaled up proportionally from small-scale reactions. *E. coli* BL21 cells containing P411_{BM3}-CIS (OD600 30, 90 mL in M9-N) were sparged with argon for 45 minutes in a round bottom flask (250 mL) containing a stir bar. Separately, glucose solution (250 mM, 11.6 mL) was sparged with argon in a conical flask. The oxygen quenching mixture (10X, 11.6 mL) was degassed in a conical flask that was placed under high vacuum until slight foaming occurred (1-2 s) and then back-filled with argon; this sequence was repeated several times. Sparged glucose solution was then added to the anaerobic cell suspension via syringe, followed by the oxygen quenching system (at which time sparging was ceased though the mixture was maintained under positive argon flow). Finally, substrate **1** (80 mM, 2.9 mL DMSO) was added dropwise via syringe, and the reaction was stirred for 24 h at room temperature under positive argon pressure. To quench the reaction, dilute HCl (3 M, 8.7 mL) and acetonitrile (125 mL) were added. Cell debris was pelleted by centrifugation (8000 x g, 10

minutes), and the supernatant was then extracted with ethyl acetate (2 x 250 mL). Solvent removal *in vacuo* left a brown oil (1 g), which was purified on silica gel via a stepwise elution (hexanes, 90/10 hexanes/ethyl acetate, 80/20 hexanes/ethyl acetate, 70/30 hexanes/ethyl acetate, ethyl acetate). Fractions containing **3** (as judged by TLC developed in 90/10 hexanes/ethyl acetate and stained with Cl_2/O -tolidine) were pooled and solvent was removed *in vacuo*. The resulting material was further purified on silica gel via an isocratic elution (50/50 hexanes/ether) affording **3** (38.6 mg, 69% yield), which was established by chiral HPLC as well as ^1H and ^{13}C NMR. Spectra are presented below.

4. Synthetic Procedures

Synthesis of Substrates and Standards. Synthesis of azide substrates and benzosultam standards was accomplished as previously described; their spectra matched those previously reported.¹⁷

2,4,6-triethylbenzenesulfonyl azide (1) ^1H NMR (500 MHz, CDCl_3): d 7.07 (2H, s), 3.06 (4H, q, $J = 7.39$ Hz), 2.66 (2H, q, $J = 7.59$ Hz), 1.29 (6H, t, $J = 7.41$ Hz), 1.26 (3H, t, $J = 7.65$ Hz); ^{13}C NMR (125 MHz, CDCl_3): d 150.9, 146.5, 132.5, 129.8, 28.7, 28.5, 17.0, 15.0.

Synthetic (3) ^1H NMR (500 MHz, CDCl_3): d 7.13 (1H, s), 6.98 (1H, s), 4.69 (m, 1H) 4.62 (s, 1H), 2.99 (2H, q, $J = 7.57$ Hz), 2.71 (2H, q, $J = 7.62$ Hz), 1.59 (3H, d, $J = 6.69$ Hz), 1.35 (3H, t, $J = 7.57$ Hz), 1.26 (3H, t, $J = 7.67$ Hz). ^{13}C NMR (125 MHz, CDCl_3): d 150.8, 142.6, 140.5, 131.5, 128.9, 120.4, 52.8, 29.2, 24.5, 21.8, 15.6, 14.8.

Enzyme synthesized (3) ^1H NMR (600 MHz, CDCl_3): d 7.13 (1H, s), 6.98 (1H, s), 4.69 (1H, m), 4.56 (1H, br), 3.00 (2H, q, $J = 7.64$ Hz), 2.71 (2H, q, $J = 7.65$ Hz), 1.59 (3H, t, $J = 6.68$ Hz), 1.35 (3H, t, $J = 7.56$ Hz), 1.26 (3H, t, $J = 7.61$ Hz); ^{13}C NMR (125 MHz, CDCl_3): 150.8, 142.6, 140.4, 131.5, 128.8, 120.4, 52.8, 29.2, 24.5, 21.8, 15.6, 14.8.

2,4,6-triethylbenzenesulfonamide (2) was synthesized by sodium borohydride reduction of **1**. ^1H NMR (500 MHz, CDCl_3): d 7.01 (2H, s), 4.80 (br), 3.07 (4H, q, $J = 7.25$ Hz), 2.63 (2H, q, $J = 7.66$ Hz), 1.29 (6H, t, $J = 7.43$ Hz), 1.24 (3H, t, $J = 7.76$); ^{13}C NMR

(125 MHz, CDCl₃): d 148.7, 144.8, 135.5, 129.4, 28.6, 28.5, 16.9, 15.2. Expected m/z for C₁₂H₁₉NO₂S⁺ 241.1136, found 241.1146.

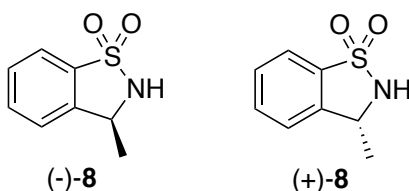
2,4,6-trimethylbenzenesulfonyl azide (4) ¹H NMR (500 MHz, CDCl₃): d 7.02 (2H, s), 2.66 (6H, s), 2.34 (3H, s); ¹³C NMR (125 MHz, CDCl₃): d 144.7, 140.1, 133.4, 132.3, 22.9, 21.3.

(5) ¹H NMR (500 MHz, CDCl₃): d 7.06 (1H, s), 6.96 (1H, s), 4.73 (1H, br), 4.43 (2H, d, $J = 5.41$), 2.59 (3H, s), 2.39 (3H, s); ¹³C NMR (125 MHz, CDCl₃): d 144.3, 137.4, 134.2, 131.7, 131.5, 122.4, 45.2, 21.7, 17.0.

(7) ¹H NMR (500 MHz, CDCl₃): d 7.22 (1H, d, $J = 1.11$ Hz), 6.98 (1H, d, $J = 1.32$ Hz), 4.45 (br, 1H), 3.61 (1H, sep, $J = 6.85$ Hz), 2.98 (1H, sep, $J = 6.88$ Hz), 1.63 (6H, s), 1.35 (6H, d, $J = 6.90$), 1.27 (6H, d, $J = 6.92$); ¹³C NMR (125 MHz, CDCl₃): d 155.7, 146.8, 145.5, 131.0, 124.5, 117.9, 59.9, 34.8, 30.0, 29.6, 24.0, 23.7.

5. Assignment of absolute configuration.

Absolute configuration of triethylsultam **3** was assigned by comparison to other compounds described in the literature.²¹ In particular, sultam **3** and monoethyl derivative **8** (shown below) were previously synthesized in enantiopure form using a BINOL-iridium catalyst, which preferentially synthesized both (-)-**3** α_D^{20} -21.3 (c = 1.01, CHCl₃) and (-)-**8** [α_D^{24}] -26.9 (c = 1.00, CHCl₃).^{21b} The absolute configuration of **8**, and the optical rotation values for its enantiomers have been previously reported (*R*)-**8** [α_D^{20}] +31.0 (c = 0.6, CHCl₃) and (*S*)-**8** [α_D^{20}] -30 (c = 1.21, CHCl₃).^{21a} By analogy, the absolute configuration of the previously reported (-)-**3** can be assigned as (*S*). Preparative chiral HPLC to separate the enantiomers of the racemic standard of **3** allowed isolation of the earlier-eluting enantiomer (which was the enzymatically preferred product). Measurement of the optical rotation of this material [α_D^{25}] -20.7 (c = 1.1, CHCl₃) revealed it to be (*S*)-**3**.



References

- (1) (a) Podust, L. M.; Sherman, D. H. *Nat. Prod. Rep.* **2012**, *29*, 1251; (b) Torres-Pazmiño, D. E. *et al. J. Biotechnol.* **2010**, *146*, 9.
- (2) (a) Newcomb, M.; Hollenberg, P. F.; Coon, M. J. *Arch. Biochem. Biophys.* **2003**, *409*, 72; (b) Guallar, V. *et al. Curr. Opin. Chem. Biol.* **2002**, *6*, 236.
- (3) (a) Heberling, M. M. *et al. Curr. Opin. Chem. Biol.* **2013**, *17*, 1; (b) Turner, N. J. *Curr. Opin. Chem. Biol.* **2011**, *15*, 234.
- (4) Zalatan, D.; Du Bois, J. *Top. Curr. Chem.* **2010**, *292*, 347.
- (5) (a) Breslow, R.; Gellman, S. H. *J. Chem. Soc. Chem. Commun.* **1982**, 1400; (b) Mahy, J. P. *et al. Tett. Lett.* **1988**, *29*, 1927.
- (6) Groves, J. T.; Nemo, T. E.; Myers, R. S. *J. Am. Chem. Soc.* **1979**, *101*, 1032.
- (7) Svastis, E. W. *et al. J. Am. Chem. Soc.* **1985**, *107*, 6427.
- (8) Dauban, P.; Dodd, R. H. *Synlett* **2003**, 1571.
- (9) White, R. E.; McCarthy, M. B. *J. Am. Chem. Soc.* **1984**, *106*, 4922.
- (10) (a) Lu, H.; Zhang, X. P. *Chem. Soc. Rev.* **2011**, *40*, 1899; (b) Caselli, A. *et al. Inorg. Chim. Acta.* **2006**, *359*, 2924.
- (11) Coelho, P. S. *et al. Science* **2013**, *339*, 307.
- (12) Coelho, P. S. *et al. Nat. Chem. Biol.* **2013**, *In press*.
- (13) Huang, W. C. *et al. Metallomics* **2011**, *3*, 410.
- (14) (a) Meunier, B.; de Visser, S. P.; Shaik, S. *Chem. Rev.* **2004**, *104*, 3947; (b) Whitehouse, C. J. C.; Bell, S. G.; Wong, L. L. *Chem. Soc. Rev.* **2012**, *41*, 1218.
- (15) Bornscheuer, U. T. *et al. Nature* **2012**, *485*, 185.
- (16) (a) Hyster, T. K. *et al. Science* **2012**, *338*, 500; (b) Köhler, V. *et al. Nat. Chem.* **2013**, *5*, 93.
- (17) Ruppel, J. V.; Kamble, R. M.; Zhang, X. P. *Org. Lett.* **2007**, *9*, 4889.
- (18) (a) Omura, T.; Sato, R. *J. Biol. Chem.* **1964**, *239*, 2370; (b) Vatsis, K. P.; Peng, H. M.; Coon, M. J. *J. Inorg. Biochem.* **2002**, *91*, 542.
- (19) Lewis, J. C. *et al. Proc. Natl. Acad. Sci. U.S.A.* **2009**, *106*, 16550.
- (20) (a) Schulz, F., Ruhr-University Bochum, 2007; (b) Pflug, S.; Richter, S. M.; Urlacher, V. B. *J. Biotechnol.* **2007**, *129*, 481.
- (21) (a) Oppolzer, W. *et al. Tetrahedron Lett.* **1990**, *31*, 4117; (b) Ichinose, M. *et al. Angew. Chem. Int. Ed. Engl.* **2011**, *50*, 9884.

*Chapter 3*ENANTIOSELECTIVE IMIDATION OF SULFIDES VIA ENZYME-CATALYZED
INTERMOLECULAR NITROGEN-ATOM TRANSFER

This chapter is published as C. C. Farwell, J. A. McIntosh, T. K. Hyster, Z. J. Wang, F. H. Arnold “Enantioselective Imidation of Sulfides via Enzyme-Catalyzed Intermolecular Nitrogen-Atom Transfer.” in *Journal of the American Chemical Society*. 2014, *136*, 8766-8771. I conducted all enzyme reactions and characterization, including protein purification, reaction set up, product quantification and determination of enantioselectivity. J.A.M. synthesized product standards and assisted in conception of enzymatic sulfimidation. T.K.H. performed initial rate experiments. Myself and Z.J.W. performed UV/Vis analysis of the enzyme oxidation state.

Abstract

Engineered enzymes with novel reaction modes promise to expand the application of biocatalysis in chemical synthesis and will enhance our understanding of how enzymes acquire new functions. The insertion of nitrogen-containing functional groups into unactivated C–H bonds is not catalyzed by known enzymes but was recently demonstrated using engineered variants of cytochrome P450_{BM3} (CYP102A1) from *Bacillus megaterium*. Here, we extend this novel P450-catalyzed reaction to include intermolecular insertion of nitrogen into thioethers to form sulfimides. An examination of the reactivity of different P450_{BM3} variants towards a range of substrates demonstrates that electronic properties of the substrates are important in this novel enzyme-catalyzed reaction. Moreover, amino acid substitutions have a large effect on the rate and stereoselectivity of sulfimidation, demonstrating that the protein plays a key role in determining reactivity and selectivity. These results provide a stepping-stone for engineering more complex nitrogen-atom transfer reactions in P450 enzymes and developing a more comprehensive biocatalytic repertoire.

Introduction

Direct oxidation of unactivated C–H bonds and heteroatoms in small molecules is a valuable method for introducing complexity into industrially and medically important compounds.¹ Modification of sulfur heteroatoms is particularly interesting given the potential for chirality in trivalent sulfur compounds and the efficacy of chiral sulfoxide therapeutics.² Enzymes catalyze a wide range of reactions in nature, and oxygenases in particular are powerful catalysts of heteroatom oxidation and C–H bond activation.³ Enzymes capable of catalyzing sulfoxidation are well documented⁴ and have even found industrial application,⁵ underscoring the utility of biocatalysis in heteroatom functionalization.

The nitrogen analogs of sulfoxides, known as sulfimides (Figure 1), are useful building blocks in chemical synthesis,⁶ ligands for metal catalysts,⁷ and are functional groups in agrochemicals.⁸ Subsequent oxidation to form sulfoximines can be achieved with good chirality transfer,⁹ and the resulting compounds are a promising source of novel derivatives of therapeutic small molecules.¹⁰ Furthermore, sulfides substituted at the sulfur position with allyl groups can undergo a 2,3-sigmatropic rearrangement upon sulfimidation, resulting in formation of a new C–N bond.^{11a} Available methods for producing sulfimides are largely based on organometallic catalytic systems using iron or rhodium, with only one example of an iron-based asymmetric sulfimidation catalyst reported.^{9,11} These methodologies typically require iminoiodinane nitrene precursors and chiral ligand frameworks to achieve stereoselectivity. Transition metal catalysts for

nitrenoid transfer also require high catalyst loadings and anhydrous conditions, and may also require high temperatures.¹²

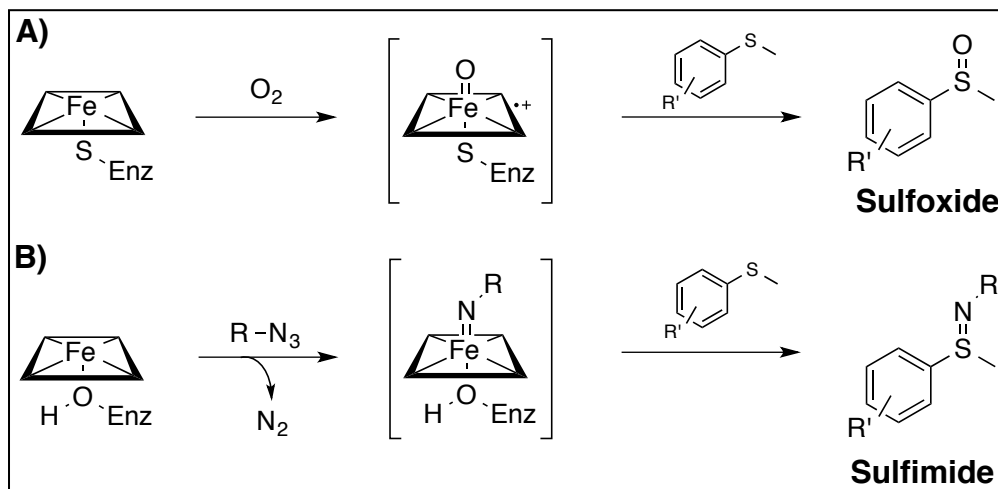


Figure 1. (A) P450-catalyzed sulfoxidation, shown proceeding through compound I. This reaction can also be mediated by compound 0 (hydroperoxy intermediate). (B) Serine-ligated P411-catalyzed sulfimide formation (this work), believed to proceed through a nitrenoid intermediate formed from an azide with N₂ as a byproduct.

Enzymes offer a “green” alternative to transition metal catalysts: they are regio- and stereoselective, non-toxic, function in aqueous media, and can be produced with ease in a suitable host organism. Whereas enzymatic sulfoxidation catalysts are well-known, enzymes that catalyze the analogous sulfimide formation have not been reported. Our laboratory has recently shown that enzymes of the iron porphyrin-containing cytochrome P450 family can catalyze carbenoid and nitrenoid insertion reactions with high activity and selectivity.¹³ Mutations to conserved residues T268 and C400 in P450_{BM3} from *Bacillus megaterium* were found to dramatically enhance reactivity for non-natural chemistry. The C400S mutation, which replaces the axial cysteine with serine, was particularly activating toward C–H amination and toward olefin cyclopropanation in whole cells.^{13b,c} The resulting shift in the ferrous-CO Soret band from 450 nm to 411 nm

prompted the ‘P411’ description for P450_{BM3} variants having the C400S mutation (Figure 1). These ‘chemo-mimetic’ enzyme systems offer several advantages over transition metal complexes. Because they are genetically encoded, tuning of selectivity and reactivity can be achieved through directed evolution. Moreover, these novel enzyme catalysts operate under mild, aqueous conditions amenable to sustainable chemical synthesis.

Previously, we and Fasan have shown that variants of P450_{BM3} catalyzed the intramolecular C–H amination of arylsulfonylazides with high selectivities and hundreds of total turnovers.^{13c,14} To further develop enzymatic nitrene transfer, we wished to explore *intermolecular* reactions, given the clear synthetic applications in building complexity in a convergent manner. Additionally, we reasoned that an intermolecular nitrene transfer reaction would allow a more detailed mechanistic characterization than was possible with the intramolecular reaction. Given that variants of P450_{BM3} are promising enantioselective sulfoxidation and C–H amination catalysts, we sought to determine whether P450 variants could catalyze the nitrogen analog of sulfoxidation, the intermolecular insertion of nitrogen into organosulfur compounds. This study describes the first report of intermolecular nitrene transfer catalyzed by an enzyme, in the context of imidation of organosulfur compounds.

Results and Discussion

In our previous work on intramolecular C–H amination, we were limited to aryl sulfonylazide substrates as nitrene precursors. Despite the success with this substrate

class, we wished to assess the influence of the R-group on the nitrenoid transfer, and thus tested a series of substrates displaying a range of stereo-electronic properties that have been shown to be effective nitrene precursors in other contexts (Figure S1, **1–6**).^{11b,12}

For the thioether acceptor substrate we chose thioanisole, which has been used in enzymatic sulfoxidation by cytochrome P450s and other oxygenase enzymes.^{4b,4d} As a catalyst, we used the P411_{BM3}-CIS T438S variant of cytochrome P450_{BM3}, possessing the aforementioned C400S mutation. This enzyme, which contains 14 mutations relative to wild-type P450_{BM3} (Table S1), was previously shown to be a good catalyst in the activation of azides for intramolecular C–H insertion.^{13c} Reaction conditions were similar to those reported previously for intramolecular C–H amination^{13c} under anaerobic conditions with NADPH supplied as a reductant.

Considering the small size of reactive oxygen species naturally produced by P450s, we anticipated that smaller azides, such as mesyl azide (**4**), would be less sterically demanding than aryl or arylsulfonyl azides and thus a more suitable partner for reaction with thioanisole. We were therefore surprised to find that of all the azides initially examined, sulfimidation activity was only observed with tosyl azide (**1**) as the nitrene source (30 total turnovers, TTN, Figure S1). Control experiments confirmed that enzyme was necessary for sulfimide formation (Table S2). Free hemin showed no activity in this transformation. As we reported previously for intramolecular C–H amination, some of the azide was reduced to sulfonamide, in this case *p*-toluenesulfonamide (**9**).^{13c}

In other non-natural P450 reactions reported to date, it was shown that amino acid substitutions could alter both the activity and stereoselectivity of the enzymes.^{13a,c} Thus we tested how the mutation of conserved residues C400 and T268 and other active-site residues affects sulfimination activity (Table 1). For these experiments we used the more reactive sulfide 4-methoxythioanisole, for which we measured 300 TTN with P411_{BM3}-CIS T438S (see below for more discussion of the effect of sulfide substituents on reactivity).

Since activating mutations T268A and C400S were already present in P411_{BM3}-CIS T438S, we tested the effects of reverting each mutation to the wild-type residue (Table 1, entries 1-3). Each revertant was much less active than the parent, supporting the benefit of having the C400S and T268A mutations for effective nitrene-transfer chemistry. Given the bulky nature of the aryl sulfonylazide nitrene sources and aryl thioethers, we next tested the C400S mutants of several P450_{BM3} variants that had been engineered via combinatorial alanine scanning to hydroxylate large substrates¹⁵ (Table 1, Entries 4-6). While P411_{BM3}-H2-5-F10 displayed comparably high levels of activity to P411_{BM3}-CIS (>100 TTN), the other mutants we tested from this library were less productive. We also tested the effects of introducing the activating mutations into wild-type P450_{BM3}. Although these wild-type derivatives were highly active and stereoselective for *intramolecular* C–H amination,^{13c} here we found that neither the single mutant (T268A or C400S) nor the double mutant (T268A + C400S) are particularly active for intermolecular sulfimination.

Table 1. Sulfimidation activity and selectivity of P450_{BM3} variants using substrates and reaction conditions shown

Reaction scheme: 4-methoxybenzenethiol (**7a**) + 4-methylbenzenesulfonyl azide (**1**) $\xrightarrow[\text{0.1 M KPi, pH= 8.0, RT, 4 hours}]{\text{Enzyme 0.2 mol \%}}$ 4-methoxy-N-(4-methylphenyl)benzenesulfonamide (**8a**)

Entry	Enzyme ^a	TTN	e.r.
1	P411 _{BM3} -CIS-T438S	300	74:26
2	P450 _{BM3} -CIS-T438S	7	nd
3	P411 _{BM3} -CIS-A268T-T438S	19	nd
4	P411 _{BM3} -H2-5-F10	140	29:71
5	P411 _{BM3} -H2-A-10	84	57:43
6	P411 _{BM3} -H2-4-D4	32	70:30
7	P450 _{BM3}	10	nd
8	P411 _{BM3}	11	nd
9	P450 _{BM3} -T268A	19	nd
10	P411 _{BM3} -T268A	17	nd
11	P411 _{BM3} -CIS-I263A-T438S	320	18:82

^a “P411” denotes Ser-ligated (C400S) variant of cytochrome P450_{BM3}. Variant IDs and specific amino acid substitutions in each can be found in Table S1. TTN = total turnover number, e.r. = enantiomeric ratio, nd = not determined.

The turnover data presented above demonstrate the sequence dependence of sulfimidation productivity. The effects, however, could be due to changes in stability of the enzymes that lead to degradation over the course of the reaction. To address this possibility, we compared the initial rates of reaction using the most productive enzyme in

terms of total turnover, P411_{BM3}-CIS-T438S, and the less productive P411_{BM3}-H2-A-10 and P411_{BM3}-H2-4-D4 enzymes (Figure S2). Differences in the total productivity (i.e., TTN) for each enzyme are mirrored in the initial rates of reaction (Table S4), suggesting that specific amino acids proximal to the heme influence binding and orientation of the substrates to effect catalytic rate enhancement.

The key role of active site architecture in guiding reaction trajectory is further supported by the effects of amino acid substitutions on the reaction stereochemistry. Indeed, we found enzymes capable of producing an excess of either sulfimide enantiomer: e.g., P411_{BM3}-CIS-T438S gives an e.r. of 74:26, while expanded active site variant P411_{BM3}-H2-5-F10 exhibited the opposite selectivity, giving 29:71 (Figure S4). Among the H2-mutants (which differ from P411_{BM3}-CIS-T438S by 3-5 amino acid substitutions, Table S1), H2-5-F10 was alone in containing the I263A mutation, suggesting that this mutation is responsible for the enantiomeric inversion observed in the P411_{BM3}-H2-5-F10 variant. When the I263A mutation was placed in the P411_{BM3}-CIS-T438S background, an even more pronounced inversion in selectivity was observed (e.r. = 18:82 for the P411_{BM3}CIS-I263A-T438S, compared to 74:26 for P411_{BM3}CIS-T438S). This enzymatic system not only induces asymmetry in sulfimide products, it also provides tunability in which selectivity can be switched with just a few mutations.

Table 2. Impact of sulfide substituents on sulfimidation activity

7a-d	1		8a-d	9
Entry	R ₁ in 7	R ₂ in 7	TTN 8	TTN 9
a	-OMe	-H	300	270
b	-Me	-H	190	400
c	-H	-Me	100	390
d	-H	-H	30	500
e	-CHO	-H	< 1*	510

* Trace product observed by LC-MS.

Previous studies of P450-catalyzed sulfoxidation¹⁶ as well as rhodium-catalyzed C–H amination¹⁷ suggest that the electronic properties of sulfide or alkyl acceptor substrates significantly impact reactivity. Thus, to better understand the mechanism of this new enzyme reaction, we sought to establish how thioether electronic properties affected enzyme-catalyzed sulfimidation. We chose a set of aryl sulfide substrates with substituents encompassing a range of electronic properties, from strongly donating to weakly withdrawing. As a first approximation of the effect of sulfide electronics, we examined the total number of turnovers catalyzed by P411_{BM3}-CIS-T438S in the reactions of different sulfides with tosyl azide (Table 2). In general, sulfides containing electron-donating substituents on the aryl sulfide ring were better substrates for sulfimidation. For example, the enzyme reaction containing 4-methoxythioanisole (**7a**) gave the highest

levels of activity (300 TTN). In contrast, the electron-deficient *p*-aldehyde substrate (**7e**) gave only trace amounts of sulfimide product. Further, some azides that initially appeared entirely inactive gave small amounts of sulfimide products when reacted with 4-methoxythioanisole, underscoring the importance of sulfide electronics in this reaction (Table S3). The identity of substrates also exerted a modest influence on the enantioselectivity of sulfimidation. In particular, P411_{BM3}-CIS-T438S gave e.r. values for substrates **8a-8d** that ranged from 59:41 for **8c** to 87:13 for **8d** (Table S5, Figures S4-S7). While it is possible that some sulfides were poorer substrates due to the steric influence of the *para* substituent, the overall trend is strongly suggestive of electron induction to the aryl sulfide being a major contributor to activity. One notable aspect of these reactions is that significantly more sulfonamide (**9**) was produced when less reactive sulfides were used.

Although the total turnover data suggest that sulfide electronics influence reactivity, this result could also be due to other factors, such as substrate-dependent enzyme inactivation. To assess the effect of sulfide substituents on reactivity more directly, we measured the initial rates of reaction of tosyl azide with the sulfides **7a-7d** in Table 2. The initial rates correlated well with the total turnover data presented above, with *p*-OMe showing the highest rate of reaction (Figure S3). Given this correlation, we sought to obtain more mechanistic information by fitting the data to a Hammett plot that correlates the observed rates with each substituent's Hammett parameter.¹⁸ We found a strong, linear relationship with a Hammett value of $\rho = -4.0$ (Figure 2), which suggests that during the rate-limiting step there is a buildup of positive charge on the sulfide that is

stabilized by electron-donating substituents. This observation is consistent with Hammett values obtained for the oxidation of thioanisoles in P450-catalyzed sulfoxidation reactions, though the magnitude of ρ for sulfimination is significantly greater than for sulfoxidation (-4.0 versus -0.2).¹⁶ One possible explanation for this difference is that the presumed nitrenoid intermediate of this reaction (Figure 1) is a weaker oxidant than compound I, making the nucleophilicity of sulfur an important contributor to the rate of nitrenoid transfer. The large difference in the magnitude of ρ could also indicate a change in mechanism relative to P450 sulfoxidation: whereas Watanabe and coworkers have proposed that sulfoxidation proceeds through a single electron transfer process,¹⁶ sulfimination may occur via direct nucleophilic attack of the thioether on the nitrenoid intermediate.

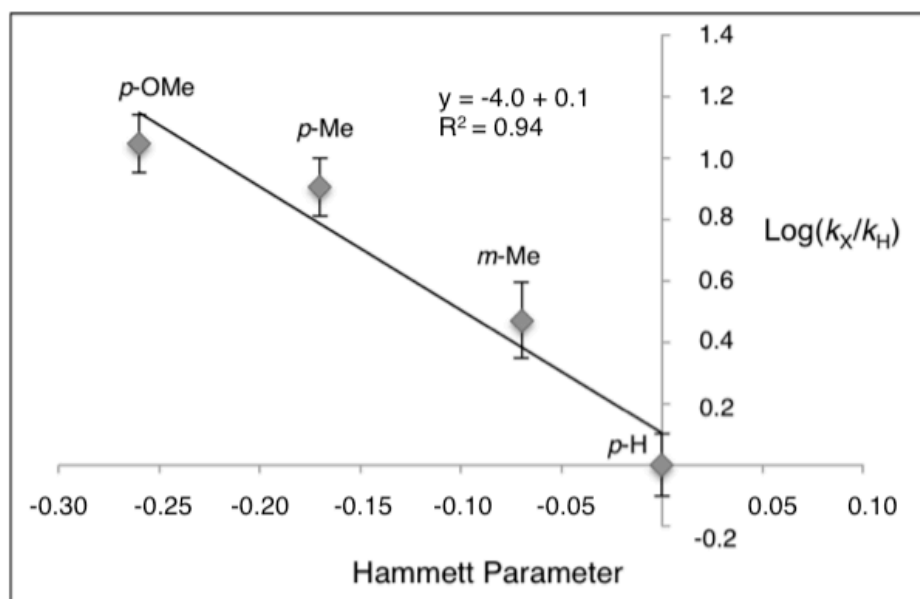


Figure 2. Plot of reaction rate versus Hammett parameter of substituted aryl sulfides using the P411_{BM3}-CIS-T438S enzyme and tosyl azide nitrogen source. Data points are labeled with aryl substituent and position (*p*- = para, *m*- = meta) and Hammett parameters obtained from Hansch et al.¹⁸

As noted above, we observed that a greater proportion of sulfonamide side product was formed when less reactive sulfides were used. The varying amounts of this side-product prompted us to examine more closely how sulfonamide might be produced. We first tested the possibility that azide is reduced by some additive in the reactions (i.e., glucose oxidase, catalase, NADPH, etc.) by simply omitting the P450 enzyme from the reactions (Table S2). We found that no-enzyme controls yielded very little reduced sulfonamide product (more than 10-fold lower than with enzyme present). While these experiments showed that enzyme was likely involved in azide reduction, this still left several possibilities. Since P411_{BM3}'s heme domain is fused to a reductase, we considered the possibility that azide reduction occurs via direct hydride transfer from the reductase, as has been observed for aldehyde reductions.¹⁹ We used carbon monoxide-inhibited reactions to investigate this possibility, since CO binding to the heme iron should have no effect on the reductase domain. In the presence of CO, we observed a significant decrease in the sulfonamide produced, suggesting that azide reduction occurs at the heme. Furthermore, only trace sulfonamide was observed when reactions were conducted in the presence of oxygen, further supporting the involvement of reduced heme in azide reduction. Since all the available evidence suggests that azide reduction and sulfimide formation both occur at the heme, the most parsimonious explanation is that both reactions stem from a common intermediate that can give rise to both sulfonamide and sulfimide products.

We propose a mechanism of sulfonamide and sulfimide formation that begins with the iron (III) heme gaining an electron from NADPH via the flavin cofactors of the reductase domain (Figure 3). Addition of azide substrate results in the formation of a formal iron (IV) nitrenoid, which can either be reduced by subsequent electron transfer or ‘trapped’ by sulfide to form sulfimide product. We hypothesize that a second electron transfer followed by protonation of the nitrenoid to generate sulfonamide restores the heme iron to its ferric state, and additional reductant is required to return to the catalytically active ferrous state (Figure 3, unproductive pathway).

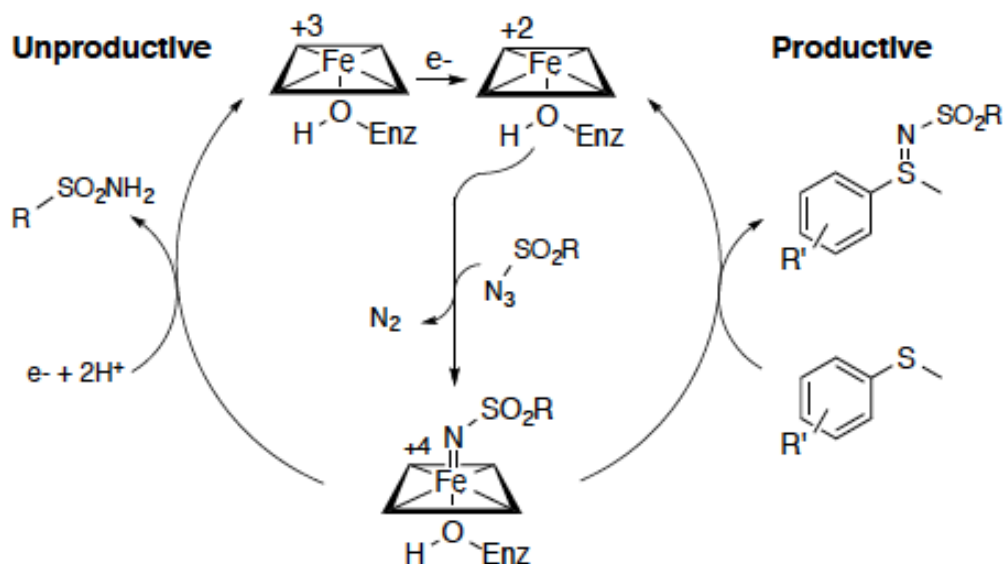


Figure 3. Proposed mechanisms of sulfimide (‘productive’) and sulfonamide (‘unproductive’) formation.

To test whether ferric heme is involved in the unproductive pathway, we monitored the change in the visible absorbance spectrum of the reduced holoenzyme P411_{BM3}-CIS-I263A-T438S upon addition of NADPH followed by azide. The Ser-ligated P411 proteins exhibit different absorbance properties in the ferric and ferrous

states compared with their Cys-ligated counterparts, such that the ferric, ferrous, and CO-ferrous Soret bands are shifted from 418, 408, and 450 nm to 405, 422, and 411 nm, respectively (Figure S8).^{13b} When NADPH was added to a solution of enzyme under an anaerobic atmosphere, we observed reduction of the heme from the ferric to the ferrous state. When a degassed solution of azide was added to the ferrous protein, we observed an immediate shift back to the ferric state, with concomitant production of sulfonamide, verified by HPLC. This observation suggests that the unproductive azide reduction pathway occurs readily in the absence of sulfide and that, when provided only with azide, the catalyst rests in the ferric state.

To determine the resting state of the P411 catalyst in sulfimination, we repeated the above experiment in the presence of both sulfide and azide. Addition of sulfide to a solution of enzyme and NADPH results in no change in the Q or Soret bands, with the iron heme remaining in the ferrous state. However, addition of azide to this solution causes the iron heme to shift to the ferric state. After 10 min, peaks corresponding to the ferrous heme begin to grow until the ferrous heme becomes the dominant species at 30 min (Figure S9). Both sulfonamide and sulfimide products are formed throughout the course of the reaction. Our observations are consistent with the competing reaction pathways outlined in Figure 3 and suggest that the catalyst rests as a mixture of ferric and ferrous hemes during sulfimination. When the concentration of azide is high, as it is at the beginning of the reaction, the unproductive pathway is favored and a ferric resting state dominates. As azide is consumed, both the ferric and ferrous resting states can be observed.

P450 monooxygenases are known to undergo an ‘oxidase uncoupling’ side reaction in which compound I is reduced by two electrons to give water, which bears some similarity to the process of azide reduction we have observed here. One difference, however, is that only a single electron transfer is required to attain a reactive state in nitrene-transfer chemistry. This stands in contrast to P450 monooxygenase chemistry, where the generation of compound I from O₂ requires the transfer of two electrons. Thus, one explanation for the relatively high proportion of reduced azide in these reactions is that the electron-transfer machinery in P450_{BM3} is evolved to carry out two-electron reductions.²⁰ In the case of nitrene-transfer chemistry, reducing the ferric heme to the +2 state allows nitrenoid formation, but a second electron transfer would generate an unreactive iron(III)-sulfonamide complex. Coupled with the fact that lower sulfide concentrations and less-reactive sulfides lead to increased azide reduction, these observations are consistent with the mechanism discussed above in which sulfimide formation competes with azide reduction. Since electron transfers from the reductase domain are quite rapid,^{21,13b} only relatively reactive sulfides can successfully compete with reduction to form sulfimide.

The mechanistic picture described above suggests that achieving higher levels of sulfide occupancy in the active site should favor sulfimide formation and inhibit azide reduction. This could be achieved with tighter binding of the sulfide acceptor substrate or by increasing the concentration of sulfide relative to azide. We therefore tested whether excess sulfide or slow addition of azide would increase sulfimide formation relative to sulfonamide. Increasing the sulfide concentration decreased reduction of azide to

sulfonamide and improved the ratio of sulfimide to sulfonamide, from 0.6 (with 0.5 eq sulfide) to 1.8 (with 4 eq sulfide) (Figure S10, Table S6). Slow azide addition slightly increased the TTN for sulfimide and decreased sulfonamide formation in a two-hour reaction (Figure S11). That higher concentrations of sulfide substrate improve sulfimide production suggests that protein engineering to improve the binding of sulfide acceptor substrates could also produce strong gains in the desired activity. Indeed, the specific activities of the enzyme catalysts reported here compare favorably with enantioselective iron-based catalysts, which routinely require catalyst loadings of 10 mol %.^{9b} Furthermore, engineering the holoenzyme or reductase domain to favor one-electron transfers might improve the proportion of desired product relative to azide reduction, which could allow reaction with more challenging organic acceptor substrates.

Conclusions

This is the first report of intermolecular nitrene transfer catalyzed by an enzyme, allowing for a mechanistic analysis of this new enzyme activity. Similar to P450-catalyzed sulfoxidation, we find that the electronic properties of the sulfide substrates strongly influence reactivity, though the magnitude of the substituent effects is greater for nitrene transfer, possibly owing to the less oxidizing nature of the presumed nitrenoid intermediate as compared to compound I. The necessity of the C400S mutation for sulfimidation can be rationalized along similar lines: the less electron-donating axial serine ligand in P411 enzymes likely makes the nitrenoid species a more potent oxidant. The impact of sulfide substituents on sulfimide formation is also reflected in the

generation of sulfonamide side product, suggesting that the nitrenoid undergoes rapid reduction and can only productively insert into sufficiently reactive sulfides. Characterization of the redox state of the heme iron in the presence and absence of nitrene source and sulfide acceptor supports the proposal that nitrenoid ‘over-reduction’ competes with productive sulfimide formation and that the former is a two-electron process resulting in regeneration of ferric heme. Another interesting aspect of this enzyme reaction is the strong preference for an *aryl* sulfonylazide nitrene source: although monooxygenation reactions use a small donor substrate (dioxygen), only trace sulfimidation was observed with small azides such as ethanesulfonyl azide (Table S3). The ability of the enzyme to accept larger aryl substrates may be beneficial for development of enantioselective intermolecular nitrene-transfer catalysts, as we have observed that a single mutation can dramatically affect the enantioselectivity of reaction. Intermolecular nitrene transfer in the form of sulfimidation can now be added to the impressive array of natural and non-natural chemistry catalyzed by cytochrome P450 enzymes.

Supplementary Materials for

Enantioselective Imidation of Sulfides via Enzyme-Catalyzed Intermolecular Nitrogen-Atom Transfer

Contents	Page
1. Materials and Methods	64
2. Confirmation of Enzyme Activity	66
3. Reaction Optimization	67
4. Determination of Initial Rates	69
5. Determination of Enantioselectivity	72
6. Synthetic Procedures	75
7. Observation of Catalytic Resting State	76
8. Effect of Excess Sulfide and Azide Slow Addition	79

1. Materials and Methods

General. Unless otherwise noted, all chemicals and reagents for chemical reactions were obtained from commercial suppliers (Sigma-Aldrich, VWR, Alfa Aesar) and used without further purification. Silica gel chromatography purifications were carried out using AMD Silica Gel 60, 230-400 mesh. ^1H spectra were recorded on a Varian Inova 500 MHz instrument in CDCl_3 , and are referenced to the residual solvent peak. Synthetic reactions were monitored using thin layer chromatography (Merck 60 gel plates) using an UV-lamp for visualization.

Chromatography. Analytical high-performance liquid chromatography (HPLC) was carried out using an Agilent 1200 series, and a Kromasil 100 C18 column (Peeke Scientific, 4.6 x 50 mm, 5 μm). Semi-preparative HPLC was performed using an Agilent XDB-C18 (9.4 x 250 mm, 5 μm). Analytical chiral HPLC was conducted using a supercritical fluid chromatography (SFC) system with isopropanol and liquid CO_2 as the mobile phase. Chiralcel OB-H and OJ columns were used to separate sulfimide enantiomers (4.6 x 150 mm, 5 μm). Sulfides were all commercially available and sulfimide standards were prepared as reported.¹ e.r. values were determined by dividing the major peak area by the sum of the peak areas determined by SFC chromatography.

Cloning and site-directed mutagenesis. pET22b(+) was used as a cloning and expression vector for all enzymes described in this study. Site-directed mutagenesis on P411_{BM3}-CIS-T438S to generate P411_{BM3}-CIS-I263A-T438S was performed using a

modified QuickChangeTM mutagenesis protocol. The PCR products were gel purified, digested with DpnI, and directly transformed into *E. coli* strain BL21 (DE3).

Table S1. Mutations present in P450_{BM3} variants used in this work.

Enzyme	Mutations relative to wild-type P450 _{BM3}
P450 _{BM3}	none
P450 _{BM3} -T268A	T268A
P411 _{BM3}	C400S
P411 _{BM3} -T268A	T268A, C400S
P450 _{BM3} -CIS-T438S	V78A, F87V, P142S, T175I, A184V, S226R, H236Q, E252G, A290V, L353V, I366V, T438S, E442K
P411 _{BM3} -CIS-T438S	P450BM3-CIS C400S, T438S
P411 _{BM3} -CIS-A268T-T438S	P450BM3-CIS, A268T, C400S, T438S
P411 _{BM3} H2-A-10	P450BM3-CIS, L75A, L181A, C400S,
P411 _{BM3} H2-5-F10	P450BM3-CIS, L75A, I263A, C400S, L437A
P411 _{BM3} H2-4-D4	P450BM3-CIS, L75A, M177A, L181A, C400S, L437A, T438S

Determination of P450 concentration. Concentration of P450/P411 enzymes was accomplished by quantifying the amount of free hemin present in purified protein using the pyridine/hemochrome assay.²²

Protein expression and purification. Enzymes used in purified protein experiments were expressed in BL21(DE3) *E. coli* cultures transformed with plasmid encoding P450 or P411 variants. Expression and purification was performed as described elsewhere,³

except that the shake rate was lowered to 130 RPM during expression. Following expression, cells were pelleted and frozen at -20 °C. For purification, frozen cells were resuspended in buffer A (20 mM tris, 20 mM imidazole, 100 mM NaCl, pH 7.5, 4 mL/g of cell wet weight) and disrupted by sonication (2 x 1 min, output control 5, 50% duty cycle; Sonicator 3000, Misonix, Inc.). To pellet insoluble material, lysates were centrifuged at 24,000 x g for 0.5 h at 4 °C. Proteins were expressed in a construct containing a 6x-His tag and were consequently purified using a nickel NTA column (5 mL HisTrap HP, GE Healthcare, Piscataway, NJ) using an AKTApurifier FPLC system (GE healthcare). P450 or P411 enzymes were then eluted on a linear gradient from 100% buffer A 0% buffer B (20 mM tris, 300 mM imidazole, 100 mM NaCl, pH 7.5) to 100 % buffer B over 10 column volumes (P450/P411 enzymes elute at around 80 mM imidazole). Fractions containing P450 or P411 enzymes were pooled, concentrated, and subjected to three exchanges of phosphate buffer (0.1 M KPi pH 8.0) to remove excess salt and imidazole. Concentrated proteins were aliquoted, flash-frozen on powdered dry ice, and stored at -20 °C until later use.

2. Confirmation of enzyme activity

Controls to confirm the enzymatic sulfimination activity of variant P411_{BM3}CIS T438S. Small-scale reactions (400 µL total volume) were set up and worked up as described above. For the reaction containing hemin as catalyst, 10 µL of a hemin solution (1 mM in 50% DMSO-H₂O) was added to a final concentration of 25 µM. TTNs were determined as described above and are presented in Table S2. CS denotes a ‘complete system’ in which all components of the reactions as described above are

present. Variations from the complete system are denoted with a “- X”, where X is the component removed.

Table S2. Control experiments using substrate **7c** yielding products **8c** (sulfimide) and **9** (sulfonamide). CS = complete system.

Condition	TTN 8c	TTN 9
P411_{BM3}-CIS T438S (CS)	90	300
CS - NADPH	1	2
CS + Na₂S₂O₄ + CO	2	40
CS boiled enzyme	1	53
CS aerobic	2.3	16
Hemin + Na₂S₂O₄	0	42
CS - P411_{BM3}-CIS T438S	0	21

3. Reaction Development and Conditions

Typical procedure for small-scale sulfimidation bioconversions under anaerobic conditions using purified enzymes. Small-scale reactions (400 μ L) were conducted anaerobically in 2 mL crimp vials as described in Chapter 2.^{13c} A solution of aryl sulfide in DMSO or methanol (100 mM, 10 μ L) was added to the reaction vial via syringe, followed by arylsulfonyl azide (100 mM, 10 μ L, DMSO). Final concentrations of the reagents were typically: 2.5 mM aryl sulfide, 2.5 mM arylsulfonyl azide, 10 mM NADPH, 25 mM glucose, 5-20 μ M P450. To the vials were then added acetonitrile (460

μL) and internal standard (1,3,5 trimethoxybenzene, 10 mM in 10% DMSO/90% acetonitrile, 1 mM final concentration). This mixture was then transferred to a microcentrifuge tube, and centrifuged at $17,000 \times g$ for 5 minutes. A portion ($20 \mu\text{L}$) of the supernatant was then analyzed by HPLC. Sulfimide formation was quantified by comparison of integrated peak areas of internal standard (1,3,5-trimethoxy benzene, 1 mM or 1,3,5-trichlorobenzene, 1 mM) and sulfimide at 220 nm to a calibration curve made using synthetically produced sulfimide and internal standard. Coefficients determined from standard curves were multiplied by a dilution factor in order to obtain sulfimide concentrations in the reaction mixture. For chiral HPLC, the quenched reaction mixture was extracted twice with ethyl acetate ($2 \times 350 \mu\text{L}$), dried under a light argon stream, and resuspended in acetonitrile ($100 \mu\text{L}$).

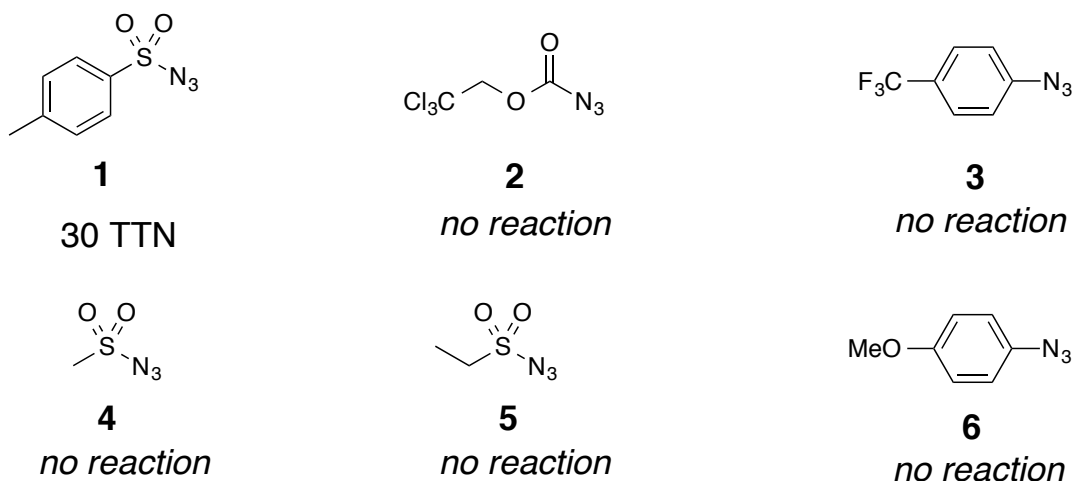


Figure S1. Azides tested as nitrene sources for sulfimidation of thioanisole using the P411_{BM3}-CIS T438S enzyme. TTN = total turnover number.

Table S3. Qualitative description of reaction productivity using para-methoxy aryl sulfide **7a** and azides shown in Figure S1.

Azide	Productivity ^a
1	+++
2	+
3	nd ^b
5	+
6	nd

^a + denotes relative amount of product, where +++ is the most productive reaction. See Figures S26 and S27 for LC-MS verification of product formation for azides **2** and **4**. ^b nd = none detected.

4. Determination of Reaction Rates

Initial rates. Four 2-ml vials were charged with a stir bar, 10x oxygen depletion system^{13c} (40 μ L), and a solution of enzyme prior to crimp sealing with a silicon septum. Once sealed, the headspace was flushed with argon for at least 10 minutes. Concurrently, a sealed 6-mL vial charged with glucose (250 mM, 400 μ L), NADPH (20 mM, 400 μ L), and KPi (pH = 8.0, 0.1 M, 2.6 mL) was sparged for 10 minutes with argon. After degassing was complete, 340 μ L of the reaction solution was transferred to the 2-mL vial via syringe. Sulfide (100 mM, 10 μ L) was added to all four 2-mL vials followed quickly (less than 20 seconds) by tosyl azide (100 mM, 10 μ L). The reactions were quenched at 1-2 minute intervals over 5-10 minutes by decapping and adding acetonitrile (460 μ L).

After 5 minutes of stirring, the vials were charged with internal standard and the reaction mixtures were transferred to 1.8 mL tubes, which were vortexed and centrifuged (14,000 x g, 5 min). The supernatant was transferred to a vial for analysis by HPLC. Initial rates are plotted for individual enzymes referenced in the text in Figure S2, and for various substituted aryl sulfides in Figure S7.

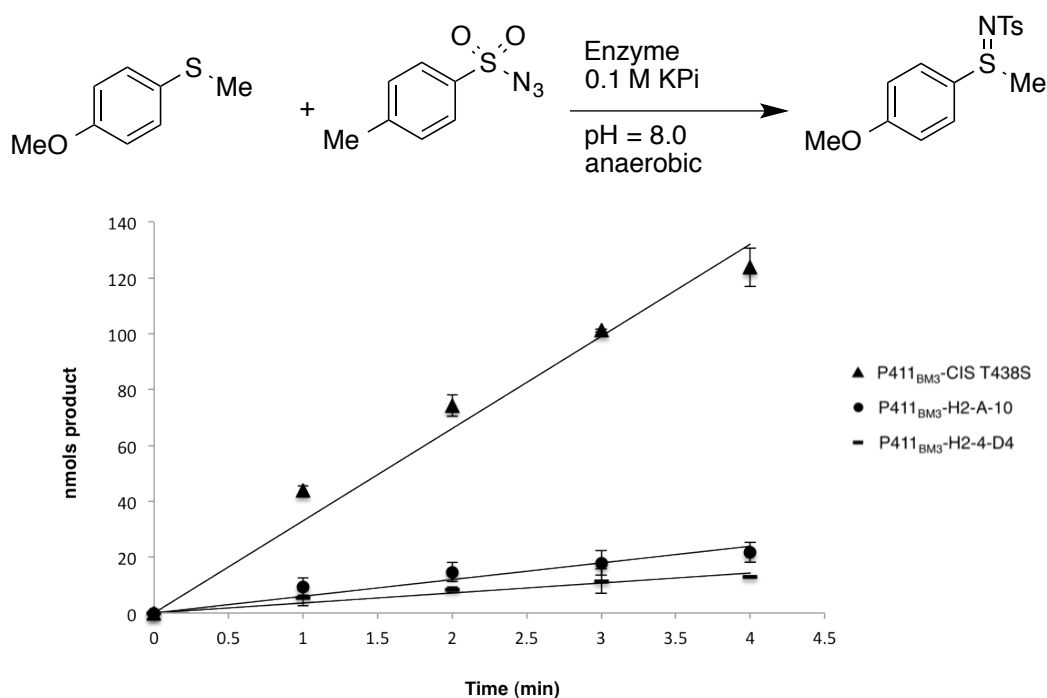


Figure S2. Data used to determine initial rates of the reaction depicted in the scheme above using the enzymes listed in the figure legend.

Table S4. Initial rates determined from data presented in Figure S2 and TTNs presented in Table 1.

Enzyme	Rate (nmol min ⁻¹)	TTN
P411 _{BM3} -CIS T438S	33	300
P411 _{BM3} -H2-A-10	3.5	32
P411 _{BM3} -H2-4-D4	5.9	84

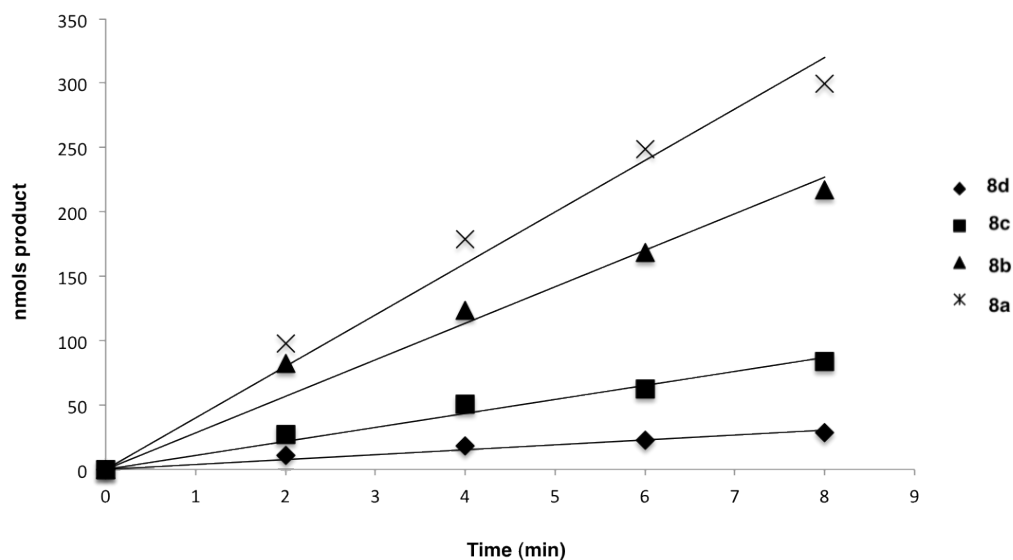
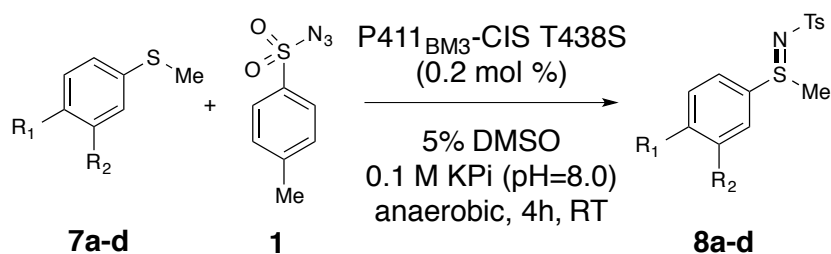


Figure S3. Data used to determine initial rates for reaction of substituted aryl sulfides with tosyl azide, using P411_{BM3}-CIS T438S as catalyst. Sulfimide products measured are as listed in Table 2 of the text.

5. Determination of Reaction Enantioselectivity

Table S5. Enantioselectivity of products **8a–8d** with P411_{BM3}-CIS T438S enzyme.



Product	e.r.	R1	R2
8a	74:26	-OMe	-H
8b	80:20	-Me	-H
8c	59:41	-H	-Me
8d	87:13	-H	-H

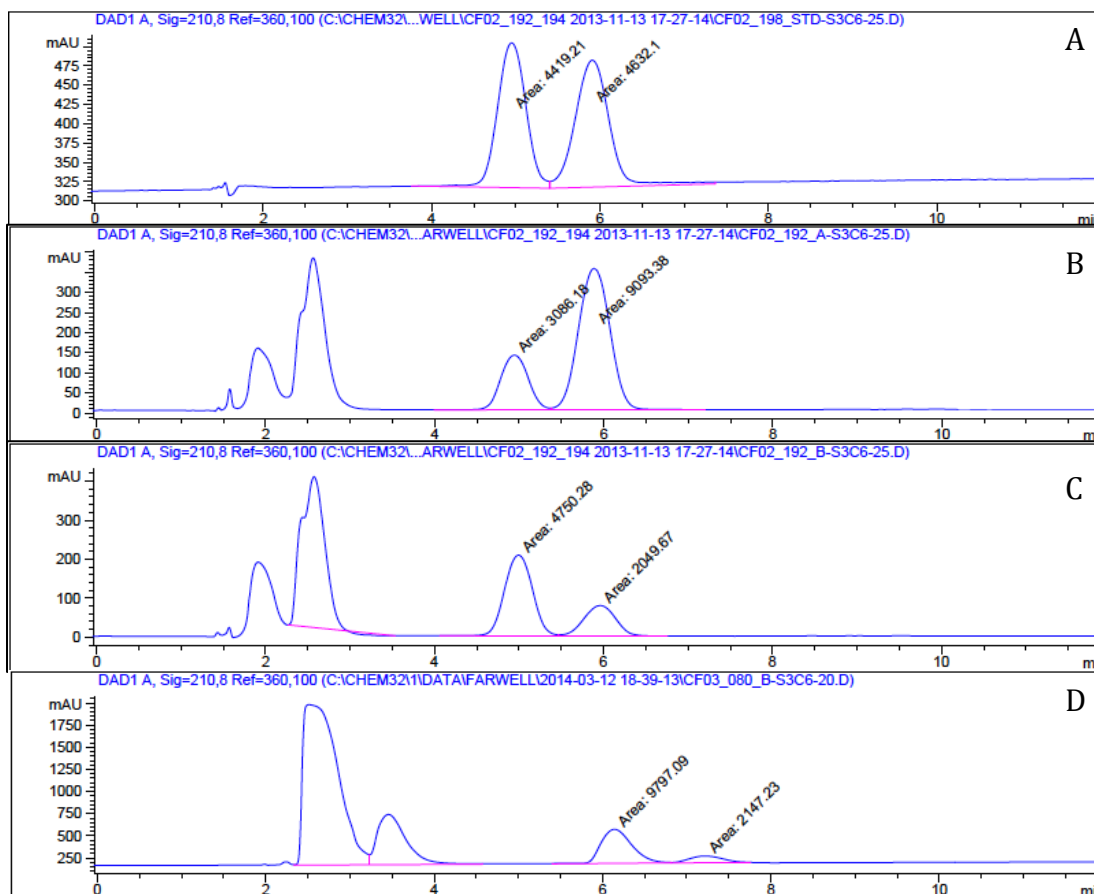


Figure S4. A) SFC trace of synthetic standard of **8a** using Chiralpak OD-H column with 25% isopropanol/75% supercritical CO₂ mobile phase. B) Trace of P411_{BM3}-CIS T438S produced **8a** under same conditions as synthetic standard. C) Trace of P411_{BM3}-H2-5-F10 produced **8a**. D) Trace of P411_{BM3}-CIS-I263A-T438S produced **8a**, using 20% isopropanol/80% supercritical CO₂ mobile phase.

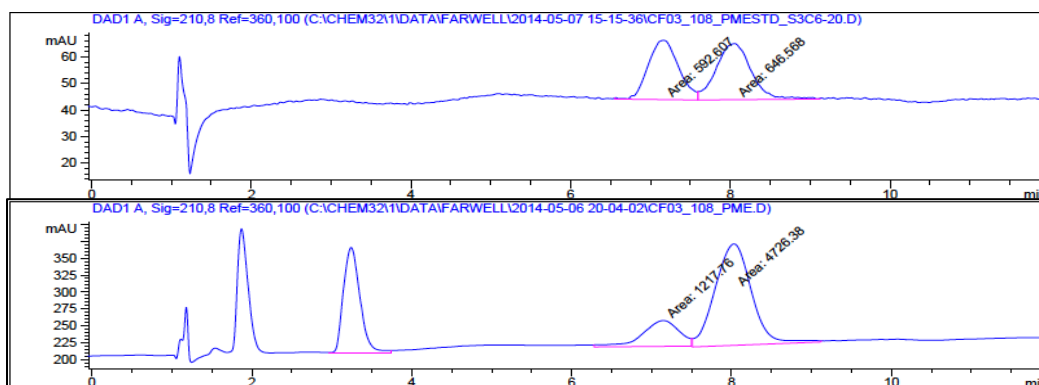


Figure S5. Top: SFC trace of **8b** synthetic standard using Chiralpak OD-H column with 20% isopropanol/80% supercritical CO₂ mobile phase. Bottom: Trace of enzyme produced **8b**.

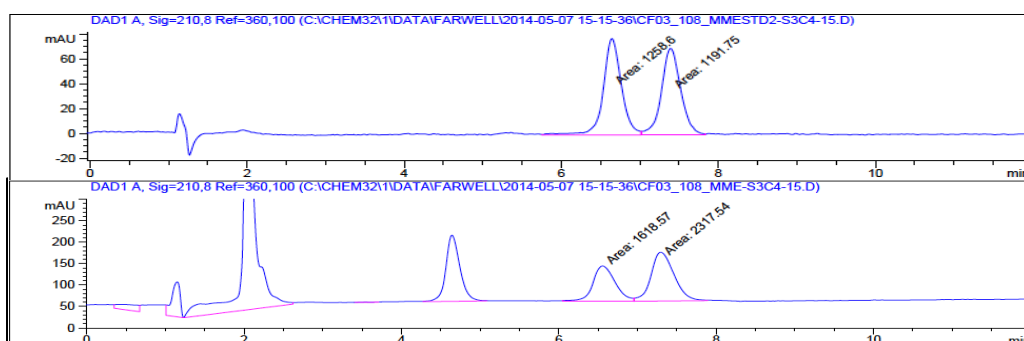


Figure S6 Top: SFC trace of **8c** synthetic standard using Chiralpak OJ column with 15% isopropanol/85% supercritical CO₂ mobile phase. Bottom: Trace of enzyme produced **8c**.

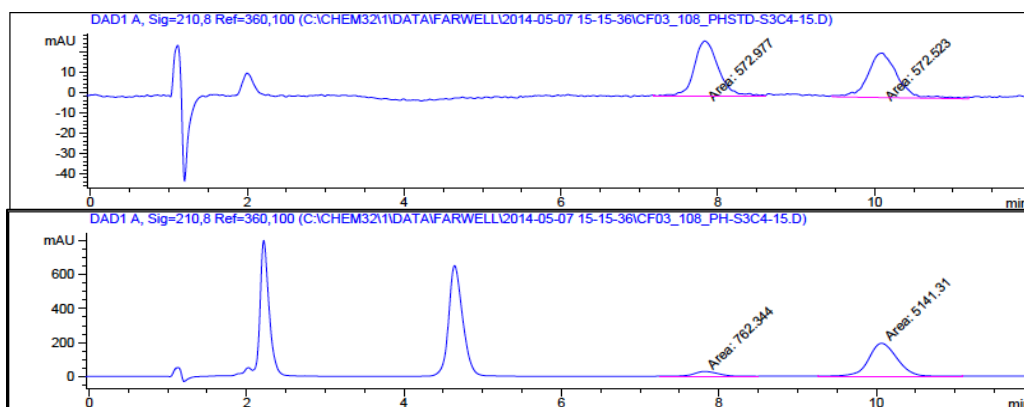
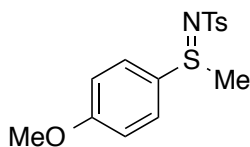


Figure S7. Top: SFC trace of **8d** synthetic standard using Chiralpak OJ column with 15% isopropanol/85% supercritical CO₂ mobile phase. Bottom: Trace of enzyme produced **8d**.

6. Synthetic Procedures

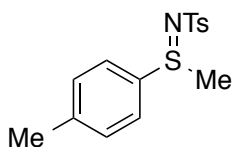
All sulfides presented in Table 2 were obtained from commercial sources (Sigma Aldrich, Alfa Aesar). Sulfimide standards were synthesized as previously reported.^{11c}

8a



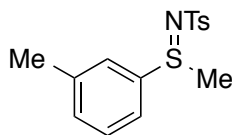
¹H NMR (500 MHz; CDCl₃): δ = 7.71 (d, J = 8.0 Hz, 2H), 7.61 (d, J = 8.9 Hz, 2H), 7.15 (d, J = 8.35 Hz, 2H), 6.96 (d, J = 8.9 Hz, 2H), 3.83 (s, 3H), 2.81 (s, 3H), 2.34 (s, 3H)

8b

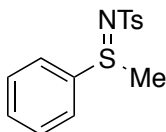


¹H NMR (500 MHz; CDCl₃): δ = 7.72 (d, J = 8.2 Hz, 2H), 7.57 (d, J = 8.2 Hz, 2H), 7.28 (d, J = 7.3 Hz, 2H), 7.16 (d, J = 8.1 Hz, 2H), 2.82 (s, 3H), 2.39 (s, 3H), 2.35 (s, 3H)

8c



¹H NMR (500 MHz; CDCl₃): δ = 7.73 (d, J = 8.0 Hz, 2H), 7.48-7.33 (m, 4H), 7.17 (d, J = 8.1 Hz, 2H), 2.82 (s, 3H), 2.36 (s, 3H), 2.35 (s, 3H)

8d

^1H NMR (500 MHz; CDCl_3): δ = 7.72 (d, J = 7.8 Hz, 2H), 7.55-7.46 (m, 5H), 7.16 (d, J = 8.1 Hz, 2H), 2.83 (s, 3H), 2.34 (s, 3H)

The ^1H NMR listings above for products **8a-8d** matched those of characterized compounds.^{9b}

7. Observation of Catalytic Resting States.

To a semi-micro anaerobic cuvette, 8 μL of P411_{BM3}CIS I263A T438S (400 μM) was added. To obtain a spectrum of the ferric protein, 0.5 mL of degassed phosphate buffer was added to the cuvette and the visible spectrum was recorded from 650 to 400 nm. To obtain a spectrum of the ferrous protein, the cuvette was sealed with a cap equipped with rubber septa and the headspace of the cuvette was purged with a gentle stream of Ar for 3 minutes. A solution of NADPH (5 mM) was added to a 6 mL crimp vial and made anaerobic by sparging with Ar for 5 minutes. The NADPH solution (0.5 mL) was then added to the anaerobic cuvette containing protein. Visible spectra of the protein sample are recorded until a stable ferrous state is reached. Representative spectra of the Fe(III)- and Fe(II)-protein are shown below (Figure S8 green and red lines, respectively).

To determine the resting state of the protein in the unproductive catalytic cycle, a degassed solution of tosyl azide (2 μL , 400 mM in DMSO) was added to a fully reduced

sample of ferrous protein. The visible spectrum of the protein shifted to the ferric heme immediately and remained unchanged for 20 minutes. The addition of an aliquot of organic solvent of similar volume did not cause the observed change in the iron oxidation state. At the end of 20 minutes (Figure S8, blue line), the cuvette was uncapped and the reaction mixture was worked up following the general procedure for small scale reactions. HPLC of the resulting solution confirmed that a substantial amount of azide is reduced to the corresponding sulfonamide.

To determine the resting state of the protein during the sulfimidation reaction, a degassed solution of sulfide **7a** (2 μ L, 400 mM in DMSO) was added to the cuvette containing P411_{BM3}CIS I263A T438S in the presence of NADPH. A visible absorbance spectrum of the mixture was recorded to ensure that the oxidation state of iron heme is unchanged. Next, a degassed solution of tosyl azide (2 μ L, 400 mM in DMSO) was added to the cuvette. Visible absorbance spectra of the solution were recorded at 5, 7, 12, 18, 22, 25, and 30 min (Figure S9). The appearance of ferrous heme is observed over time. HPLC confirmed formation of both sulfimide and sulfonamide.

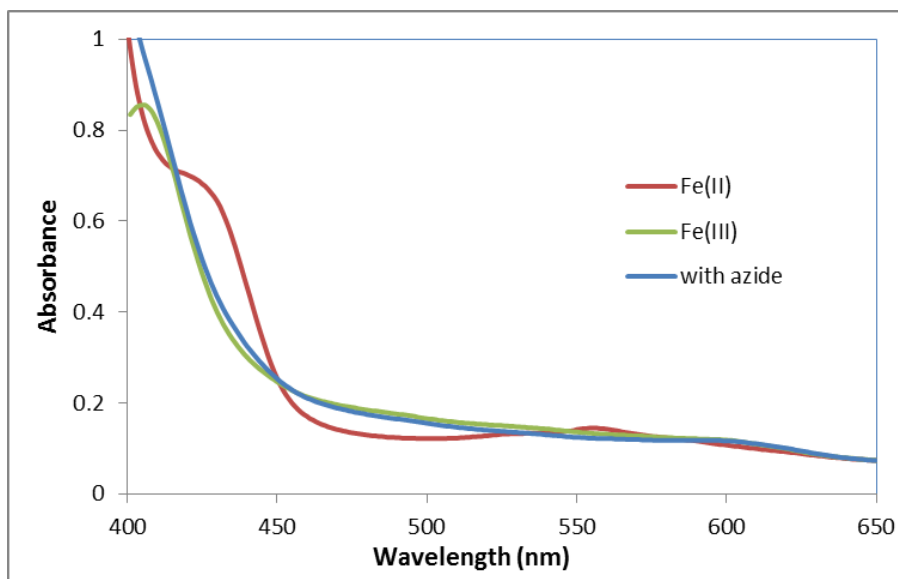


Figure S8. Visible spectroscopy of Fe(III) (green) and Fe(II)-P411_{BM3}CIS I263A T438S in the presence of NADPH (red), followed by azide addition (blue).

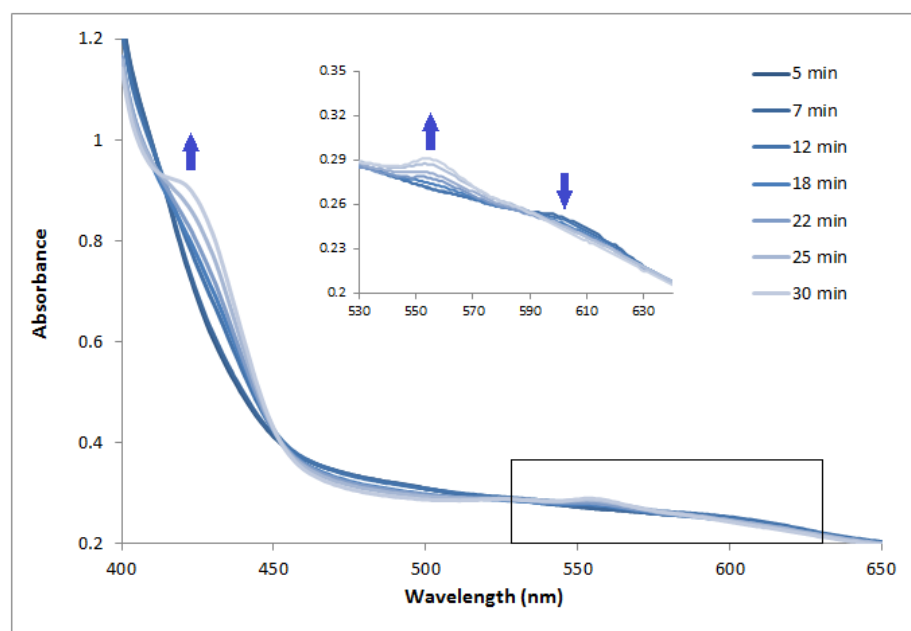


Figure S9. Monitoring the iron heme during the sulfimidation reaction with azide and sulfide. As shown in Figure S8, the Soret peak for the Fe(III) state is obscured by NADPH. Therefore the Q-band region (enlarged box from 530-640 nm) was used to assess the transition from Fe(III) to Fe(II) as the reaction proceeds as described in the supplemental text.

8. Excess sulfide and azide slow addition experiments.

To assess the impact of sulfide concentration on overall productivity of the reaction, sulfide was added to the reaction ranging from 0.5 eq to 4 eq relative to azide. 1 eq of azide denotes 1 mM in the small scale reactions described above. Results are plotted in Figure S10 below as a ratio of the TTN for sulfimide vs. TTN for sulfonamide. Slow addition was accomplished by adding 1 μ L of a 100 mM (100 nmol) tosyl azide solution (DMSO) at 15 minute intervals to a reaction set up, as described previously, with 0.4% catalyst loading and containing 2.5 mM **7a**. Azide was added over 150 minutes until equimolar final concentrations of sulfide and azide were achieved. Results of the slow addition are presented in Figure S11.

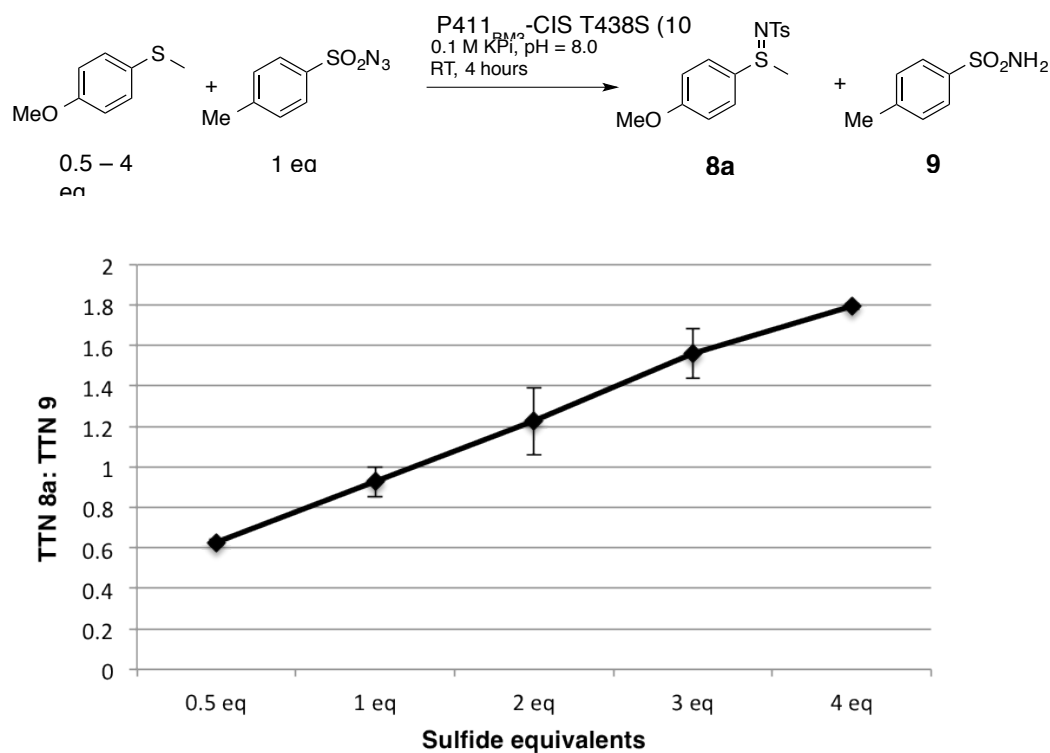


Figure S10. Ratio of sulfimide TTN to sulfonamide TTN as sulfide concentration is varied, using P411_{BM3}-CIS T438S enzyme, as shown in the scheme. Reactions were assembled as described above, with azide concentration held constant at 1 mM and sulfide concentration varied from 0.5 mM to 4 mM.

Table S6: Production of sulfimide **8a** and sulfonamide **9** in the presence of varying levels of sulfide acceptor substrate, as described above.

Sulfide	Azide	TTN 8a	TTN 9
0.5eq	1 eq	71	110
1 eq	1 eq	97	100
2 eq	1 eq	110	93
3 eq	1 eq	130	85
4 eq	1 eq	140	80

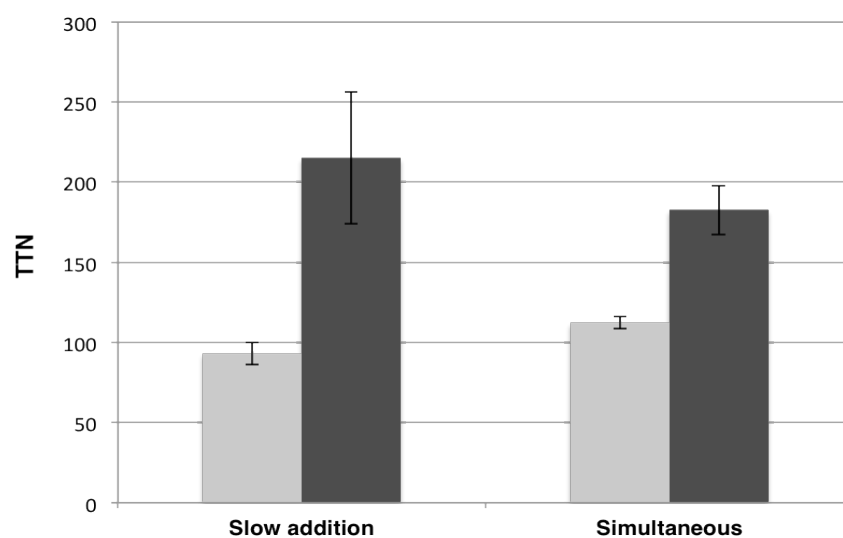


Figure S11. TTN values measured for slow addition vs. adding substrates simultaneously, using P411BM3-CIS T438S enzyme and the substrates shown in Figure S10. Light gray bar shows TTN for sulfonamide, **9**, dark gray shows TTN for the sulfimide, **8a**.

References

- (1) (a) Davies, H. M. L.; Manning, J. R. *Nature* **2008**, *451*, 417-424. (b) Paddon, C. J. *et al. Nature* **2013**, *496*, 528.
- (2) (a) Carreno, M. C. *Chem. Rev.* **1995**, *95*, 1717. (b) Fernandez, I.; Khair, N. *Chem. Rev.* **2003**, *103*, 3675.
- (3) (a) de Gonzalo, G.; *et al. Tetrahedron-Asymmetr.* **2006**, *17*, 130. (b) Feingersch, R. *et al. Appl. Environ. Microbiol.* **2008**, *74*, 1555. (c) Colonna, S.; Gaggero, N.; Pasta, P.; Ottolina, G. *Chem. Comm.* **1996**, 2303. (d) Allenmark, S. G.; Andersson, M. A. *Tetrahedron: Asymmetry* **1996**, *7*, 1089. (e) Colonna, S. *et al. Biochem.* **1990**, *29*, 10465-10468. (f) Colonna, S. *et al. J. Chem. Soc., Chem. Comm.* **1992**, 357. (g) Dai, L. H.; Klivanov, A. M. *Biotechnology and Bioengineering* **2000**, *70*, 353. (h) Fruetel, J. *et al. J. Am. Chem. Soc.* **1994**, *116*, 11643.
- (4) (a) Zhang, J. D. *et al. Appl. Microbiol. Biotechnol.* **2010**, *85*, 615. (b) Schallmeyer, A. *et al. Appl. Microbiol. Biotechnol.* **2011**, *89*, 1475. (c) Pordea, A. *et al. J. Am. Chem. Soc.* **2008**, *130*, 8085-8088. (d) O'Reilly, E. *et al. Catal. Sci. Technol.* **2013**, *3*, 1490. (e) Nikodinovic-Runic, J. *et al. Appl. Microbiol. Biotechnol.* **2013**, *97*, 4849.
- (5) (a) Bong, Y. K. *et al.*; WO Patent 2,011,071,982: 2011. (b) Ang, E. L. *et al.* WO Patent 2,012,078,800: 2012. (c) Huisman, G. W.; Collier, S. J. *Curr. Opin. Chem. Biol.* **2013**, *17*, 284.
- (6) (a) Raghavan, S.; Kumar, C. N. *Tetrahedron Lett.* **2006**, *47*, 1585. (b) Padwa, A.; Nara, S.; Wang, Q. *Tetrahedron Lett.* **2006**, *47*, 595.
- (7) (a) Thakur, V. V.; Kumar, N.; Sudalai, A. *Tetrahedron Lett.* **2004**, *45*, 2915. (b) Takada, H. *et al. Chirality* **2000**, *12*, 299.
- (8) (a) Gilchrist, T. L.; Moody, C. J. *Chem. Rev.* **1977**, *77*, 409. (b) Park, S.J. *et al. ChemMedChem* **2013**, *8*, 217. (c) Chen, X.Y.; Buschmann, H.; Bolm, C. *Synlett* **2012**, *23*, 2808.
- (9) (a) Collet, F.; Dodd, R. H.; Dauban, P. *Org. Lett.* **2008**, *10*, 5473. (b) Wang, J.; Frings, M.; Bolm, C. *Angew. Chem., Int. Ed.* **2013**, *52*, 8661.
- (10) Lücking, U. *Angew. Chem., Int. Ed.* **2013**, *52*, 9399.
- (11) (a) Murakami, M. *et al. Chirality* **2003**, *15*, 116. (b) Murakami, M.; Uchida, T.; Katsuki, T. *Tetrahedron Lett.* **2001**, *42*, 7071-7074. (c) Mancheno, O. G.; Bolm, C. *Org. Lett.* **2006**, *8*, 2349. (d) Mancheno, O. G.; Bolm, C. *Chem. – Eur. J.* **2007**, *13*, 6674. (e) Mancheno, O. G. *et al. Org. Lett.* **2009**, *11*, 2429.
- (12) (a) Cramer, S. A.; Jenkins, D. M. *J. Am. Chem. Soc.* **2011**, *133*, 19342. (b) Ruppel, J. V. *et al. Org. Lett.* **2008**, *10*, 1998. (c) Fiori, K.W.; Du Bois, J. *J. Am. Chem. Soc.* **2007**, *129*, 562.
- (13) (a) Coelho, P. S. *et al. Science* **2013**, *339*, 307. (b) Coelho, P. S.; *et al. Nat. Chem. Biol.* **2013**, *9*, 485. (c) McIntosh, J. A. *et al. Angew. Chem., Int. Ed.* **2013**, *52*, 9309. (d) Wang, Z. J. *et al. Chem. Sci.* **2014**, *5*, 598.
- (14) (a) Singh, R.; Bordeaux, M.; Fasan, R. *ACS Catal.* **2014**, *4*, 546. (b) Bordeaux, M.; Singh, R.; Fasan, R. *Bioorg. Med. Chem.* **2014** (In press).
- (15) Lewis, J. C. *et al. Chembiochem* **2010**, *11*, 2502.

- (16) (a) Watanabe, Y.; Iyanagi, T.; Oae, S. *Tetrahedron Lett.* **1982**, 23, 533. (b) Watanabe, Y.; Iyanagi, T.; Oae, S. *Tetrahedron Lett.* **1980**, 21, 3685.
- (17) Collet, F. *et al. Dalton Trans.* **2010**, 39, 10401.
- (18) Hansch, C.; Leo, A.; Taft, R. W. *Chem. Rev.* **1991**, 91, 165.
- (19) Kaspera, R. D. *et al. Biochem. Biophys. Res. Commun.* **2012**, 418, 464.
- (20) McIntosh, J. A.; Farwell, C. C.; Arnold, F. H. *Curr. Opin. Chem. Biol.* **2014**, 19, 126.
- (21) Daff, S. N. *et al. Biochem.* **1997**, 36, 13816-13823.
- (22) Berry, E. A.; Trumpower B. L. *Anal. Biochem.* **1987**, 161, 1.

*Chapter 4*ENZYME-CONTROLLED NITROGEN-ATOM TRANSFER ENABLES
REGIODIVERGENT C–H AMINATION

This chapter is published as T. K. Hyster, C. C. Farwell, A. R. Buller, J. A. McIntosh, F. H. Arnold “Enzyme-controlled nitrogen-atom transfer enables regiodivergent C–H amination.” in *Journal of the American Chemical Society*. 2014, *136*, 15505-15509. T.K.H synthesized all compounds, and performed initial rate experiments. I conducted enzyme characterization, library construction and screening, and crystallographic analysis of an engineered enzyme variant.

Abstract

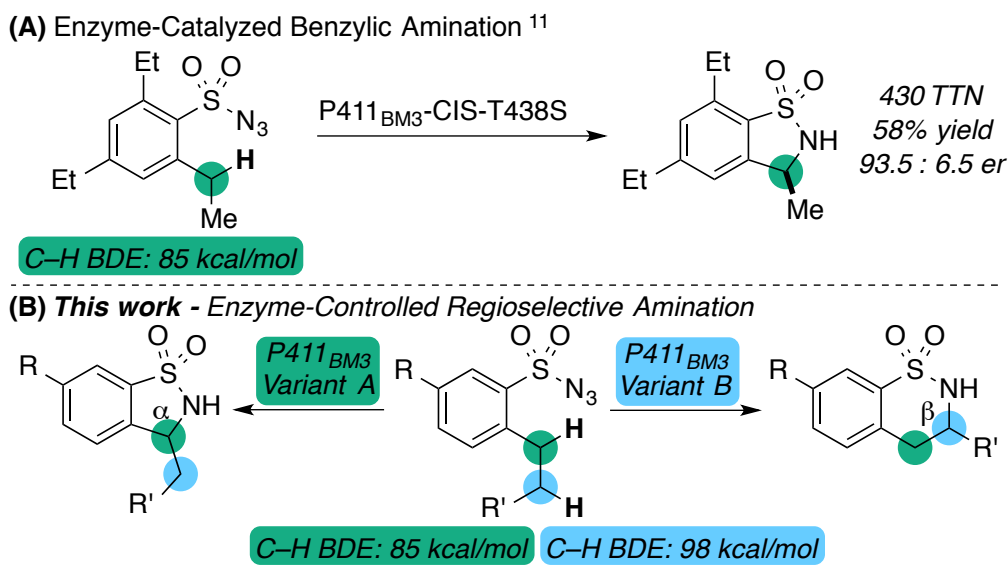
We recently demonstrated that variants of cytochrome P450_{BM3} (CYP102A1) catalyze the insertion of nitrogen species into benzylic C–H bonds to form new C–N bonds. An outstanding challenge in the field of C–H amination is catalyst-controlled regioselectivity. Here, we report two engineered variants of P450_{BM3} that provide divergent regioselectivity for C–H amination, one favoring amination of benzylic C–H bonds while the other favors homo-benzylic C–H bonds. The two variants provide nearly identical kinetic isotope effect (KIE) values (2.8-3.0) that suggest C–H abstraction is rate limiting. The 2.66-Å crystal structure of the most active enzyme suggests that the engineered active site can preorganize the substrate for reactivity. We hypothesize that the enzyme controls regioselectivity through localization of a single C–H bond close to the iron nitrenoid.

Main Text

The presence of nitrogen atoms in the vast majority of drugs drives the search for efficient and selective methods to form new C–N bonds.¹ Traditional approaches for forming aliphatic C–N bonds utilize the intrinsic nucleophilicity of nitrogen and the electrophilicity of a vast array of carbon species to facilitate bond formation.² Nature utilizes a similar reactivity profile, as exemplified by transaminase and amino acid dehydrogenase enzymes.³ An alternative means to C–N bond formation reverses the traditional reactivity profiles by utilizing an electrophilic nitrogen species.⁴ This is typically achieved *via* generation of a transition metal-bound nitrenoid intermediate that can react with alkenes, nucleophilic heteroatoms, and C–H bonds.⁵ This approach is attractive because new C–N bonds can be accessed directly from unactivated carbon atoms.

With the exception of the unusual cytochrome P450 TxtE-catalyzed nitration of tryptophan,⁶ the machinery to generate and use electrophilic nitrogen species has not been found in nature. Cytochrome P450s, however, have evolved to generate and use electrophilic oxygen species capable of reacting with alkenes, heteroatoms, and C–H bonds.⁷ This feat is possible because P450s can form a highly reactive iron-oxo intermediate known as compound I.⁸ Inspired by the similarity between compound I and the carbenoid and nitrenoid intermediates invoked in transition metal-catalyzed reactions, our group recently discovered that P450s could catalyze reactions thought to proceed through these intermediates.^{9,10,11,12}

C–H amination activity is particularly sensitive to the nature of the residue ligating the axial position of the iron-heme prosthetic group, with serine-ligated P411_{BM3} variants providing reactivity superior to cysteine-ligated variants in the amination of secondary benzylic C–H bonds (Scheme 1).¹¹ We refer to the serine-ligated enzymes as P411s, because the diagnostic Soret peak shifts from 450 nm (cysteine-ligated) to 411 nm and the enzymes no longer catalyze their native oxygenation reactions. Complementary work by Fasan showed that variants of P450_{BM3} and other hemoproteins bearing different axial ligands (cysteine, histidine, or tyrosine) will catalyze this type of transformation, although they require more activated tertiary benzylic C–H bonds to >50% yield.¹³ The need for relatively weak C–H bonds ($\text{BDE} \leq 85$) can be understood, in part, by considering the reaction mechanism.¹⁴ Iron-catalyzed aminations are understood to proceed *via* a mechanism in some ways reminiscent of P450-catalyzed C–H oxidation, where C–H bond cleavage generates a radical species that can rebound to form the new C–N bond.¹⁵ White found that the C–H cleavage is sensitive to bond strength, where C–H bonds with lower bond dissociation energies (BDE) are aminated preferentially to C–H bonds with greater BDE.¹⁶ Fasan corroborated this result using enzymes, reporting a linear relationship between reaction rate and C–H bond strength.^{13b}



Scheme 1. Enzyme-catalyzed C–H amination.

This observation indicates that it could be challenging to aminate strong C–H bonds of substrates having alternative, weak C–H bonds. Given that C–H amination is kinetically controlled, Du Bois found that substrate geometry can influence selectivity. Rather than substrate control, it would be more attractive to have selectivity controlled by the catalyst, such that different products could be generated from a single starting material, depending on the catalyst. In select examples, Du Bois and Katsuki found that modulating the steric properties of the ligand on rhodium and iridium catalysts can shift selectivity in favor of stronger, but less hindered, C–H bonds.¹⁷

We hypothesized that enzymes could provide an elegant solution to this regioselectivity challenge. Since P450s can be engineered to alter the regioselectivity of hydroxylation,¹⁸ we imagined that active site engineering could similarly generate catalysts with high selectivity for amination (Scheme 1). As a model system, we selected 2,5-di-*n*-propyl benzene sulfonyl azide **1** because it contains two potential sites for C–H

amination: the benzylic position (α -position) and the homo-benzylic position (β -position) with disparate C–H bond strengths (85 kcal/mol and 98 kcal/mol).¹⁹ Furthermore, Zhang showed that this substrate could undergo amination of both positions under cobalt-porphyrin catalysis, although amination of the α -position was favored.²⁰

We began by testing variants from our previous reports on C–H amination and sulfimination.^{11,21} The best variant was P411_{BM3}-CIS-T438S (15 mutations from wild type). It gave low activity with sulfonylazide 1 (32 TTN) (Table 1, entry 1), but was modestly selective for β -amination (84:16), establishing that a P411-based amination biocatalyst is capable of cleaving bonds significantly stronger than previously reported.

Expanded active sites have been key for superior reactivity in some of our previous studies.^{21,22} Unfortunately, low reactivity and selectivity were observed for mutants containing alanine mutations in the active site (Table 1, entries 2-4). We thus focused on engineering new variants for amination. We selected five positions in the active site, F87, L181, I263, T268, and T438, and screened libraries made by site-saturation mutagenesis at each position in the P411_{BM3}-CIS-T438S parent. Mutation at four of the positions failed to provide more-active variants. The I263 library, however, yielded a substantially improved enzyme: variant P411_{BM3}-CIS-T438S-I263F showed an 11-fold increase in activity and 97:3 selectivity favoring amination at the β -position (Table 1, entry 5). Reverting the previously identified activating mutations C400S and T268A decreased the desired reactivity, confirming their importance to catalysis (Table 1, entries 6-7).¹¹

Table 1. Comparison of activities (TTN) and regioselectivities of P411BM3 variants for the reaction of azide **1** to sultams **2** and **3**.

Reaction scheme: Azide **1** (1,3-dipropylbenzene-1,3-diazide) reacts with an enzyme at 25 °C, 12 hr to yield sultams **2** (1,3-dipropyl-2-methyl-1,2,3,4-tetrahydro-1,2,3-benzodithiazine 1,1-dioxide) and **3** (1,3-dipropyl-2-ethyl-1,2,3,4-tetrahydro-1,2,3-benzodithiazine 1,1-dioxide).

Entry	Catalyst	TTN	2:3
1	P411 _{BM3} -CIS-T438S	32	84:16
2	P411 _{BM3} -H2-5-F10	56	53:47
3	P411 _{BM3} -H2-4-D4	19	66:44
4	P411 _{BM3} -H2-A10	31	44:54
5	P411_{BM3}-CIS-T438S-I263F	361	97:3
6	P450 _{BM3} -CIS-T438S-I263F	<1	n.d.
7	P411 _{BM3} -CIS-T438S-I263F-A268T	12	33:64
8	P411 _{BM3} -CIS-T438S-F87A	70	25:75
9	P411_{BM3}-T268A-F87A	187	30:70
10	P411 _{BM3} -B1-T268A-M263I	35	38:62
11	P411 _{BM3} -Man1-T268A	7	34:66
12	P411 _{BM3} -T268A-F87V	25	99:1
13	P411 _{BM3} -CIS-T438S-I263F-F87A	10	66:34

In the course of screening site saturation mutagenesis libraries, F87A was identified as a mutation that switched selectivity to favor amination at the α -position, albeit with low turnover (Table 1, entry 8). Since F87A is present in many P450_{BM3} variants engineered as hydroxylation catalysts, we elected to screen a set of F87A variants to determine if this mutation would continue to provide selectivity for the α -

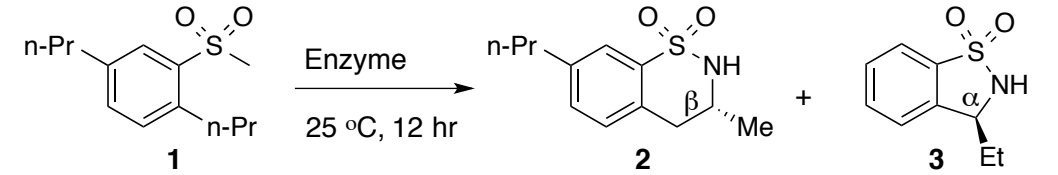
position in those variants and whether the additional mutations could further increase activity. In all cases tested, the F87A mutation favored α -amination, albeit with low levels of activity (Table 1, entries 9-11). The most active variant is P411_{BM3}-T268A-F87A (3 mutations from wild type), providing 187 TTNs and modest selectivity (30:70 (2:3)) for the α -amination product (Table 1, entry 9). Reverting the F87A mutation to F87V (the mutation present in the P411_{BM3}-CIS backbone) switched the selectivity to the to 6-position, demonstrating the importance of the residue at this position for controlling C-H amination regioselectivity (Table 1, entry 12). We were also interested in testing the impact of F87A in the presence of the I263F mutation. The double F87A+I263F variant continued to be selective for β -amination, but with substantially decreased selectivity and activity (Table 1, entry 13). These results support the lynchpin role of the F87 position in controlling the regioselectivity of amination.

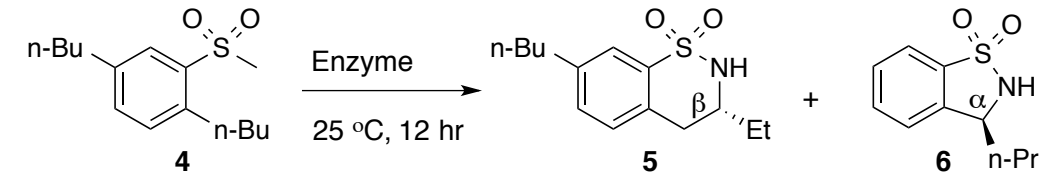
Having identified two enzyme variants with divergent regioselectivity, P411_{BM3}-CIS-T438S-I263F and P411_{BM3}-T268A-F87A, we then explored the ability of these enzymes to control regioselectivity and enantioselectivity on different substrates (Table 2). In addition to providing excellent regioselectivity, P411_{BM3}-CIS-T438S-I263F and P411_{BM3}-T268A-F87A furnished sultams **2** and **3** with excellent enantioselectivity (99.5:0.5 er in both cases) (Table 2, entries 1 and 2). These enzymes are effective at controlling regioselectivity for substrates bearing longer alkyl chains, although with diminished activity (Table 2, entry 4). Surprisingly, P411_{BM3}-T268A-F87A affords even greater regioselectivity (3:97 (**5:6**)) for α -amination on these substrates when compared to the parent substrate (Table 3, entry 5). Changing the substituent on the aromatic ring

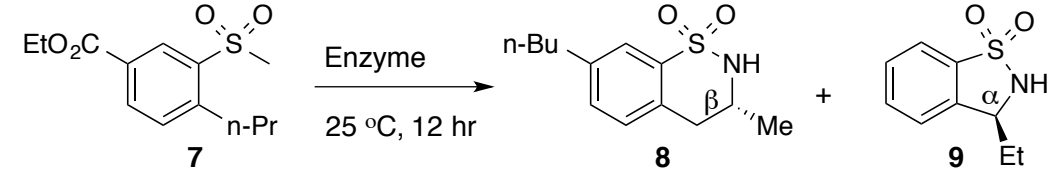
from an alkyl group to an ester did not negatively impact the reaction. The two variants continued to strongly favor their respective regioisomers with good yields and comparable enantioselectivities (Table 2, entries 5 and 6).

In order to gain insight into how these enzymes determine regioselectivity, we considered the possibility of mechanistic differences between amination at the α -position and β -position. To probe this, we measured the kinetic isotope effects with **1** and **D₁₄-1**. When P411_{BM3}-CIS-T438S-I263F was tested, a ¹H-KIE value of 2.8 was observed, whereas P411_{BM3}-T268A-F87A afforded a ¹H-KIE value of 3.0 (Figures S1 and S2). These values are consistent with C–H abstraction being rate-determining in the catalytic cycle and suggest a similar C–H cleavage mechanism despite the divergent selectivities. Since C–H abstraction is kinetically controlled, reactivity depends on the proximity of the C–H bond to the metal nitrenoid. In light of the exquisite regio- and enantioselectivities provided by the two P411 variants, we hypothesize that the enzyme active sites situate the substrate such that a different C–H bond is kinetically accessible in each variant.

Table 2. Comparison of activities (TTN), regioselectivities, and enantioselectivities for azides **1**, **4**, and **7** with P411_{BM3}-CIS-T438S-I263F and P411_{BM3}-T268A-F87A

				
Variant	TTN	Selectivity 2:3	e.r. ^a (2)	e.r. (3)
P411 _{BM3} -CIS-T438S-I263F	361	97:3	99.5 : 0.5	
P411 _{BM3} -T268A-F87A	187	30:70		99 : 1

				
Variant	TTN	Selectivity 5:6	e.r. ^a (5)	e.r. (6)
P411 _{BM3} -CIS-T438S-I263F	178	90:10	99.5 : 0.5	
P411 _{BM3} -T268A-F87A	128	3:97		99.5 : 0.5

				
Variant	TTN	Selectivity 8:9	e.r. ^a (8)	e.r. (9)
P411 _{BM3} -CIS-T438S-I263F	192	95:5	98.5 : 1.5	
P411 _{BM3} -T268A-F87A	130	5:95		99.5 : 0.5

^a e.r. = enantiomeric ratio.

To aid in understanding how the active site architecture of these P411 enzymes controls regioselectivity, we pursued their structural characterization through X-ray crystallography. Although high-quality crystals of P411_{BM3}-T268A-F87A were not forthcoming, crystals of P411_{BM3}-CIS-T438S-I263F diffracted to 2.66 Å and molecular replacement readily yielded a structure. This new structure represents a substantial improvement on the previously reported P411_{BM3}-CIS structure, which was determined at 3.3 Å-resolution.^{12a} The global features remain identical, but the higher resolution data enable more-accurate placement of the side chains lining the active site, the heme vinyl and propionate moieties, and the position of the L437 sidechain (Figure S3).^{12a} Importantly, the F263 sidechain is resolved and populates a non-favored rotamer extending into the active site. Interestingly, the location of the F263 sidechain does not substantially change the location of the I-helix (on which F263 resides) by comparison to the I263 parent. It does, however, cause repacking of the flanking residues on the F-helix (Figure S3). Alignment of the structure of P411_{BM3}-CIS-T438S-I263F with that of wild-type P450_{BM3} bound to palmitoic acid shows that I263F occludes binding of the native substrate. This is consistent with previous reports that showed that the I263F mutation shut down the native hydroxylation activity.²³ Docking the sultam product into the active site clearly demonstrates that I263F is positioned to pack against the benzene ring of the substrate. These complementary van Der Waals interactions could decrease the conformational freedom of the nitrenoid intermediate and thereby promote reactivity at the higher-energy C–H bond (Figure S5).

In summary, we have discovered two P411_{BM3} variants that offer different and complementary regioselectivities for C–H amination. Mutation at the F87 position is crucial for controlling selectivity, with F87V favoring the β -amination of 2,5-disubstituted benzene sulfonyl azides, whereas F87A favors α -amination. Introduction of phenylalanine at position I263 provides a 11-fold increase in β -amination activity. Given that the C–H cleavage is rate-limiting, regioselectivity is likely kinetically controlled, wherein the C–H bond cleaved is the one closest to the iron-nitrenoid, as dictated by the enzyme. Crystallographic analysis reveals that the I263F mutation has little effect on the secondary and tertiary structure of the protein and primarily decreases the volume of the active site.

While catalyst-controlled divergent regioselectivity remains a challenge for small molecule catalysts, enzyme catalysts can be readily engineered by mutagenesis and screening for the desired selectivity. Combined with their ability to take on non-natural activities such as direct C–H amination, enzymes represent a versatile platform for catalyst development to solve challenging selectivity problems in organic chemistry.

Supplementary Materials for

Enantioselective Imidation of Sulfides via Enzyme-Catalyzed Intermolecular Nitrogen-Atom Transfer

Contents	Page
1. Materials and Methods	98
2. Determination of Initial Reaction Rates	99
2. Crystal Structure of P411BM3-CIS T438S I263F	101
3. Synthetic Procedures	107

1. Materials and Methods

Small scale reaction conditions were as described in Chapter 2. Protein expression, purification, and molecular cloning protocols were performed as described in Chapter 3.

Reaction screening in 96-well plate format. Site-saturation libraries were generated by employing the “22-codon” method.²⁴ *E. coli* libraries were generated and culture in 200 μ L of LB_{AMP} and stored as glycerol stocks at -80 °C in 96-well plates. 50 μ L of the preculture was transferred to a 1200 μ L of Hyperbroth using a multichannel pipette. The cultures were incubated at 37 °C, 200 rpm, 80% humidity until the OD₆₀₀ = 4 (approx. 2.5 hours). The plates were cooled on ice for 30 minutes before expression was induced (0.5 mM IPTG, 1 mM Ala final concentration. Expression was conducted at 20 °C, 180 rpm, 20 hours. The cells were pelleted (4000 x g, 10 min, 4 °C) and the 96-well plate was transferred to an anaerobic chamber. The pellets were resuspended in 300 μ L argon sparged reaction buffer (4:1 M9-N/glucose (250 mM)). GOX solution (10x, 40 μ L/well) was added to each well followed by azide **1** (100 mM, 10 μ L/well). The plate was sealed with aluminum sealing tape, removed from the anaerobic chamber, and shaken at 40 rpm. After 12 hours, the seal was removed and 500 μ L of acetonitrile and 10 μ L of standard (10 mM) were added to each well. The plate was vortexed and centrifuged (4000g, 30 minutes) and 500 μ L aliquots were transferred to a shallow-well plate for analysis by HPLC.

TABLE S1: Mutations (relative to wild-type P450_{BM3}) in enzymes used in this study.

Enzyme	Mutations relative to wild-type P450 _{BM3}
P450 _{BM3}	None
P411 _{BM3} -T268A	C400S-T268A
P450 _{BM3} -CIS	V78A, F87V, P142S, T175I, A184V, S226R, H236Q, E252G, T268A, A290V, L353V, I366V, E442K
P411 _{BM3} -CIS	P450 _{BM3} -CIS C400S
P411 _{BM3} -H2-5-F10	P411 _{BM3} -CIS L75A, I263A, L437A
P411 _{BM3} -H2-4-D4	P411 _{BM3} -CIS M177A, L181A, L437A
P411 _{BM3} -H2-A10	P411 _{BM3} -CIS L75A, L181A
P411 _{BM3} -CIS-T438S	P411 _{BM3} -CIS T438S
P411 _{BM3} -CIS-T438S-I263F	P411 _{BM3} -CIS T438S, I263F
P411 _{BM3} -CIS-T438S-I263F-A268T	P411 _{BM3} -CIS T438S, I263F, A268T
P450 _{BM3} -CIS-T438S-I263F	P450 _{BM3} -CIS T438S, I263F
P411 _{BM3} -MAN1-T268A	V78A, F81L, A82T, F87A, P142S, T175I, A184V, F205C, S226R, H236Q, E252G, R255S, A290V, L353V, C400S
P411 _{BM3} -MAN1-T268A-M263I	V78L, F87A, P142S, T175I, A184T, F205C, S226R, H236Q, E252G, R255S, A290V, G315S, A330V, L353V, T268A, C400S
P411 _{BM3} -T268A-F87A	C400S-T268A-F87A
P411 _{BM3} -T268A-F87V	C400S-T268A-F87V
P411 _{BM3} -CIS-T438S-I263F-F87A	P411 _{BM3} -CIS T438S, I263F

2. Determination of reaction rates

Determination of initial rates. All initial rate experiments were set up in an anaerobic chamber. Four 2-ml vials were charged with a stir bar, GOX 10x (40 μ L), glucose (250 mM, 40 μ L), NADPH (20 mM, 40 μ L), and KPi (pH = 8.0, 0.1 M, 260 μ L). The vials were sealed with a silicon crimp cap and removed from the anaerobic chamber. The reactions were placed on a stir plate and charged with azide **1** or azide **1'** (100 mM, 10 μ L). The reactions were quenched at 2-3 minute intervals over 8-12 minutes by

decapping and adding acetone (500 μ L) and internal standard (1,3,5-trimethoxybenzene 10 mM, 10 μ L). After 5 minutes of stirring, the reaction mixtures were transferred to 1.8 mL tubes, which were vortexed and centrifuged (14,000 \times g, 10 min). The supernatant was transferred to a vial for analysis by HPLC. Kinetic isotope effects for P411_{BM3}-CIS-T438S-I263F and P411_{BM3}-T268A-F87A are plotted in Figures S2 and S3.

Figure S1. Initial Rate Plots of Azide **1** (blue diamonds) and Azide **1'** (red squares) with P411_{BM3}-CIS-T438S-I263F. Each point is an average of 3 runs.

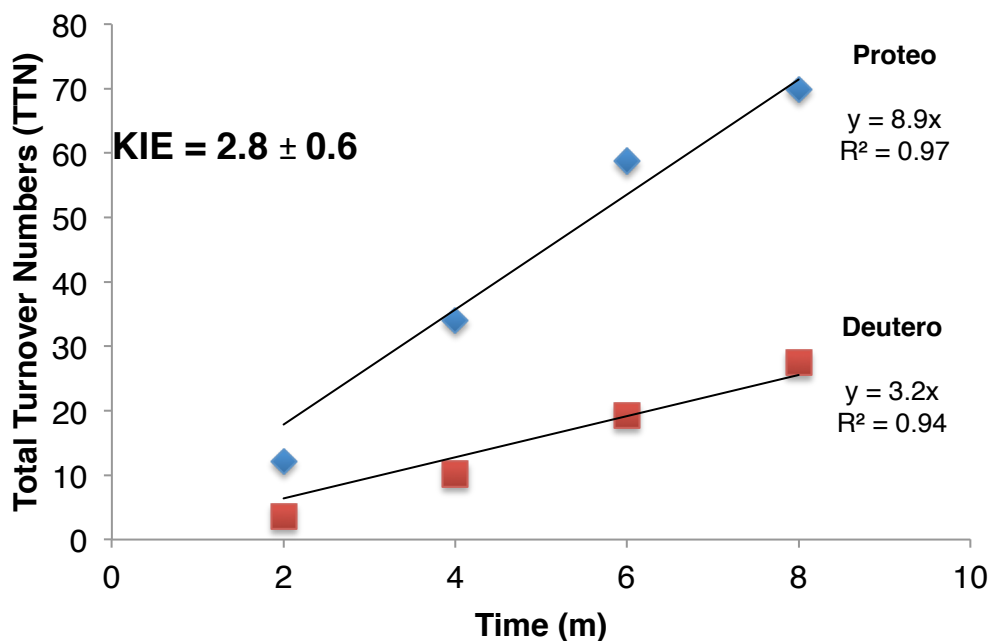
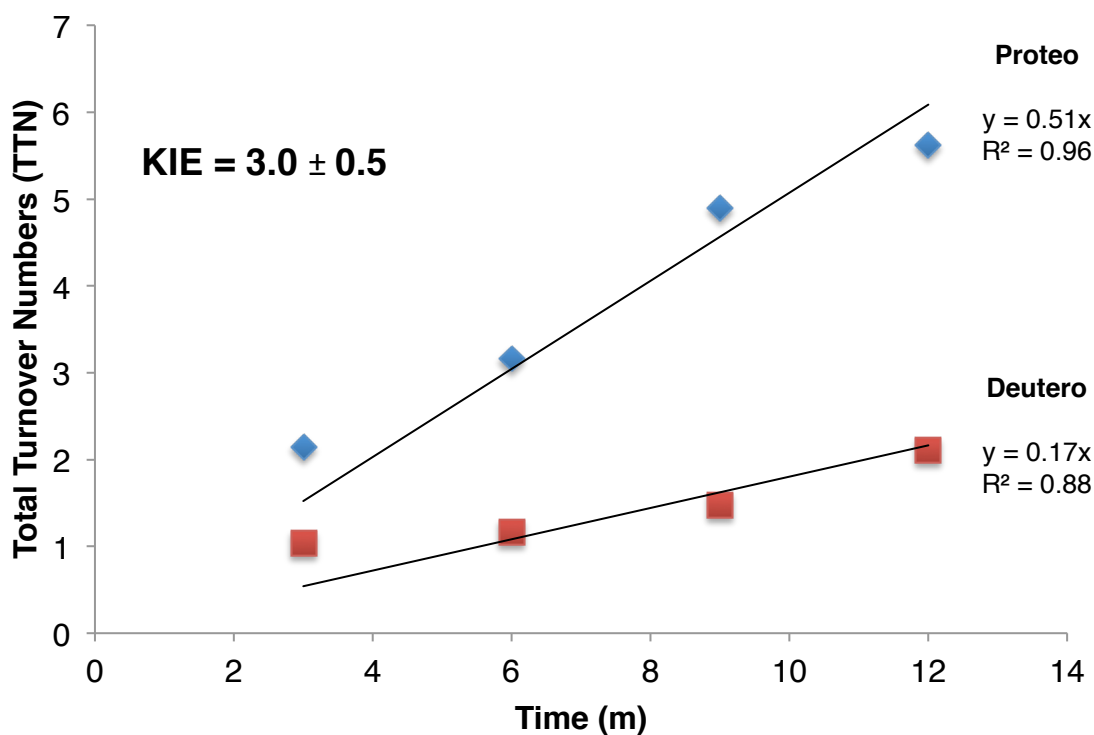


Figure S2. Initial Rate Plots of Azide **1** (blue diamonds) and Azide **1'** (red squares) with P411_{BM3}-T268A-F87A. Each point is an average of 3 runs.



3. Crystal structure of P411_{BM3}-CIS-T438S-I263F

Crystallization, data collection, and structure determination. The heme domain of P411_{BM3}-CIS-T438S-I263F was purified, flash frozen in liquid N₂, and stored at -80 °C until crystallization. Sitting drop vapor diffusion experiments were performed by generating a 1:1 mixture of protein stock (12 mg/mL in 0.1 M KPi, pH = 8.0) and well solution in a 96-well sitting-drop plate with a final drop volume of 0.4 μ L and a reservoir volume of 400 μ L. Crystals grew over 5-10 days in 0.1 M Tris/HCl (pH = 7.0), 2.0 M ammonium sulfate, 0.2 M lithium sulfate. Crystals were cryoprotected by immersion into well solution with 20% glycerol before being flash-frozen in liquid N₂. Diffraction data

were collected on the Stanford Synchrotron Radiation Laboratory Beamline 12-2. Data were processed using XDS in the spacegroup $P4_22_12$ to 2.66 Å resolution.²⁵

The structure of P411_{BM3}-CIS-T438S-I263F was solved by molecular replacement using the Phaser program,²⁶ as implemented in CCP4,²⁷ using the P411_{BM3}-CIS structure [PDB ID: 4H23] as the search model. Model building was performed in Coot and restrained refinement in Refmac5.²⁸ Model quality was assessed with the MolProbity online server.²⁹ TLS operators were included in the last round of refinement.³⁰ Crystallographic and model statistics are described in Table S1.

Table S2. Data processing and refinement statistics

Data processing	P411BM3-CIS-T438S-I263F
Wavelength	
Spacegroup	P4 ₂ 2 ₁ 2
Unit cell dimensions	= 90°
a = b , c	206.9 , 119.39
$\alpha = \beta = \gamma$	90
Beamline	SSRL 12-2
Wavelength	0.9795 Å
Resolution (Å)	39.1 – 2.66
Last bin (Å)	2.8 – 2.66
Number of Observations	1,031,477
Completeness (%)	100 (100)
R _{meas} (%)	0.25 (2.1)
R _{pim} (%)	0.067 (0.550)
I/σI	11.0 (1.44)
CC1/2	0.996 (0.534)
Redundancy	13.8 (14.5)
Refinement	
Number of reflections	70732
Number of atoms	10947
Last bin (Å)	2.73 – 2.66
R _{work}	19.7 (34.7)
R _{free}	23.5 (37.5)
Average B factor (Å ²)	36.2
Ramachandran Plot	
Most favored (%)	96.4
Allowed (%)	99.9
Outliers (%)	0.1

Values in parenthesis are for the highest resolution shell;

R_{merge} is $\Sigma |I_o - I| / \Sigma I_o$, where I_o is the intensity of an individual reflection, and I is the mean intensity for multiply recorded reflections;

R_{pim} is $1/(N-1) \Sigma |I_o - I| / \Sigma I_o$, where N is the number of observations for a given reflection;

R_{work} is $\|F_o - F_c\| / F_o$, where F_o is an observed amplitude and F_c a calculated amplitude;

R_{free} is the same statistic calculated over a 5.1% subset of the data that has not been included during refinement.

Figure S3. P411_{BM3}-CIS-T438S-I263F (blue) and P411_{BM3}-CIS-T438S (green) overlaid with key residues displayed and labeled.

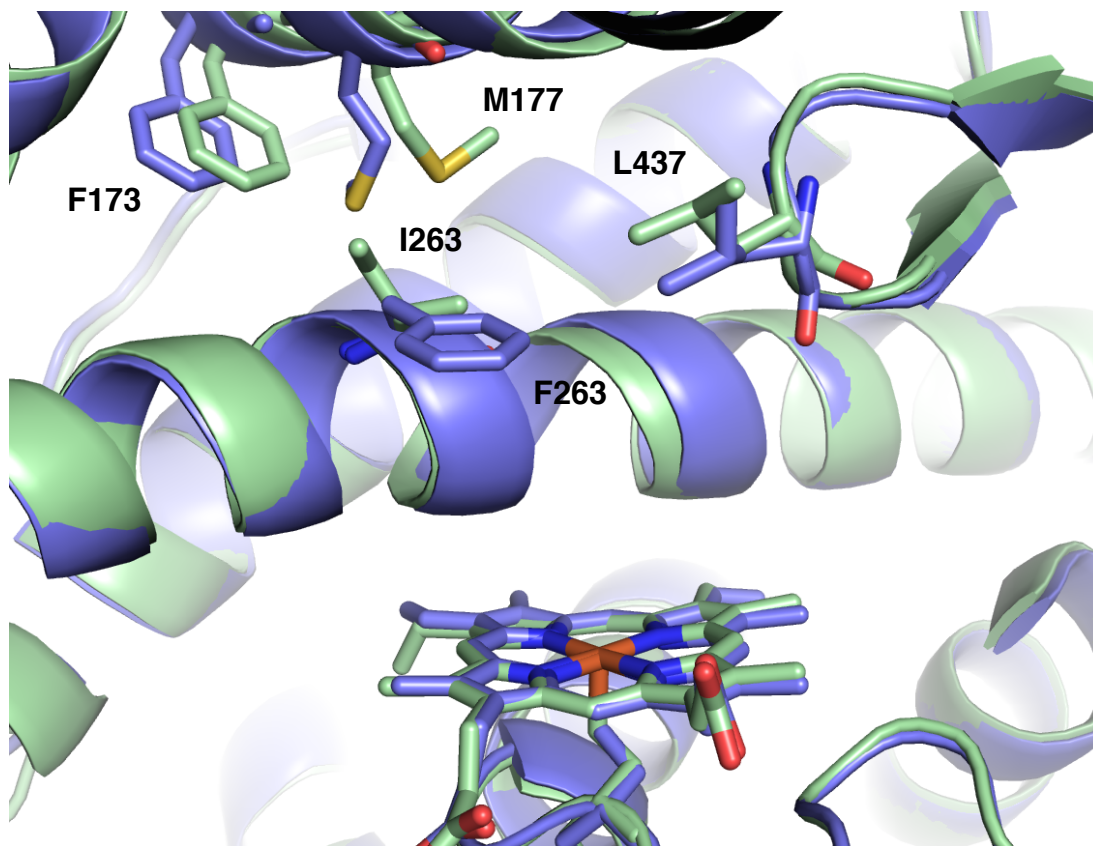


Figure S4. (Left) P411_{BM3}-CIS-T438S-I263F (blue) occluding C16-C18 of PAM. **(Right)** and P450_{BM3} (green) containing PAM.

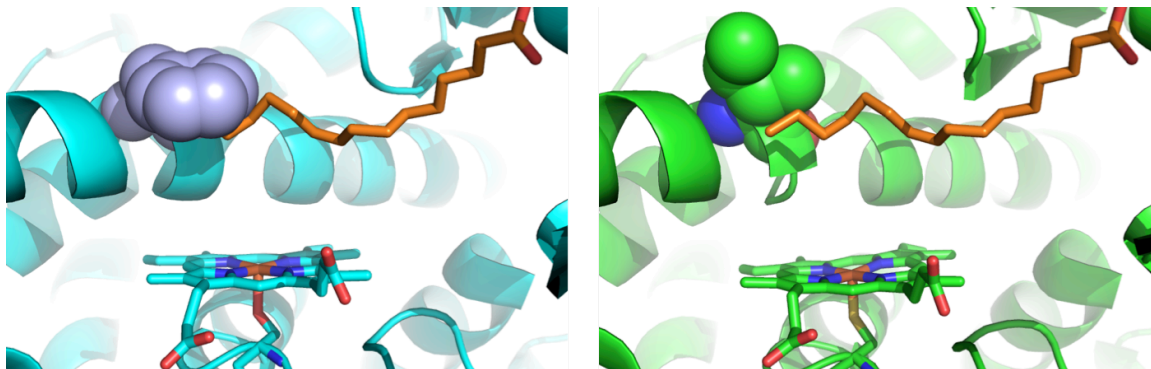
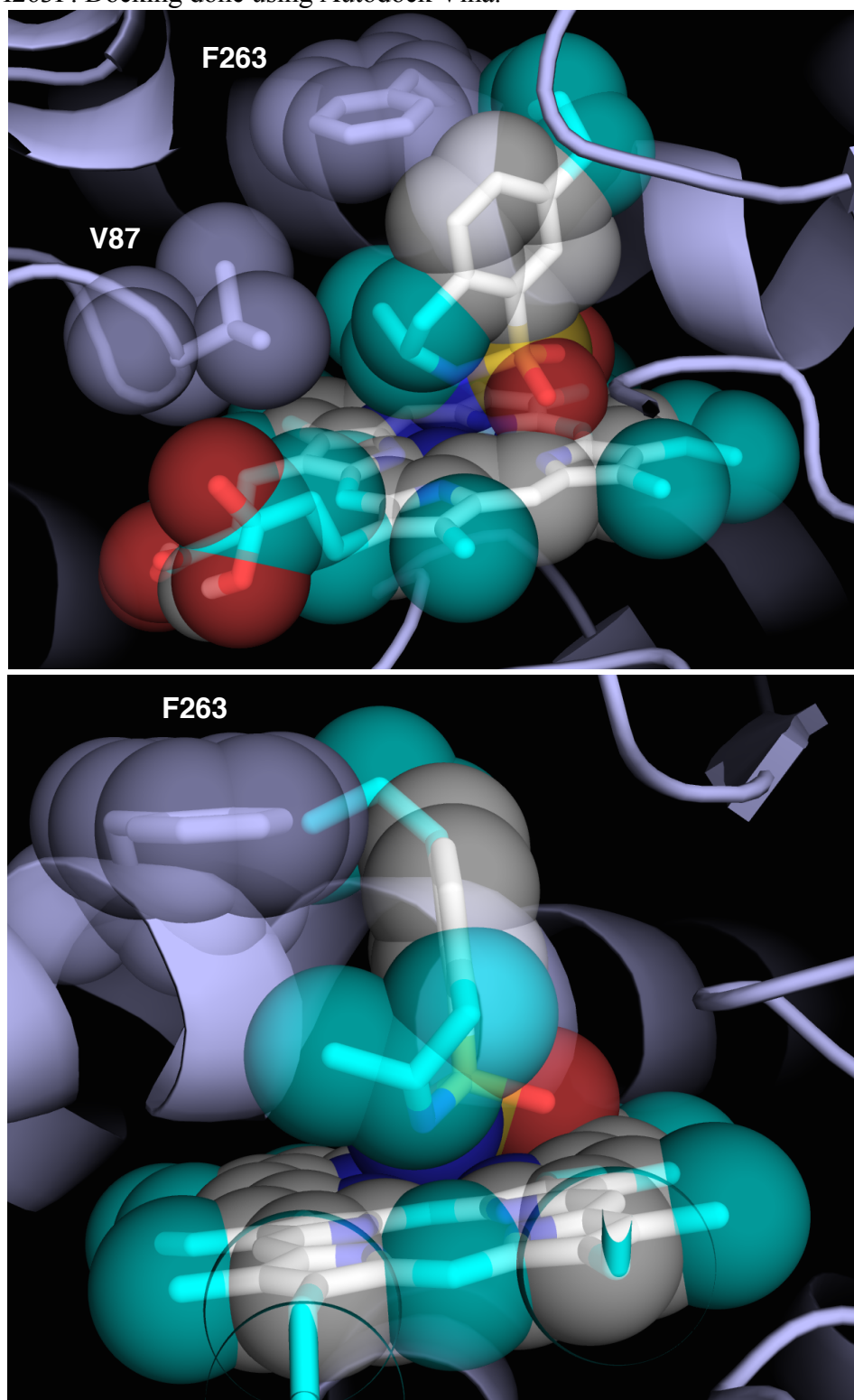
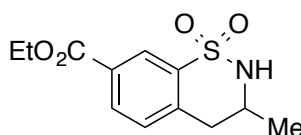


Figure S5. Docking Model of Sultam **3** covalently bound to heme with P411_{BM3}-CIS-T438S-I263F. Docking done using Autodock Vina.³¹



4. Synthetic Procedures

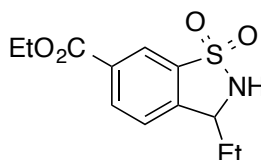
Sultams **2** and **3** were previously reported by Katsuki.³²



ethyl 3-methyl-3,4-dihydro-2H-benzo[e][1,2]thiazine-7-carboxylate 1,1-dioxide (9)

¹H 500 MHz (DMSO *d*₆): 8.17 (d, 1H, *J* = 1.8 Hz), 8.06 (d, 1H, *J* = 1.8, 8.2 Hz), 7.53 (m, 2H), 4.34 (q, 2H, *J* = 7.25 Hz), 3.83 (m, 1H), 3.06 (dd, 1H, *J* = 17.6, 3.7 Hz), 2.79 (dd, 1H, *J* = 17.6, 11.4 Hz), 1.34 (3H, t, *J* = 7.1 Hz), 1.28 (3H, d, *J* = 6.6 Hz).

¹³C 125 MHz (DMSO *d*₆): 164.4, 141.4, 137.9, 131.8, 130.7, 128.9, 123.7, 61.3, 48.6, 34.9, 21.0, 14.1.



ethyl 3-ethyl-2,3-dihydrobenzo[d]isothiazole-6-carboxylate 1,1-dioxide (10)

¹H 500 MHz (DMSO *d*₆): 8.23 (dd, 1H, *J* = 8.1, 1.5 Hz), 8.20 (d, 1H, *J* = 1.5 Hz), 8.16 (d, 1H, *J* = 4.2 Hz), 7.77 (d, 1H, *J* = 8.1 Hz), 4.72 (ap p, 1H, *J* = 4.0 Hz), 4.37 (q, 2H, *J* = 7.1 Hz), 1.97 (m, 1H), 1.68 (m, 1H), 1.35 (t, 3H, *J* = 7.1 Hz), 0.90 (t, 3H, *J* = 7.3 Hz).

¹³C 125 MHz (DMSO *d*₆): 164.3, 145.3, 136.9, 133.3, 131.1, 125.7, 121.1, 61.5, 58.2, 27.9, 14.1, 9.8.

REFERENCES

- (1) Roughley, S. D.; Jordan, A. M. *J. Med. Chem.* **2011**, *54*, 3451. (b) Carey, J. S.; et al. *Org. Biomol. Chem.* **2006**, *4*, 2337.
- (2) Baxter, E. W.; Reitz, A. B. *Organic Reactions* **2002**, *59*, 1.
- (3) (a) Matthew, S.; Yun, H. *ACS Catalysis* **2012**, *2*, 993. (b) Heberling, M. M.; Wu, B.; Bartsch, S.; Janssen, D. B. *Curr. Opin., Chem. Biol.* **2013**, *17*, 250. (c) Turner, N. J. *Curr. Opin. Chem. Biol.* **2011**, *15*, 234.
- (4) Driver, T. G. *Nat. Chem.* **2013**, *5*, 736.
- (5) (a) Davies, H. M. L.; Manning J. R. *Nature* **2008**, *451*, 417. (b) Muller, P.; Fruit, V. *Chem. Rev.* **2003**, *103*, 2905. (b) Halfen, J. A. *Curr. Org. Chem.* **2005**, *9*, 657.
- (6) (a) Barry, S. M. et al. *Nat. Chem. Biol.* **2012**, *8*, 814. (b) Dodani, S. C; et. al. *ChemBioChem* **2014** DOI: 10.1002/cbic.201402241.
- (7) (a) McIntosh, J. A.; Farwell, C. C.; Arnold, F. H. *Curr. Opin. Chem. Biol.* **2014**, *19*, 126. (b) Fasan, R. *ACS Catal.* **2012**, *2*, 647. (c) Lewis, J. C.; Coelho, P. S.; Arnold, F. H. *Chem. Soc. Rev.* **2011**, *40*, 2003. (d) Jung, S. T.; Lauchli, R.; Arnold, F. H. *Curr. Opin. Biotech.* **2011**, *22*, 201.
- (8) (a) Schlichting, L. et al. *Science* **2000**, *287*, 1615-1622. (b) Rittle, J.; Green, M. T. *Science* **2010**, *330*, 933. (c) Montellano, P. R. O. *Chem. Rev.* **2010**, *110*, 932. (d) Whitehouse, C. J.; Bell, S. G.; Wong, L. L. *Chem. Soc. Rev.* **2012**, *41*, 1218.
- (9) (a) Kornecki, K. P. et al. *Science* **2013**, *342*, 351. (b) Fischer, E. O.; Dötz, K. H. *Chem. Ber.* **1970**, *103*, 1273. (c) Hyster, T. K.; Arnold, F. H. *Isr. J. Chem.* **2014**, DOI:10.1002/ijch.201400080.
- (10) Coelho, P. S.; et al. *Science* **2013**, *339*, 307.
- (11) McIntosh, J. A. et al. *Angew. Chem.-Int. Ed.* **2013**, *52*, 9309.
- (12) (a) Coelho, P. S. et al. *Nat. Chem. Biol.* **2013**, *9*, 485. (b) Wang, Z. J. et al. *Angew. Chem. Int. Ed.* **2014**, *126*, 6928. (c) Heel, T. et al. *ChemBioChem* **2014**, *15*, 2556.
- (13) (a) Singh, R.; Bordeaux, M.; Fasan, R. *ACS Catalysis* **2014**, *4*, 546. (b) Bordeaux, M.; Singh, R.; Fasan, R. *Bioorg. Med. Chem.* **2014** DOI: 10.1016/j.bmc.2014.05.015.
- (14) Matthew, M. L. et al. *J. M. Nat. Chem. Biol.* **2014**, *10*, 209.
- (15) (a) Mansuy, D. et al. *J. Chem. Soc., Chem. Commun.* **1984**, 1161. (b) Mahy, J. P.; et al. *Tetrahedron Lett.* **1988**, *29*, 1927. (c) Moreau, Y.; et al. *J. Phys. Chem. B* **2007**, *111*, 10288. (d) Lu, H.; et al. *Organometallics* **2010**, *29*, 389. (e) Lu, H.; et al. *Angew. Chem.-Int. Ed.* **2010**, *49*, 10192. (f) Badieli, Y. M. et al. *Angew. Chem.-Int. Ed.* **2008**, *47*, 9961.
- (16) Paradine, S. M.; White, M. C. *J. Am. Chem. Soc.* **2012**, *134*, 2036.
- (17) (a) Fiori, K. W.; Fleming, J. J.; Du Bois, J. *Angew. Chem.-Int. Ed.* **2004**, *43*, 4349. (b) Ichinose, M.; et al. *Angew. Chem. Int. Ed.* **2011**, *50*, 9884.
- (18) (a) Kolev, J. N.; et al. *ChemBioChem* **2014**, *15*, 1001. (b) Kolev, J. N.; et al. *ACS Chem. Biol.* **2014**, *9*, 164. (c) Dennig, A.; et al. *Angew. Chem.-Int. Ed.* **2013**, *52*, 8459. (d) Zhang, K.; et al. *J. Am. Chem. Soc.* **2012**, *134*, 18695. (e) Zhang, K.; Damaty, S. E.; Fasan, R. *J. Am. Chem. Soc.* **2011**, *133*, 3242. (f) Peters, M. W.; et al. *J. Am. Chem. Soc.* **2003**, *125*, 13442. (g) Cirino, P. C.; Arnold, F. H. *Adv. Synth. Catal.* **2002**, *344*, 932.
- (19) *CRC Handbook of Chemistry and Physics*, 91st ed.; Haynes, W. M., Ed.; CRC Press: Boca Raton, FL, 2010; pp 9–65.

- (20) Ruppel, J. V.; Kamble, R. M.; Zhang, X. P. *Org. Lett.* **2007**, *9*, 4889.
- (21) Farwell, C. C.; et al. *J. Am. Chem. Soc.* **2014**, *136*, 8766.
- (22) (a) Lewis, J. C.; et al. *ChemBioChem* **2010**, *11*, 2502. (b) Wang, Z. J.; et al. *Chem. Sci.* **2014** *5*, 598.
- (23) Chen, C.-K.; et al. *J. Biol. Inorg. Chem.* **2010**, *15*, 159.
- (24) S. Kille, *et al.*, *ACS Synth. Biol.* **2013**, *2*, 83–92.
- (25) Kabsch, W. *Acta Cryst.* **2010**, D66, 125.
- (26) McCoy, A. J. *et al.* *J. Appl. Cryst.* **2007**, *40*, 658.
- (27) Bailey, S. *Acta Cryst.* **1994**, D50, 760.
- (28) (a) Emsley, P.; Cowtan, K. *Acta Cryst.* **2004**, D60, 2126. (b) Winn, M. D. *et al.* *Macromolecular Crystallography, Pt D* **2003**, 374, 300.
- (29) Chen, V. B. ; Arendall III, W. B.; Headd, J. J.; Keedy, D. A.; Immormino, R. M.; Kapral, G. J.; Murray, L. W.; Richardson, J. S.; Richardson, D. C. *Acta Cryst.* **2010**, D66, 12.
- (30) Painter, J.; Merritt, E. A. *J. Appl. Cryst.* **2006**, *39*, 109.
- (31) Trott, O.; Olson, J. A. *J. Comp. Chem.* **2010**, *31*, 455.
- (32) Ichinose, M. *et al.* *Angew. Chem.-Int. Ed.* **2011**, *50*, 9884-9887.

*Chapter 5***ENANTIOSELECTIVE ENZYME-CATALYZED AZIRIDINATION ENABLED BY
ACTIVE-SITE ENGINEERING OF A CYTOCHROME P450**

This chapter is prepared for submission to ACS Central Science as C. C. Farwell, R. K. Zhang, J. A. McIntosh, T. K. Hyster, F. H. Arnold “Enantioselective enzyme-catalyzed aziridination enabled by active-site engineering of a cytochrome P450.” I performed all initial characterization of the enzymatic aziridination reaction, including discovery of the beneficial effects of I263F in this reaction. R.K.Z. synthesized product standards, quantified reaction products, and performed enzyme mutagenesis and screening for aziridination. J.A.M and T.K.H. performed analytical experiments to characterize the initial reaction. Myself and F.H.A. wrote the paper.

Abstract

One of the greatest challenges in protein design is creating new enzymes, something evolution does all the time. Using some of nature's evolutionary tricks, we have engineered a bacterial cytochrome P450 to catalyze highly enantioselective intermolecular aziridination, a synthetically useful reaction that has no natural biological counterpart. The new enzyme is fully genetically encoded and can be optimized rapidly by protein engineering to exhibit very high enantioselectivity (up to 99% *ee*) and high activity (>1,000 catalytic turnovers) for intermolecular aziridination, demonstrated here with tosyl azide and substituted styrenes. Together with carbene (olefin cyclopropanation and N-H insertion) and nitrene transfer (C-H amination and sulfimination) activities reported previously, this new aziridination activity highlights the remarkable ability of a natural enzyme to adapt to non-natural substrates and take on new functions. Once discovered in an evolvable enzyme such as the P450, non-natural reactivity can be improved and selectivity tuned by protein engineering to create a new catalyst family.

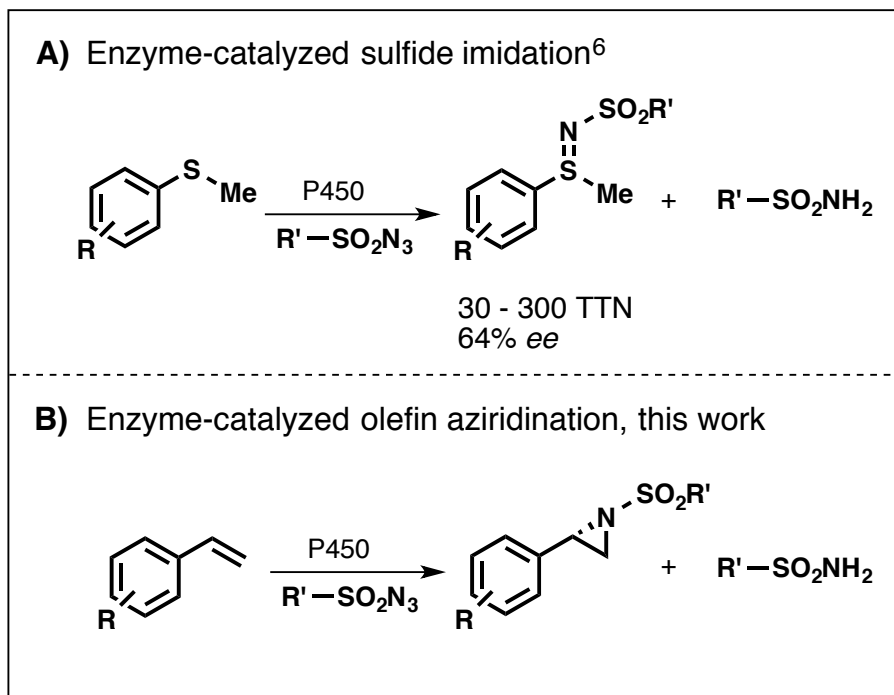
Introduction

The impressive catalytic diversity of enzymes illustrates the breadth of reaction space explored throughout biological evolution. Chemists are taking advantage of this vast repository of biocatalysts for chemical synthesis; they are also mimicking nature's engineering strategy of mutation and selection to optimize enzyme function for a myriad of applications.¹ A remaining challenge is to create new enzymes for the many useful reactions that are not known in the biological world. We and others have argued that learning from nature's mechanisms for catalytic innovation—exploiting enzyme catalytic promiscuity and retaining key elements of structure and mechanism while exploring new functions—can help us discover new biocatalysts starting from nature's vast repertoire.² The discovery and optimization of enzyme catalysts for non-natural reactions has provided alternative routes to important molecules that would otherwise be unattainable through biocatalysis.³

Our group⁴ and that of Rudi Fasan⁵ recently reported that heme proteins can catalyze intramolecular direct C–H amination via formation of reactive metallonitrenoid species and nitrene transfer. We extended this novel biocatalytic activation mode to intermolecular sulfimination and showed that the enzyme, derived from a cytochrome P450, could be tuned by mutation to catalyze the reaction with good activity and moderate enantioselectivity (Scheme 1A).⁶ Carrying out non-natural reactions with an enzyme provides the opportunity for unprecedented control over selectivity: we recently showed, for example, that engineering the active site could even override the preference for sites

with lower bond dissociation energies that governs regioselectivity of small-molecule C-H amination catalysts.⁷

Among the various nitrene transfer reactions used in synthetic chemistry, aziridination with azide nitrene sources is a compelling transformation (Scheme 1B), given its high atom-economy and the utility of the aziridine functional group in chemical synthesis.⁸ The oxygen equivalent to aziridines, epoxides, are prevalent in natural products, and their biosynthesis involves oxygenation via enzyme-activated electrophilic oxygen species.⁹ However, aside from the TxtE-catalyzed nitration of tryptophan,¹⁰ no natural enzyme is known to use electrophilic nitrogen species for the direct transfer of nitrogen atoms to olefins or C-H bonds. Aziridine rings are much less common in natural products than epoxides, and aziridine biosynthesis is believed to involve intramolecular nucleophilic displacement (e.g., activation by vicinal alcohols, as depicted in Figure 1).¹¹ This step is thought to occur late in biosynthesis and can involve anchoring of the substrate to peptidyl carrier proteins (Figure 1). The dearth of knowledge about the enzymes responsible for this transformation, along with the extremely limited set of substrates investigated so far, makes applying natural aziridination pathways for chemical synthesis infeasible. An enzymatic reaction analogous to epoxidation would be highly attractive given the utility of enantioselective convergent synthesis with electrophilic metal-nitrogen species.¹²

Scheme 1. Enzyme-catalyzed intermolecular nitrogen-atom transfer

In our previous work on the intermolecular imidation of sulfides catalyzed by variants of cytochrome P450_{BM3}, two factors appeared to limit reactivity. First, the reaction was promoted by electron-rich sulfides, and second, enzyme-catalyzed azide reduction represented a significant side reaction, particularly with less reactive, electron-deficient sulfides.⁶ Increasing the sulfide substrate loading improved the sulfimide product to side product ratio, which suggested that increasing the effective concentration of sulfide ‘nitrene acceptor’ in the enzyme active site might improve sulfimidation productivity. Given the less reactive nature of olefins relative to sulfides along with operational limitations to increasing olefin effective concentration (i.e., their limited solubility in aqueous media), we surmised that intermolecular aziridination would be a challenging activation mode for the

enzyme. However, we hypothesized that protein engineering would allow us to circumvent these limitations if the enzyme could more effectively bind and orient the substrates in the enzyme active site for productive nitrene transfer. Here we demonstrate that active-site engineering can indeed enable intermolecular enzyme-catalyzed nitrene transfer to olefins.

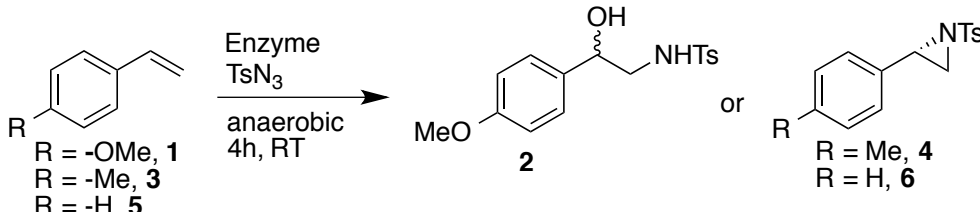
Results and Discussion

We started this investigation of enzyme-catalyzed aziridination with an engineered variant of cytochrome P450_{BM3}, P411_{BM3}-CIS-T438S, found previously to be effective for intramolecular C–H amination and sulfide imidation (see table S1 for mutations from wild-type P450_{BM3}).^{4b,6} We call this enzyme a “P411” due to mutation of the cysteine residue that coordinates the heme iron to serine (C400S), which changes the characteristic CO-bound Soret peak from 450 to 411 nm.^{4b,7,14} This axial cysteine is completely conserved among the cytochrome P450s and is required for the native monooxygenation activity. Thus the P411 enzyme is no longer a ‘cytochrome P450’, nor does it exhibit its native monooxygenation activity.¹⁴⁻¹⁵ However, the C400S mutation increases the non-natural carbene and nitrene transfer activities of P450_{BM3}.^{4b,6-7,14} Two crystal structures of P411 variants of P450_{BM3} show that the serine coordinates the iron and causes no significant structural perturbation in the substrate binding pocket.^{7,14}

Mechanistic analysis of sulfide imidation suggested that electron-rich sulfides promote nitrene transfer.⁶ Reasoning that aziridination could also be influenced by the electronic properties of the olefin substrate, we tested reactivity towards 4-methoxystyrene, bearing the strong electron-inducing p-OMe substituent, and tosyl azide (TsN₃) as the

nitrene precursor (Figure 2). The major product of the reaction was tosyl sulfonamide **3**, as also observed with intermolecular imidation of sulfides.⁶ The minor product was not the aziridine, however, but amido-alcohol **2**. Control experiments showed that a synthetic aziridine standard (**S1**) rapidly decomposes under aqueous reaction conditions to the corresponding amido-alcohol **2** (Figure S1). Degradation of this aziridine product has also been observed in studies with small-molecule catalysts.¹⁶ We therefore inferred that production of **2** is directly related to the nitrene transfer activity of the enzyme towards this olefin substrate.

Table 1. Total turnovers (TTN) to product and enantioselectivities for aziridination catalyzed by P411_{BM3}-CIS-T438S (P) and P411_{BM3}-CIS-T438S-I263F (P-I263F) with selected styrenyl olefins **1**, **3**, and **5** and tosyl azide using purified holoenzymes. Reactions were done in 0.1 M KPi buffer pH = 8.0 using NADPH as reductant, using 0.2 mol% enzyme, with 2.5 mM TsN₃ and 7.5 mM styrene. Detailed reaction conditions can be found in the supporting information.

				
P411_{BM3}-CIS-T438S (P)			P-I263F	
Product	TTN	% ee	TTN	% ee
2	15	rac	150	rac
4	8	nd	160	70 (<i>S</i>)
6	5	nd	190	74 (<i>S</i>)

^a TTN = Total turnover number. ^b % ee determined as $((S - R)/(S + R))$ for *S*-selective reactions, and $((R - S)/(R + S))$ for the *R*-selective reaction, nd = not determined, rac = racemic.

The low level of nitrene transfer activity to 4-methoxystyrene with P411_{BM3}-CIS-T438S prompted us to investigate other enzyme variants. We chose a small set of cytochrome P450_{BM3} variants and heme proteins prepared for other studies in order to assess how changes in the protein sequence affect nitrene transfer to olefin substrates (Tables S1 and S2). P450_{BM3} sequences lacking the C400S and/or T268A mutations⁶⁻⁷ were not productive in the aziridination reaction. Nor did the Fe(II)-protoporphyrin IX (PPIX) cofactor catalyze aziridination under these conditions. (In previous work we found that Fe(II)-PPIX was active for intramolecular C–H bond amination, depending on the C–H bond strength,⁴ but did not catalyze intermolecular nitrene transfer to sulfides.⁶) Mutants differing from P411_{BM3}-CIS-T438S by 2-5 alanine mutations in the active site¹⁷ showed some aziridination activity (4-8 TTN), but none was more productive than P411_{BM3}-CIS-T438S. We also tested a set of enzymes containing different axial mutations, including the S400H, S400D, and S400M mutants of P411_{BM3}-CIS-T438S. These enzymes were also only weakly active, giving **2** at levels similar to P411_{BM3}-CIS-T438S (3-4 TTN). Myoglobin (horse heart), cytochrome c (bovine heart), and cytochrome P450_{Rhf} (from *Rhodococcus* sp. NCIMB 9784) were all inactive for this intermolecular aziridination (Table S2). The thermostable cytochrome P450 CYP119 from *Sulfolobus sulfataricus* with the axial C317S mutation¹⁸ did catalyze aziridination (~ 7 TTN), demonstrating that axial mutants of other cytochrome P450s may be active and suitable starting points for further engineering.

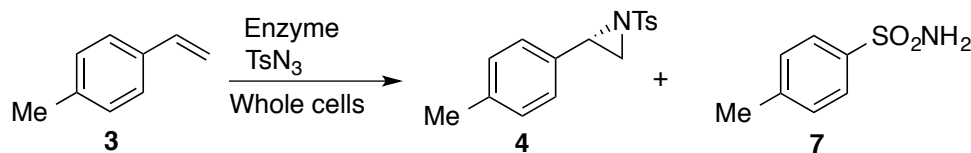
Of all the enzymes tested, a variant of P411_{BM3}-CIS-T438S having a single active-site substitution, I263F, was the most reactive toward 4-methoxystyrene by a wide margin (150 TTN, Table 1). This variant, which promoted regioselective intramolecular C–H

amination in a previous study,⁷ supported aziridination at 10-fold increased total turnover compared to the P411_{BM3}-CIS-T438S parent enzyme. Comparison of these two enzymes' activities with a set of styrenyl olefins showed that the I263F variant was also more productive with the comparatively electron-deficient 4-methylstyrene (**4**) and styrene (**6**) substrates. Furthermore, P411_{BM3}-CIS-T438S-I263F (henceforth referred to as P-I263F) is more active with styrenes **4** and **6** than with 4-methoxystyrene **1**. This trend in substrate specificity is inverted compared to the parent enzyme (Table 1) and the previously observed trend for intermolecular imidation of sulfides.⁶ Unlike the aziridine product that leads to **2**, aziridine products **4** and **6** were stable in the reaction conditions. The P411_{BM3}-CIS-T438S-I263F variant displayed moderate *S* enantioselectivity with 4-methylstyrene and styrene (70 and 74% *ee* (*S*), respectively). Racemic product was observed for both enzymes with 4-methoxystyrene **1**, consistent with non-enzymatic degradation of the aziridine to amido-alcohol **2**.

The P-I263F enzyme was even more productive when the reactions were carried out using whole *E. coli* cells expressing this enzyme (Figure S2). These observations are consistent with previous studies demonstrating improved enzyme-catalyzed metal nitrenoid and carbenoid transfer in whole-cell reactions.^{4, 14} No aziridine product was observed when cells without enzyme were used, although tosyl azide was converted to tosyl sulfonamide over the course of the reaction, consistent with previous observations (**7**, Table 2).⁴ Indeed, the P-I263F enzyme gave enough product in whole-cell reactions to allow for screening in 96-well plate format (see supporting material for library construction and screening procedures). Having observed a large increase in aziridination activity upon a

single active site mutation, we attempted to improve the activity further by performing saturation mutagenesis at selected active site residues and screening for product formation by HPLC. Site-saturation mutagenesis (SSM) libraries were created in P-I263F at several active-site positions that were previously shown to influence productivity and enantioselectivity in non-natural reactions (A78, L181, T268, A328).^{3a,7} Screening of these single SSM libraries on 4-methylstyrene for aziridination productivity revealed one hit, P-I263F-A328V, with slightly improved TTN values but substantially improved % *ee* (96% *ee*, Table 2). Another round of SSM was performed on this variant at additional active site positions (A82, F87, L437, T438). A second hit was isolated, P-I263F-A328V-L437V, with further improved aziridination productivity. Although yield improvements were modest (40% **5** with P-I263F to 43% with P-I263F-A328V and 58% with P-I263F-A328V-L437V, Table 2), a very significant increase in enantioselectivity, up to > 99% *ee* (S), was observed with the A328V-L437V double mutant. The P-I263F-L437V and P-I263F-A328V single mutants were both less productive and less selective than the P-I263F-A328V-L437V double mutant, demonstrating that the two mutations both contribute to achieving this very high enantioselectivity.

Table 2. Improvement in yield and % *ee* for aziridine product **4** with active-site engineering starting with P411_{BM3}CIS-T438S (P). Reactions were carried out using whole *E. coli* cells resuspended in M9-N reaction buffer under anaerobic conditions. Yield is based on TsN₃. See SI methods for detailed reaction set up and quantification procedures.

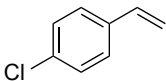
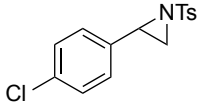
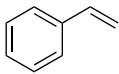
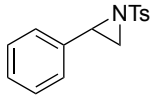
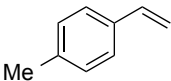
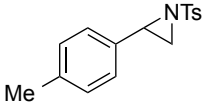
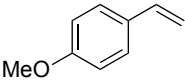
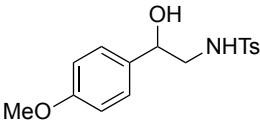
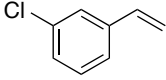
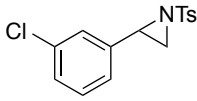
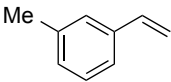
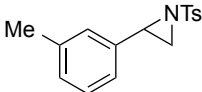
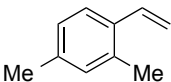
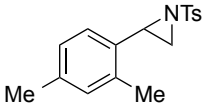
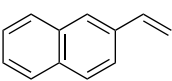
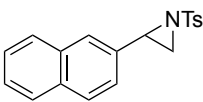
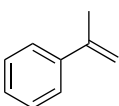
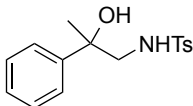


Entry	Enzyme	% yield 4	% yield 7	% <i>ee</i> 4
1	pET22b-empty	0	96	nd
2	P411 _{BM3} -CIS T438S	1.1	95	25
3	P-I263F	40	54	55
4	P-I263F-A328V	43	50	96
5	P-I263F-L437V	37	52	95
6	P-I263F-A328V-L437V	58	40	> 99

We hypothesized that the improved aziridine yield observed with P-I263F-A328V-L437V might stem from a decrease in the rate of azide reduction catalyzed by the evolved enzyme. Initial rate measurements performed using purified enzymes are consistent with this view, showing decreased rates of azide reduction in P-I263F-A328V (27 min⁻¹) and P-I263F-A328V-L437V (14 min⁻¹) compared to P-I263F (33 min⁻¹) (Table S4). Somewhat unexpectedly, P-I263F-A328V-L437V also gives a slower rate of aziridination compared to P-I263F and P-I263F-A328V (6.0 min⁻¹, 9.7 min⁻¹, and 9.6 min⁻¹, respectively), although the relative rate of aziridination to azide reduction was the highest for this enzyme (Table S4). Indeed, the productivities of purified enzymes reflect the relative rates of aziridine formation to azide reduction, where P-I263F-A328V-L437V shows improved azide utilization over the course of the reaction than P-I263F.

Having obtained a variant with high enantioselectivity for aziridination of **3**, we next investigated reactions with different substituted styrene substrates in whole-cell reactions (Table 3). As observed with P-I263F, we saw no correlation between the electronic inductivity of the aryl substituent and productivity. In general, the evolved enzyme was more productive with styrenes substituted at the 4-position, though the highest productivity was observed with styrene itself (1020 TTN, entry 2). Both 3-methylstyrene and 3-chlorostyrene were significantly less reactive than their 4-substituted counterparts, giving 120 and 17 TTN, respectively. In contrast, 2,4-dimethyl styrene gave 200 TTN, suggesting that 2-substitution is less detrimental to reactivity. The evolved enzyme is exceptionally selective with styrene and all 4-substituted styrenes tested, with the exception of 4-methoxystyrene, while alternative substitution results in decreased enantioselectivity (95% *ee* and 81% *ee* for entries 6 and 7, respectively). Taken together, these results suggest that the P-I263F-A328V-L437V enzyme active site is preferentially configured for non-substituted and 4-substituted styrene aziridination. Both 4-methoxystyrene and α -methylstyrene (entries 4 and 9, respectively) gave exclusively racemic amido-alcohol product. Formation of the amido-alcohol may result from carbocation stabilization at the benzylic position, resulting in decomposition of the aziridine product and subsequent carbocation quenching with water. For these substrates, the resonance and hyperconjugative stabilization provided by the p-OMe and α -Me groups is likely responsible for this effect. The fact that 4-methoxystyrene and α -methylstyrene both yield a racemic mixture of their respective amido-alcohols suggests that the carbocation is quenched by water in a step-wise, rather than concerted, process.

Table 3. Substrate scope of P-I263F-A328V-L437V enzyme, showing productivity in terms of TTN and selectivity in % *ee* for each product.

Entry	Olefin	Product	TTN ^a	% <i>ee</i> ^b
1			320	99
2			1020	99
3			500	99
4			550	rac
5			17	95
6			120	95
7			200	81
8			61	88
9			51	rac

^a Reaction productivity and enantioselectivity determined as described in SI methods. ^b % *ee* determined as $(S - R)/(S + R)$. rac = racemic.

The highly enantioselective P-I263F-A328V-L437V variant has three mutations in its active site compared to the enzyme used in initial reaction characterization, P411_{BM3}-

CIS-T438S. The crystal structure of the heme domain of P-I263F was recently solved and shows how the F263 side chain is oriented within the active site, directly above the heme cofactor (PDB ID: 4WG2, Figure S2). Considering I263F in the context of two other mutations in P411_{BM3}-CIS-T438S that promote nitrene transfer activity, F87V and T268A, provides insight into the effect of active site structure on reaction productivity. Mutation of F87 to either V or A can be activating in various P450_{BM3}-catalyzed nitrene transfer reactions described so far.^{2b,4a,6-7} The F87G mutation has been shown to negatively impact native fatty acid hydroxylation by P450_{BM3},¹⁹ whereas F87V promotes hydroxylation of naphthalene and indole substrates.²⁰ These results suggest steric hindrance at F87 that is relieved upon substitution with smaller residues and enhances reactivity with bulkier substrates. Reversion of either T268A or F87V to the wild-type residue in P-I263F reduces aziridination productivity (Table S1). The combined effects of the I263F, F87V, T268A, and other active site residues suggest that active site ‘reshaping’ promotes olefin aziridination. The data in Tables 1 and 3 suggest that active site structure can override the influence of substrate electronic properties by more effectively orienting substrates in a favorable configuration for nitrene transfer to occur.

The difference between the active sites of P411_{BM3}-CIS-T438S (P) and P-I263F is dramatic: the F263 side chain fills space above the heme cofactor whereas the I263 side chain is pointed up and away from the heme (Figure S6A and S6B). Given their more conservative nature relative to the I263F mutation, the A328V and L437V substitutions likely exert only subtle influences on active site structure yet give a significant boost to aziridination enantioselectivity (68% *ee* vs. 99% *ee* with styrene). The fact that the improved selectivity provided by A328V and L437V comes at the expense of aziridination

rates *in vitro* could suggest that these mutations may block alternative approaches of the aziridine, thus leading to decreased rates, but higher selectivities. The improved overall yield in whole cell conditions with P-I263F-A328V-L437V also suggests a role for these mutations in a more favorable partition between azide reduction and aziridine formation.

The rate of nitrene transfer in P411-catalyzed intermolecular sulfimidation depended on the electronic properties of the substrates, where more electron-rich sulfides gave higher rates of sulfide imidation.⁶ The productivities of the evolved intermolecular aziridination catalysts do not follow this trend: for example, styrene is substantially more reactive than the more electron-rich 4-methoxystyrene (Tables 1 and 3). Our results for intermolecular aziridination thus suggest that nitrene transfer is driven more by favorable substrate binding for aziridination than substrate electronic properties. Analysis of regioselective intramolecular C–H amination suggests a similar role for substrate positioning by the enzyme in governing the position of C–H amination.⁷ These observations reinforce the strong influence of active site structure in promoting enzyme-catalyzed intermolecular nitrene transfer. It is possible that further engineering could enable the enzyme to catalyze even more challenging reactions such as intermolecular C–H amination.

Conclusions

In this first example of enzyme-catalyzed aziridination, we report intermolecular aziridination of styrenyl olefins using tosyl azide catalyzed by a serine-ligated “P411” variant of cytochrome P450_{BM3}. The specific active site sequence is critical to achieving high productivity. Reaction enantioselectivity and productivity could be tuned through active-site mutations, such that variant P-I263F-A328V-L437V exhibited very high

enantioselectivity (99% *ee*) and significantly improved azide utilization compared to the parental enzyme, P411_{BM3}-CIS-T438S. Indeed, the results of active site engineering for aziridination productivity are consistent with the hypothesis that improving nitrogen-atom ‘acceptor’ (olefin) binding is a viable route to improving reactivity in intermolecular nitrene transfer. These results demonstrate the critical role for protein engineering in optimizing non-natural reactivity, and suggest that the well-known plasticity of the P450 active site can be leveraged to target challenging chemical transformations. Taking advantage of the catalytic promiscuity of natural enzymes and protein engineering will enable us to further expand the reaction space of genetically encoded biocatalysts.

Supplementary Materials for

Enantioselective enzyme-catalyzed aziridination enabled by active-site engineering of a cytochrome P450

Contents	Page
1. Materials and Methods	127
2. Synthetic Procedures	132
3. Characterization of Enzymatic Aziridination	136
4. Structural Analysis of Aziridination Catalysts	139
5. Assignment of Absolute Configuration	141
6. Initial Rates of Aziridine and Sulfonamide Formation	142

1. Materials and Methods

General procedures, protein expression, and protein purification performed as described in Chapter 3.

Chromatography. Analytical high-performance liquid chromatography (HPLC) was carried out using an Agilent 1200 series, and a Kromasil 100 C18 column (4.6 x 50 mm, 5 μ m). Semi-preparative HPLC was performed using an Agilent XDB-C18 (9.4 x 250 mm, 5 μ m). Analytical chiral HPLC was conducted using a supercritical fluid chromatography (SFC) system with isopropanol and liquid CO₂ as the mobile phase. Chiral OB-H and AS-H columns were used to separate aziridine and amido-alcohol enantiomers (4.6 x 150 mm, 5 μ m). Olefins were all commercially available; amido-alcohol and aziridine standards were prepared as reported (see Synthetic Procedures).

Typical procedure for small-scale aziridination bioconversions under anaerobic conditions using whole cells and purified enzymes. *E. coli* BL21(DE3) cells containing P450 or P411 enzymes were expressed and resuspended to an OD₆₀₀ = 30 in M9-N), and then degassed by sparging with argon in a sealed 6 mL crimp vial for at least 10 minutes. To 2 mL crimp vials were added glucose (250 mM in M9-N, 40 μ L) and the oxygen quenching mixture (14,000 U/ml catalase and 1,000 U/ml glucose oxidase, 20 μ L). The headspace of the sealed 2 mL reaction vial was made anaerobic by flushing argon over the solution. Resuspended cells (320 μ L), followed by olefin substrate (10 μ L, 300 mM in DMSO) and then tosyl azide (10 μ L, 100 mM in DMSO), were added to a 2 mL reaction vial via syringe under a continuous flow of argon. Final concentrations of reagents were typically: 2.5 mM tosyl azide, 7.5 mM olefin, 25 mM glucose. Sealed reaction vials were wrapped in parafilm and shaken (40 rpm) at room temperature for 4 hours.

For purified enzyme reactions, a buffer solution composed of 5 mM NADPH and 25 mM glucose in 0.1 M KPi pH = 8.0 was prepared and sparged for 20 minutes with argon. Reaction vials were charged with 5 or 7.5 μ M enzyme and oxygen quenching mixture (as above) and headspaces flushed with argon for 10 minutes. Degassed buffer solution was then added to the vials, followed by olefin substrate and tosyl azide to final concentrations of 7.5 mM and 2.5 mM, respectively. For reactions with myoglobin, cytochrome C, CYP119, and P450_{Rhf}, 5 mM sodium dithionite was used as reductant. Reactions were quenched by adding acetonitrile (460 μ L). The mixture was then transferred to a microcentrifuge tube and centrifuged at 14,000 rpm for 5 minutes. The solution (540 μ L) was transferred to an HPLC vial, charged with internal standard (60 μ L, 10 mM 1,3,5-trichlorobenzene in acetonitrile), and analyzed by HPLC for yield.

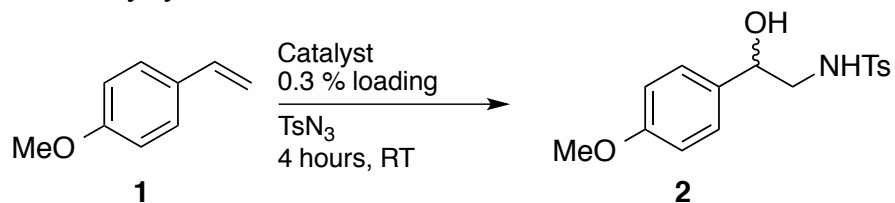
For chiral HPLC reactions were performed on a 2 mL scale with the same concentration of reagents using a similar procedure. Chiral HPLC reactions were quenched with 2 mL acetonitrile, extracted with ethyl acetate, dried and resuspended in acetone (200 μ L), and purified by C18 semi-preparative HPLC. The purified material was dried, resuspended in acetonitrile, and injected onto the chiral HPLC system for analysis.

Reaction screening in 96-well plate format.

Site-saturation libraries were generated by employing the “22-codon” method.²¹ *E. coli* libraries were generated and cultured in 300 μ L of LB with 100 μ g/ml ampicillin and stored as glycerol stocks at -80 °C in 96-well plates. 50 μ L of the pre-culture was transferred to a 1000 μ L of Hyperbroth using a multichannel pipette. The cultures were incubated at 37 °C, 220 rpm, 80% humidity for 3 hours. The plates were cooled on ice for 15 minutes before

expression was induced (0.5 mM IPTG, 1mM 5-aminolevulinic acid final concentration). Expression was conducted at 20 °C, 120 rpm, 20 h. The cells were pelleted (3000 x g, 5 min) and re-suspended in 40 µL/well oxygen quenching solution. The 96-well plate was transferred to an anaerobic chamber. 300 µL per well argon sparged reaction buffer (4:1 M9-N : 250mM glucose in M9-N) was added followed by 4-methylstyrene (300 mM, 10 µL/well) and tosyl azide (100 mM, 10 µL/well). The plate was sealed with aluminum sealing tape, removed from the anaerobic chamber, and shaken at 40 rpm. After 16 hours, the seal was removed and 400 µL of acetonitrile was added to each well. The contents of each well were mixed by pipetting up and down using a multichannel pipette. Then the plate was centrifuged (4000 x g, 5 minutes) and 500 µL of the supernatant was transferred to a shallow-well plate for analysis by HPLC.

Table S1. Panel of P450_{BM3} enzymes tested for aziridination reactivity with 4-methoxystyrene **1**.



Entry	Enzyme	TTN 2
1	P411 _{BM3} -CIS T438S	15
2	P450 _{BM3} -CIS T438S	< 1
3	P450 _{BM3} -CIS T438S C400H	3
4	P450 _{BM3} -CIS T438S C400D	4
5	P450 _{BM3} -CIS T438S C400M	4
6	P411 _{BM3} -CIS A268T T438S	< 1
7	P411 _{BM3} -H2-5-F10	8
8	P411 _{BM3} -H2-A-10	4
9	P411 _{BM3} -H2-4-D4	5
10	P450 _{BM3}	< 1
11	P411 _{BM3}	3
12	P450 _{BM3} -T268A	2
13	P411 _{BM3} -T268A	4
14	P411 _{BM3} -CIS T438S I263F	150
14	P411 _{BM3} -CIS T438S I263F V87F	19
15	P411 _{BM3} -CIS T438S I263F A268T	< 1

Table S2. Non-P450_{BM3} catalysts tested for activity in the above reaction for nitrene transfer to 4-methoxystyrene. Myoglobin and cytochrome C were purchased as lyophilized powder from Sigma Aldrich. CYP119 and P450_{Rhf} mutants were expressed and purified as described above.

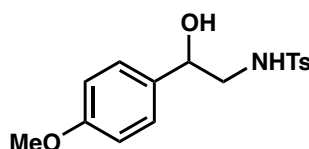
Entry	Catalyst	TTN 2
1	Hemin	< 1
2	Hemin + BSA	< 1
3	Myoglobin	< 1
4	Cytochrome C	< 1
5	P450 _{CYP119} C317S	7
6	P450 _{CYP119} T213A C317H	< 1
7	P450 _{Rhf}	< 1
8	P450 _{Rhf} T275A	< 1

Table S3. Mutations present in P450_{BM3} variants used in this work.

Enzyme	Mutations relative to wild-type P450 _{BM3}
P450 _{BM3}	none
P450 _{BM3} -T268A	T268A
P411 _{BM3}	C400S
P411 _{BM3} -T268A	T268A, C400S
P450 _{BM3} -CIS T438S	V78A, F87V, P142S, T175I, A184V, S226R, H236Q, E252G, A290V, L353V, I366V, T438S, E442K
P411 _{BM3} -CIS T438S	P450 _{BM3} -CIS C400S, T438S
P-I263F	P411 _{BM3} -CIS T438S I263F
P-I263F-A328V	P411 _{BM3} -CIS T438S I263F A328V
P-I263F-A328V-L437V	P411 _{BM3} -CIS T438S I263F A328V L437V
P411 _{BM3} -CIS A268T T438S	P450 _{BM3} -CIS, A268T, C400S, T438S
P411 _{BM3} H2-A-10	P450 _{BM3} -CIS, L75A, L181A, C400S,
P411 _{BM3} H2-5-F10	P450 _{BM3} -CIS, L75A, I263A, C400S, L437A
P411 _{BM3} H2-4-D4	P450 _{BM3} -CIS, L75A, M177A, L181A, C400S, L437A, T438S

2. Synthetic Procedures

Synthesis of substrates and standards. All olefins presented in main text Table 1 were obtained from commercial sources (Sigma Aldrich).

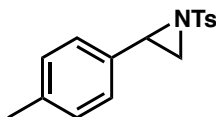


***N*-(2-hydroxy-2-(4-methoxyphenyl)ethyl)-4-methylbenzenesulfonamide (2).** Synthesized as previously reported.²²

¹H NMR (400 MHz, CDCl₃): δ 7.72 (d, 2H, *J* = 8.1 Hz), 7.29 (d, 2H, *J* = 8.3 Hz), 7.19 (d, 2H, *J* = 8.6 Hz), 6.84 (d, 2H, 8.6 Hz), 5.06 (dd, 1H, *J* = 8.1, 4.6 Hz), 4.73 (dd, 1H, *J* = 8.7, 3.7 Hz), 3.78 (s, 3H), 3.20 (ddd, 1H, *J* = 13.3, 8.1, 3.7 Hz), 3.01 (ddd, 1H, *J* = 13.2, 8.6, 4.6 Hz), 2.42 (s, 3H)

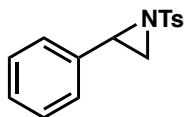
¹³C NMR (101 MHz, CDCl₃): δ 159.66, 143.69, 136.86, 133.00, 129.90, 127.26, 127.21, 114.16, 72.50, 55.44, 50.30, 21.66

HRMS (FAB⁺): calculated for C₁₆H₁₈NO₄S ([M+H]⁺): 320.0956; found: 320.0950



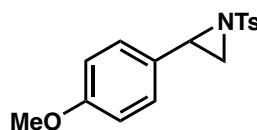
***N*-(*p*-Tolylsulfonyl)-2-(*p*-methylphenyl)aziridine (5).** Synthesized as previously reported^{S2} with spectral data in agreement with literature reported values.²³

¹H NMR (300 MHz, CDCl₃): δ 7.86 (d, 2H, *J* = 8.3 Hz), 7.32 (d, 2H), 7.10 (m, 4H), 3.74 (dd, 1H, *J* = 7.2, 4.5 Hz), 2.97 (d, 1H, *J* = 7.2 Hz), 2.43 (s, 3H), 2.38 (d, 1H, *J* = 4.5 Hz), 2.31 (s, 3H).



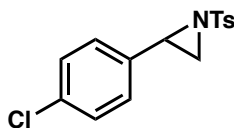
***N*-(*p*-Tolylsulfonyl)-2-phenylaziridine (7).** Synthesized as previously reported²⁴ with spectral data in agreement with literature reported values.²³

¹H NMR (300 MHz, CDCl₃): δ 7.87 (d, 2H, J = 8.3 Hz) 7.19-7.36 (m, 7H), 3.77 (dd, 1H, J = 7.2, 4.5 Hz), 2.98 (d, 1H, J = 7.2 Hz), 2.43 (s, 3H), 2.39 (d, 1H, J = 4.5 Hz)



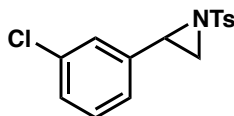
***N*-(*p*-Tolylsulfonyl)-2-(*p*-methoxyphenyl)aziridine (S1).** Synthesized as previously reported^{S2} with spectral data in agreement with literature reported values.²³

¹H NMR (500 MHz, CDCl₃): δ 7.87 (d, 2H, J = 8.3 Hz), 7.34 (d, 2H, J = 8.5 Hz), 7.14 (d, J = 8.7 Hz, 2H), 6.83 (d, J = 8.7, 2H), 3.78 (s, 3H), 3.75 (dd, 1H, J = 7.2, 4.5 Hz), 2.97 (d, 1H, J = 7.2 Hz), 2.44 (s, 3H), 2.39 (d, 1H, J = 4.5 Hz)



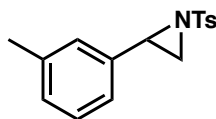
***N*-(*p*-Tolylsulfonyl)-2-(*p*-chlorophenyl)aziridine (S2).** Synthesized as previously reported^{S2} with spectral data in agreement with literature reported values.²³

¹H NMR (300 MHz, CDCl₃): δ 7.86 (d, 2H, J = 8.3 Hz), 7.34 (d, 2H, J = 7.9 Hz), 7.26 (d, 2H, J = 8.5 Hz), 7.15 (d, 2H, J = 8.5 Hz), 3.73 (dd, 1H, J = 7.2, 4.4 Hz), 2.98 (d, 1H, J = 7.2 Hz), 2.44 (s, 3H), 2.34 (d, 1H, J = 4.4 Hz)



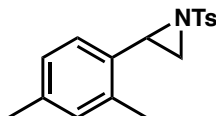
***N*-(*p*-Tolylsulfonyl)-2-(*m*-chlorophenyl)aziridine (S3).** Synthesized as previously reported^{S2} with spectral data in agreement with literature reported values.²⁵

¹H NMR (400 MHz, CDCl₃): δ 7.87 (d, 2H, *J* = 8.3 Hz), 7.35 (d, 2H, *J* = 7.7 Hz), 7.19 – 7.26 (m, 3H), 7.12 (dt, 1H, *J* = 6.8, 1.8 Hz), 3.73 (dd, 1H, *J* = 7.2, 4.3 Hz), 2.97 (d, 1H, *J* = 7.2 Hz), 2.44 (s, 3H), 2.35 (d, 1H, *J* = 4.4 Hz)



***N*-(*p*-Tolylsulfonyl)-2-(*m*-methylphenyl)aziridine (S4).** Synthesized as previously reported^{S2} with spectral data in agreement with literature reported values.²⁶

¹H NMR (400 MHz, CDCl₃): δ 7.87 (d, 2H, *J* = 8.3 Hz), 7.33 (d, 2H, *J* = 8.6 Hz), 7.01 – 7.20 (m, 4H), 3.74 (dd, 1H, *J* = 7.2, 4.5 Hz), 2.96 (d, 1H, *J* = 7.2 Hz), 2.43 (s, 3H), 2.38 (d, 1H, *J* = 4.5 Hz), 2.30 (s, 3H)

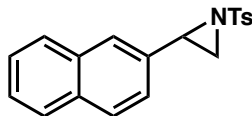


***N*-(*p*-Tolylsulfonyl)-2-(2,4-dimethylphenyl)aziridine (S5).** Synthesized as previously reported.²⁴

¹H NMR (400 MHz, CDCl₃): δ 7.90 (d, 2H, *J* = 8.4 Hz), 7.34 (d, 2H, *J* = 8.5 Hz), 6.91 – 7.00 (m, 3H), 3.84 (dd, 1H, *J* = 7.2, 4.6 Hz), 2.97 (d, 1H, *J* = 7.2 Hz), 2.44 (s, 3H), 2.35 (s, 3H), 2.32 (d, 1H, *J* = 4.6 Hz), 2.28 (s, 3H)

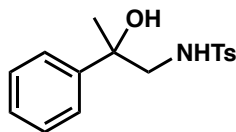
¹³C NMR (101 MHz, CDCl₃): δ 144.72, 137.95, 136.72, 135.15, 130.89, 130.32, 129.84, 128.11, 126.82, 125.98, 39.61, 35.07, 21.75, 21.11, 19.08

HRMS (FAB⁺): calculated for C₁₇H₂₀NO₂S ([M+H]⁺): 302.1215; found: 302.1210



***N*-(*p*-Tolylsulfonyl)-2-(naphthalene-2-yl)aziridine (S6).** Synthesized as previously reported²⁴ with spectral data in agreement with literature reported values.²³

^1H NMR (400 MHz, CDCl_3): δ 7.90 (d, 2H, $J = 8.3$ Hz), 7.75 – 7.81 (m, 3H), 7.73 (s, 1H), 7.45 – 7.49 (m, 2H), 7.33 (d, 2H, $J = 8.3$ Hz), 7.25 – 7.30 (m, 1H), 3.93 (dd, 1H, $J = 7.2, 4.4$ Hz), 3.07 (d, 1H, $J = 7.2$ Hz), 2.50 (d, 1H, $J = 4.5$ Hz), 2.42 (s, 3H)



***N*-(2-hydroxy-2-phenylpropyl)-4-methylbenzenesulfonamide (S7).** Synthesized as previously reported.²²

^1H NMR (400 MHz, CDCl_3): δ 7.67 (d, 2H, $J = 8.3$ Hz), 7.24 – 7.38 (m, 7H), 4.59 (s, 1H), 3.22 (dd, 1H, $J = 12.8, 8.5$ Hz), 3.12 (dd, 1H, $J = 12.8, 4.8$ Hz), 2.42 (s, 3H), 1.56 (s, 3H)

^{13}C NMR (101 MHz, CDCl_3): δ 144.87, 143.73, 136.73, 129.93, 128.75, 127.60, 127.19, 124.93, 73.81, 53.99, 27.62, 21.68

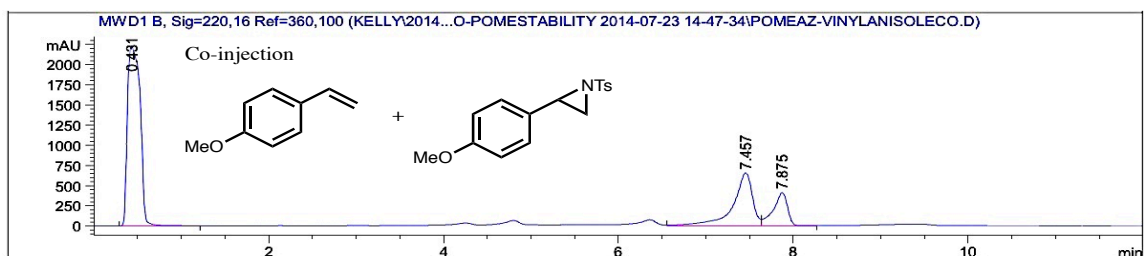
HRMS (FAB⁺): calculated for $\text{C}_{16}\text{H}_{20}\text{NO}_3\text{S}$ ($[\text{M}+\text{H}]^+$): 306.1164; found: 306.1160

3. Characterization of Enzymatic Aziridination

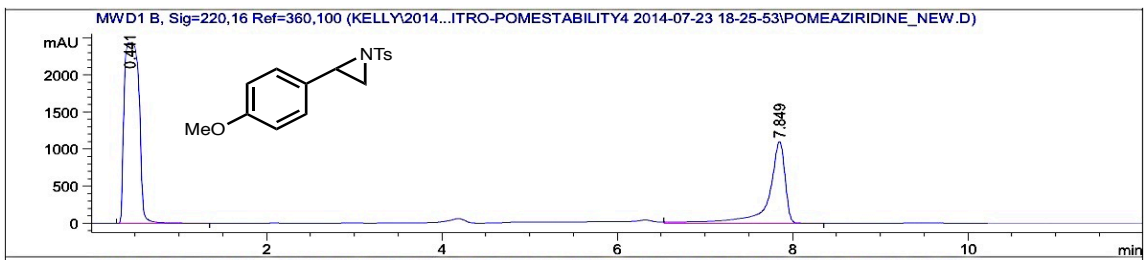
Figure S1. Demonstration of enzymatic synthesis and degradation of aziridine S1 in reaction conditions

A. HPLC 220 nm chromatogram of controls.

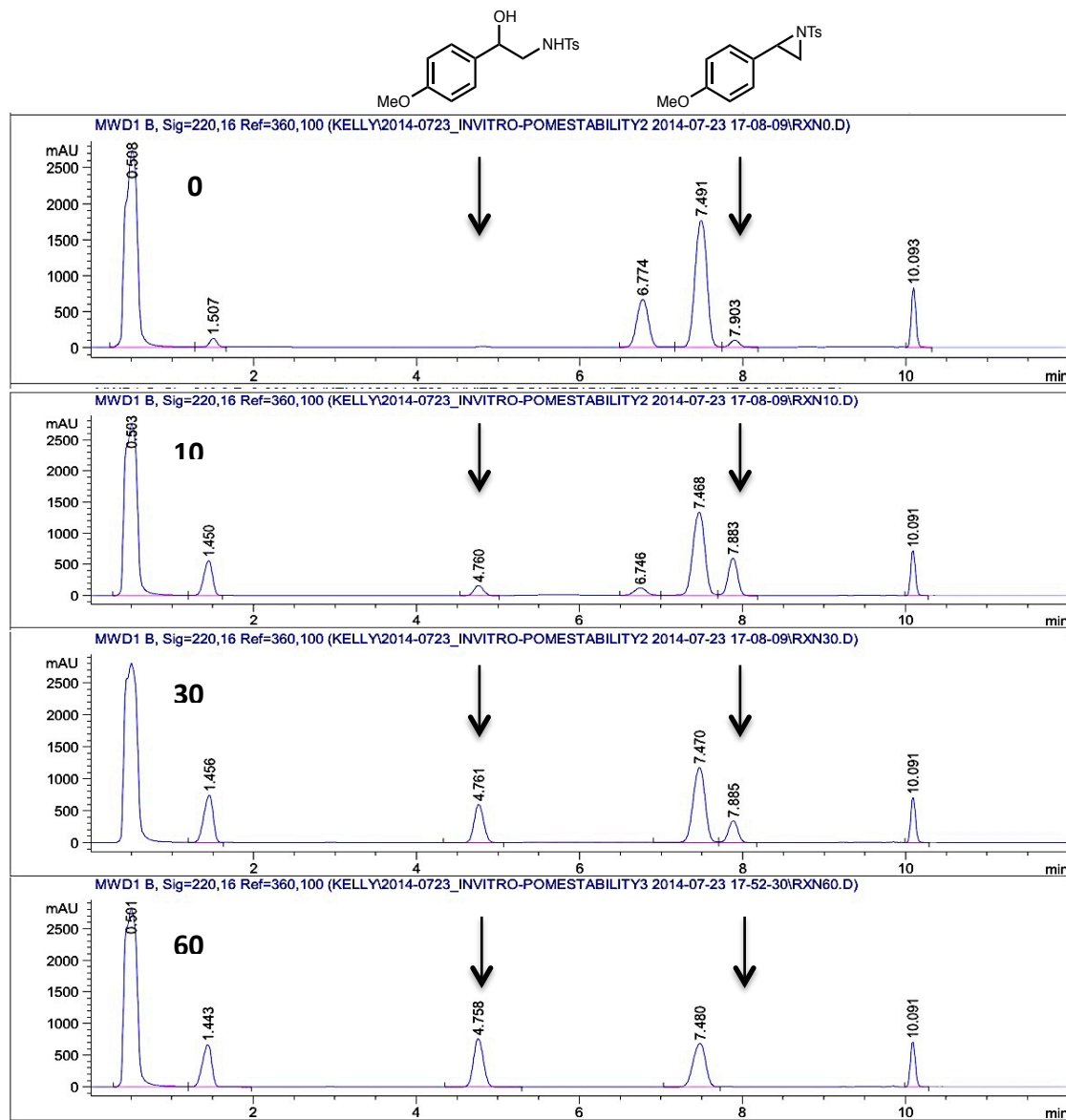
Co-injection of 4-methoxystyrene (Sigma Aldrich) and synthetic standard S1, confirmed by NMR.



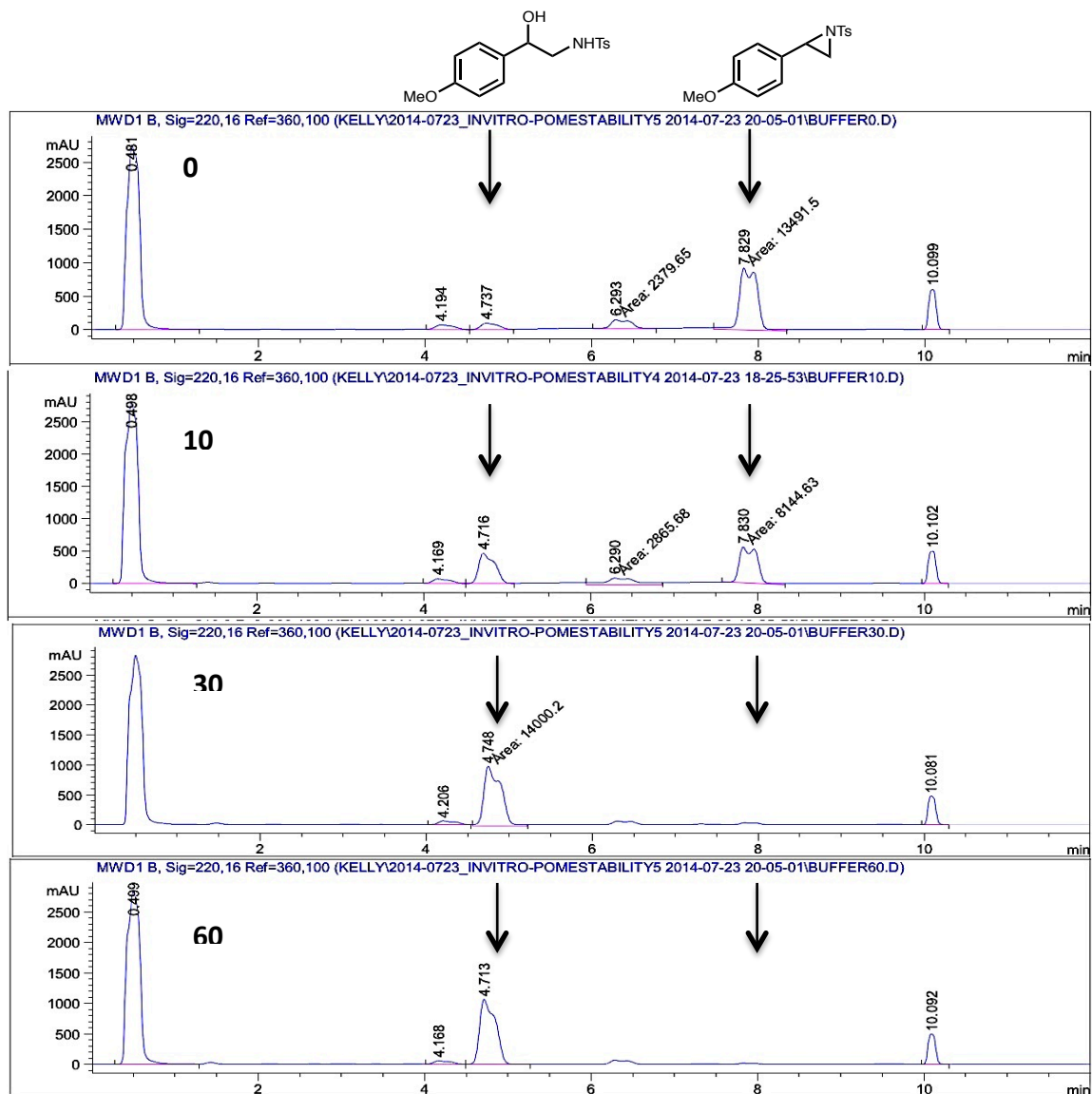
Synthetic standard S1, confirmed by NMR.



B. HPLC 220 nm chromatograms of P411-enzymatic reaction with 4-methoxystyrene **1** and tosyl azide as substrates analyzed at different time points. Putative aziridine **S1** and amido-alcohol **2** are marked with arrows.



C. HPLC 220 nm chromatograms of synthetic standard **S1** in reaction conditions *without* P411 catalyst at several time points. Putative aziridine **S1** and amido-alcohol **2** are marked with arrows.



4. Structural Analysis of Aziridination Catalysts

Figure S2. Representation of the P411_{BM3}-CIS-I263F-T438S active site.

P411_{BM3}-CIS-I263F-T438S active site is modeled from a previously solved structure (PDB ID: 4WG2).⁷ Active site residues V87, F263, and A268 are shown as pink sticks, with the heme cofactor as green sticks.

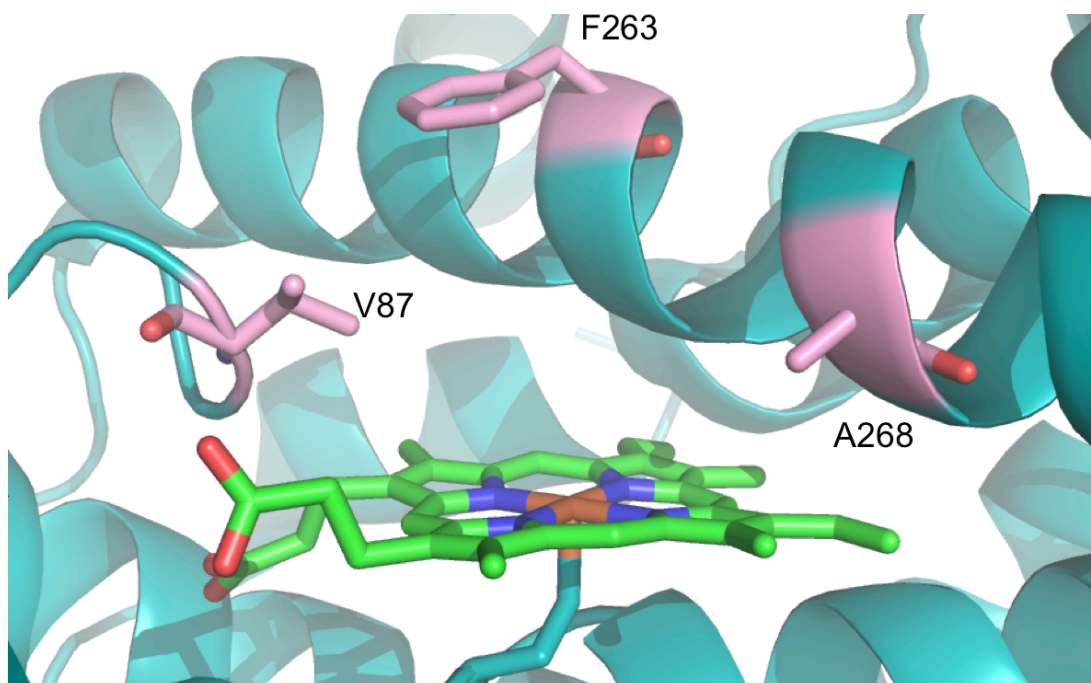
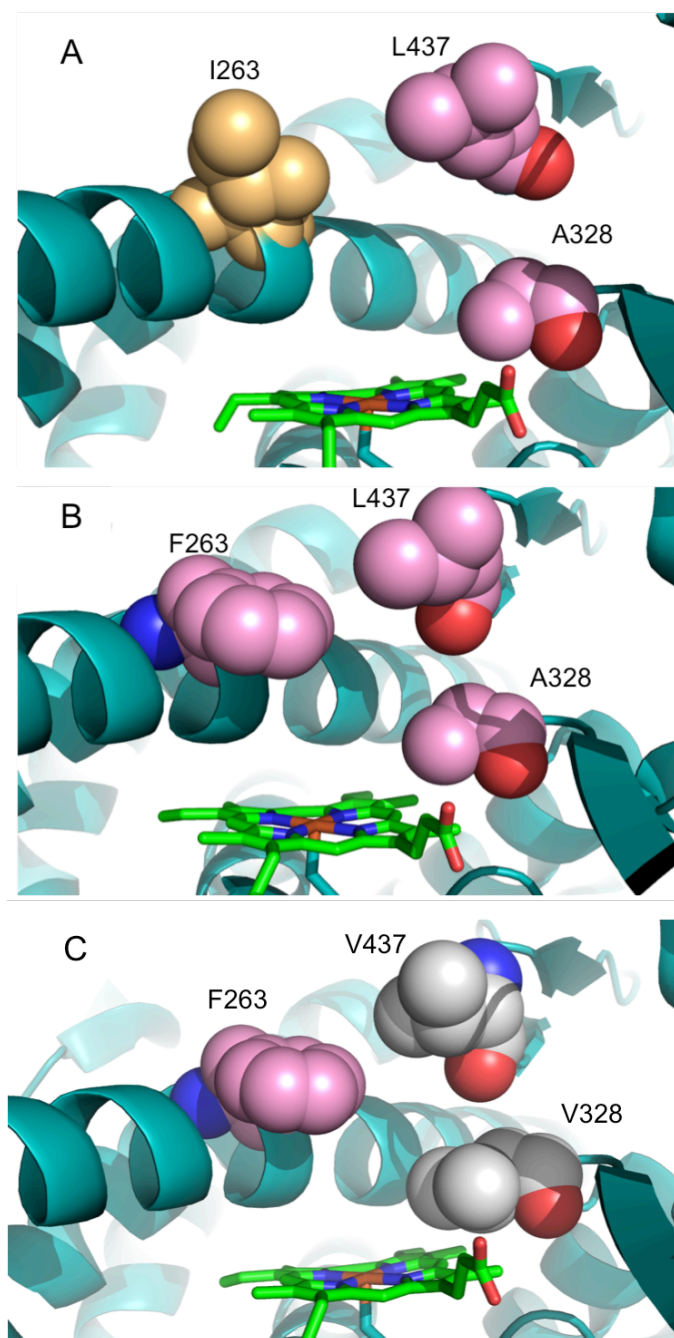


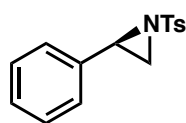
Figure S3. Comparison of active site residues in P-I263F and P-I263F-A328V-L437V

A) P411_{BM3}-CIS-T438S structure (PDB ID: 4H23) with I263 shown as van Der Waals spheres in gold, L437 and A328 shown in pink. B) P-I263F structure (PDB ID: 4WG2) showing the active site and residues F263, A328, and L437 as in pink. C) P-I263F structure with A328V and L437V mutations implemented *in silico* using Pymol shown as gray van Der Waals spheres.

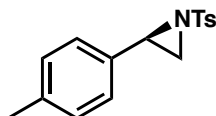
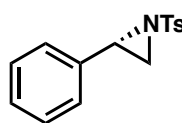


5. Assignment of Absolute Configuration.

Absolute stereochemistry of enzyme-produced aziridine **7** was assigned by chiral HPLC analysis and optical rotation. In particular, absolute stereochemistry of **7** was previously assigned by chiral HPLC using Chiracel OJ column (isopropanol/n-hexane mobile phase), with (*S*)-**7** the earlier eluting enantiomer.²⁷ Analytically enantiopure **7** produced by P-I263F-A328V-L437V was subjected to the same chiral HPLC conditions and observed to be the earlier eluting enantiomer (Figure S11), leading to an assignment of (*S*)-**7**. Further support for this assignment came from measuring optical rotation. The optical rotation values for enantiomers of **7** have been previously reported (*R*)-**7** [α_D^{25}] -80.25 ($c=0.8$, CHCl₃) and (*S*)-**7** [α_D^{20}] +26.7 ($c=0.7$, CHCl₃).²⁸ Optical rotation measurement of analytically enantiopure **7** produced by P-I263F-A328V-L437V gave [α_D^{25}] +80.2 ($c=1.2$, CHCl₃), revealing it to be (*S*)-**7**. Similarly, the optical rotation of P-I263F-A328V-L437V produced **5** (analytically enantiopure) was measured to be [α_D^{25}] +106.1 ($c=0.45$, CHCl₃). By analogy, the configuration of enzymatically preferred (+)-**5** is assigned as (*S*)-**5**.



(-)-**7**



(-)-**5**

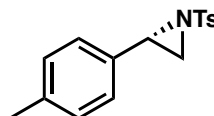
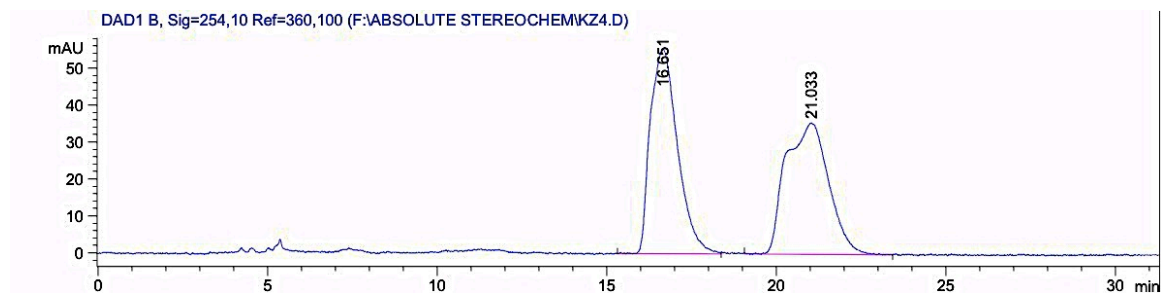
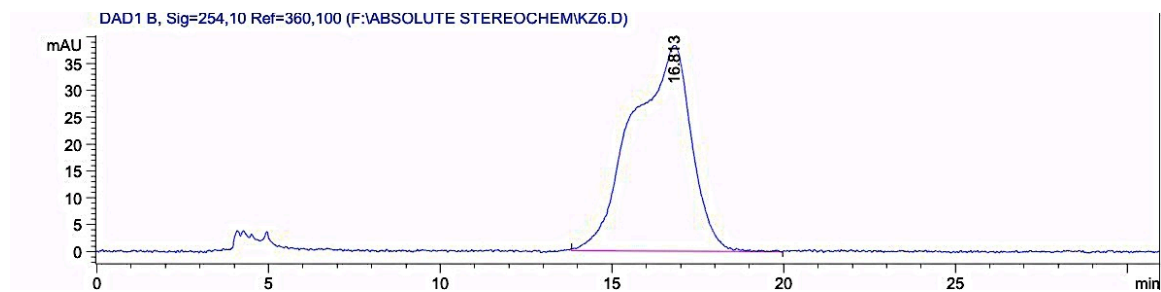


Figure S12. Assignment of absolute stereochemistry of enzymatically produced aziridine 7 by chiral HPLC (Chiracel OJ, 30% isopropanol : 70% n-hexane, 210 nm).

Racemic synthetic aziridine 7, $t_R = 16.7$ min and 21.0 min.

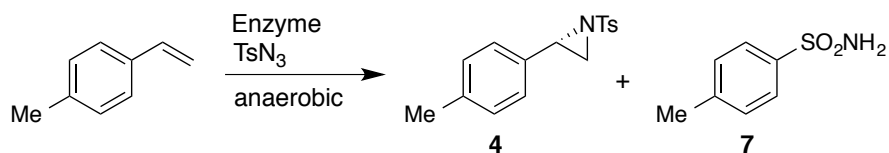


P-I263F-A328V-L437V produced aziridine 7, $t_R = 16.8$ min.



6. Initial rates for aziridination and azide reduction.

Table S4. Initial rates for each enzyme and product were determined as described in Chapter 3, with reaction conditions as described above (Materials and Methods, 2.5 mM tosyl azide, 7.5 mM styrene **4**). Rates of sulfonamide (**7**) formation were determined in the presence of styrene **4**



Enzyme	TOF 4 (min^{-1})	TOF 7 (min^{-1})	TOF 4 / TOF 7	TTN 4	TTN 7	TTN 4 / TTN 4 + 7
P411 _{BM3} -CIS T438S ("P")	0.36	13.2	0.027	8	320	0.024
P-I263F	9.2	28.1	0.34	139	261	0.34
P-I263F-A328V	9.6	27.6	0.35	nd	nd	nd
P-I263F-A328V-L437V	6.0	14.2	0.42	168	228	0.42

References

- (1) (a) Bornscheuer, U. T. *et al. Nature* **2012**, 485, 185; (b) Savile, C. K. *et al. Science* **2010**, 329, 305.
- (2) (a) Bornscheuer, U. T.; Kazlauskas, R. J. *Angew. Chem.-Int. Edit.* **2004**, 43, 6032; (b) McIntosh, J. A.; Farwell, C. C.; Arnold, F. H. *Curr. Opin. Chem. Biol.* **2014**, 19, 126; (c) Renata, H.; Wang, Z. J.; Arnold, F. H. *Angew. Chem.-Int.Edit.* **2014**, (*In press*); (d) Toscano, M. D.; Woycechowsky, K. J.; Hilvert, D. *Angew. Chem.-Int. Edit.* **2007**, 46, 3212.
- (3) (a) Wang, Z. J. *et al. Angew. Chem.-Int. Edit.* **2014**, 126, 6928; (b) Seitz, M. *et al. ChemBioChem* **2013**, 14, 436; (c) Hammer, S. C. *et al. Tetrahedron* **2012**, 68, 7624.
- (4) McIntosh, J. A. *et al. Angew. Chem.-Int. Edit.* **2013**, 52, 9309
- (5) (a) Bordeaux, M.; Singh, R.; Fasan, R. *Bioorgan. Med. Chem.* **2014**, 22, 5697; (b) Singh, R.; Bordeaux, M.; Fasan, R. *ACS Catal.* **2014**, 4, 546.
- (6) Farwell, C. C. *et al. J. Am. Chem. Soc.* **2014**, 136, 8766.
- (7) Hyster, T. K. *et al. J. Am. Chem. Soc.* **2014**, 136, 15505.
- (8) (a) Degennaro, L.; Trinchera, P.; Luisi, R. *Chem. Rev.* **2014**, 114, 7881; (b) Yudin, A. K. *Aziridines and Epoxides in Organic Synthesis*; Wiley-VCH Verlag GmbH, 2006.
- (9) (a) Ortiz de Montellano, P. R.; De Voss, J. J. *Nat. Prod. Rep.* **2002**, 19, 477; (b) Liu, P. *et al. J. Am. Chem. Soc.* **2001**, 123, 4619.
- (10) (a) Dodani, S. C. *et al. ChemBioChem* **2014**, 15, 2259; (b) Barry, S. M. *et al. Nat. Chem. Biol.* **2012**, 8, 814.
- (11) Thibodeaux, C. J.; Chang, W.-c.; Liu, H.-w. *Chem. Rev.* **2011**, 112, 1681.
- (12) Davies, H. M. L.; Manning, J. R. *Nature* **2008**, 451, 417.
- (13) Ogasawara, Y.; Liu, H.-w. *J. Am. Chem. Soc.* **2009**, 131, 18066.
- (14) Coelho, P. S. *et al. Nat. Chem. Biol.* **2013**, 9, 485.
- (15) Perera, R. *et al. Arch. Biochem. Biophys.* **2011**, 507, 119.
- (16) (a) Ando, T. *et al. Tetrahedron* **1998**, 54, 13485; (b) Kiyokawa, K.; Kosaka, T.; Minakata, S. *Org. Lett.* **2013**, 15, 4858.
- (17) Lewis, J. C. *et al. ChemBioChem* **2010**, 11, 2502.
- (18) Heel, T. *et al. ChemBioChem* **2014**, n/a.
- (19) Noble, M. A. *et al. Biochem. J.* **1999**, 339, 371.
- (20) (a) Misawa, N. *et al. Appl. Microbiol. Biotech.* **2011**, 90, 147; (b) Li, Q. S. *et al. Chemistry-a European Journal* **2000**, 6, 1531.
- (21) Kille, S. *et al. ACS Synth Biol.* **2013**, 2, 83.
- (22) Srinivas, B. *et al. J. Mol. Cat. A: Chem* **2007**, 261, 1.
- (23) (a) Huang, C.Y.; Doyle, A.G. *J. Am. Chem. Soc.* **2012**, 134, 9541. b) Kiyokawa, K. *et al. Org. Lett.* **2013**, 15, 4858; c) Evans, D.A.; Faul, M.M.; Bilodeau, M.T. *J. Am. Chem. Soc.* **1994**, 116, 2742.
- (24) Ando, T. *et al. Tetrahedron* **1998**, 54, 13485.
- (25) Craig II, R.A. *et al. Chem. Eur. J.* **2014**, 20, 4806.
- (26) Gao, G.Y.; Harden, J.D.; Zhang, X.P. *Org. Lett.* **2005**, 7, 3191.
- (27) Takeda, Y. *et al. J. Am. Chem. Soc.* **2014**, 136, 8544.

- (28) (a) Alonso, D.A.; Andersson, P.G.; *J. Org. Chem.* **1998**, *63*, 9455; b) Wang, X.; Ding, K. *Chem. Eur. J.* **2006**, *12*, 4568.